AN EXPERIMENTAL STUDY OF A POPULATION OF PHASE-REPELLING RELAXATION OSCILLATORS

by

ADAM ALEXANDER BRAILOVE

B. Sc. Massachusetts Institute of Technology

(1985)

SUBMITTED IN PARTIAL FULFILLMENT

OF THE REQUIREMENTS FOR THE DEGREE OF

DOCTOR OF PHILOSOPHY

at the

MASSACHUSETTS INSTITUTE OF TECHNOLOGY

June, 1995

Signature of Author_____

Department of Physics

June, 1995

Certified by_____

Paul S. Linsay

Thesis Supervisor

Accepted by_____

George Koster

Chairman, Department Committee

AN EXPERIMENTAL STUDY OF A POPULATION OF PHASE-REPELLING RELAXATION OSCILLATORS

by

ADAM ALEXANDER BRAILOVE

Submitted to the Department of Physics in May, 1995 in partial fulfillment of the requirements for the degree of Doctor of Philosophy in Physics.

ABSTRACT

The dynamical behavior of a system of coupled relaxation oscillators is studied experimentally. A population of up to 15 coupled electronic op-amp relaxation oscillators is used as a prototype for the real collections of limit-cycle oscillators frequently found in many physical, biological and technological systems. The oscillators interact via an all-to-all or mean-field coupling. The rarely studied case of anti-ferromagnetic interactions, in which oscillators tend to repel each other in phase, is considered. The behavior of the system is significantly different from the predictions of the limited theory that is currently available. The novel behavior observed includes the existence of numerous distinguishable phase-locked states and an exponential distribution of the duration of transients. The critical coupling strength necessary for the oscillator system to completely phase-lock is measured.

A simple geometrical model of the dynamics of the system during the transient is presented as a means of understanding the exponential distribution of transient lengths. In addition, a phase-response oscillator model is shown to exhibit similar transient behavior.

Thesis Supervisor: Dr. Paul S. Linsay
Title: Senior Research Scientist

ACKNOWLEDGMENTS

I would like to thank here all the people who have helped and supported me during my time as an M.I.T. graduate student:

First and foremost, let me thank my supervisor Dr. Paul Linsay who has tolerated my stubbornness and has given me the time and space to do a bit of intellectual roaming. He provided the original idea for these experiments and was always available for discussions and always had new things to try. He gave me a level of independence many graduate students don't have and I am appreciative.

Credit is also due to the M.I.T. Physics Department, which has generously provided me with financial support in the face of a continuing decline in funding for academic physics research. Thanks go to the department for four years of Teaching Assistantships, without which this thesis wouldn't have been possible, and to Professors Baranger and Rosenberg who agreed to read this thesis.

I would also like to thank all the wonderful folks in Junior Lab where I performed my teaching duties (time-consuming though they have been.) Thanks are due to Dr. J. Kirsch, Professors Henry Kendall, David Pritchard, George Clark, Ranier Weiss and Leslie Rosenberg for teaching me by example, as much as the students, about both teaching and physics. Thanks, also, to all the students for their enthusiasm and curiosity.

On a personal level, credit and thanks and love go, of course, to my family. For the emotional support, financial support, encouragement, nagging, advice (useful and otherwise) and all the other little benefits that come from a family, I give great thanks to my parents and grandparents and sister.

Finally, thanks are owed to the guys in the office at the P.F.C. and the founders of C.P.O.: Tom, John, Darren and Chris. The Chinese lunches, the calculating, dreaming, and planning; the friendship, camaraderie, good humor and perspective made this whole experience so much easier.

TABLE of CONTENTS

1. INTRODUCTION

Limit-cycle oscillators are an ubiquitous feature of the physical, technological and biological worlds. In general terms, every dissipative physical system which oscillates autonomously, is a limit-cycle oscillator. This thesis concerns experiments which were performed upon a small collection of electronic limit-cycle oscillators, coupled to each other with an all-to-all or mean field coupling. The behavior of the experimental system is novel and, as will be seen, it differs markedly from the simple theoretical treatment currently available. In order to gain a more complete understanding, however, it is useful to place this work in its proper historical context. This will be followed by a brief survey of some of the physical applications of coupled oscillator systems. Next, we give a more formal statement of the purpose for our experiments, and finally, we lay out a road map to the remainder of the thesis.

1.1 Historical Context

The problem considered here lies at the intersection of three important areas of physics: non-linear dynamics, oscillator synchronization, and statistical mechanics. Each of these areas has a long and rich history, infused more recently with a new vitality resulting from recent discoveries.

1.1.1 Nonlinear Dynamics

The first such area, non-linear dynamics, dates back at least as far as Henri Poincaré [Poincaré, 1881] who originated the use of phase space to describe dynamical systems. The phase space of a physical system is constructed so that each independent physical variable forms one coordinate in phase space. The entire state of the system is then compactly described by a point in phase space. A geometrical or topological understanding of a system's phase space often provides an alternative way of viewing the system and can lead to fresh insights into its dynamics. It is a testament to the importance of the phase space approach to dynamical systems that it is essentially taken for granted today. Indeed, it will prove to be a valuable tool in the work presented here.

Most of the great mathematical tools of science and technology, such as those found in mechanical and electrical engineering, have been based largely on a linear view of the world. Although small forays into the nonlinear realm were made, these usually took the form of perturbative extensions of linear problems. This focus on linear problems was in

no small measure due to the analytical tractability of such problems. The advent of the digital computer and its rapidly increasing computational power has, in the last few decades, ushered in a new era of research in physics and has reopened and reinvigorated the field of dynamical systems.

The discovery of chaos – irregular, aperiodic motion in simple, low dimensional, deterministic dynamical systems – was the key development from which so much renewed interest in this field has flowed. Lorenz discovered [Lorenz, 1963] that a highly simplified, purely deterministic, three dimensional model of atmospheric convection, exhibited aperiodic behavior. This early numerical discovery of chaos, however, went unrecognized for some time. It is now well known that dissipative systems can posses states, known as strange attractors, toward which initial conditions eventually evolve. The existence of a strange attractor is stable under variations in system parameters, yet the motion of a point on the attractor is chaotic, and highly sensitive to small perturbations. This notion was advanced by Smale [Smale, 1967] who introduced the geometrical view of strange attractors (the Smale 'horseshoe') as transformations on phase space which involve both stretching and folding.

The discovery of chaos led to renewed hope that the long unresolved problem of fluid turbulence might be understood, since chaos formed a bridge between the deterministic world of the Navier-Stokes equation and the clearly disordered and unpredictable motion of turbulent fluids. As its parameters are varied, a system may undergo bifurcations which introduce oscillations at new frequencies. Seminal work by Ruelle, Takens [Ruelle & Takens, 1971] and later Newhouse [Newhouse *et al.*, 1978] proved that, under relatively general conditions, as few as three incommensurate (having mutually irrational ratios) frequencies are sufficient for a chaotic attractor to arise.

1.1.2 Oscillator Synchronization

The study of oscillator synchronization has a long and rich history, as well. The measurement of time played a crucial role in the early development of science. To make accurate measurements of time, Christiaan Huygens [Huygens, 1673] invented the pendulum clock in 1657. It is interesting to note that, like our own experimental oscillators, the pendulum clock is a limit-cycle oscillator: a constant source of energy (from a falling weight) is used to produce oscillations of constant amplitude and frequency. Huygens also made what is probably the first scientifically recorded observation of oscillator synchronization. He wrote:

> "It is quite worth noting that when we suspended two clocks so constructed from two hooks imbedded in the same wooden beam, the motions of each pendulum in opposite swings were so much in agreement that they never receded the least bit from each other and the sound of each was always heard simultaneously. Further, if this agreement was disturbed by some interference, it reestablished itself in a short time. For a long time I was amazed at this unexpected result, but after careful examination finally found that the cause of this is due to the motion of the beam, even though this is hardly perceptible. The cause is that the oscillations of the pendula, in proportion to their weight, communicate some motion to the clocks. This motion, impressed onto the beam, necessarily has the effect of making the pendula come to a state of exactly contrary swings if it happened that they moved otherwise at first, and from this finally the motion of the beam completely ceases."

His astonishment and excitement is palpable even today. As Huygens' found, it is quite common to find synchronization occurring in groups of oscillators, when no intentional effort has been made at causing synchronization. This spontaneous creation of temporal order and agreement among elements with so little internal 'intelligence' is perhaps inherently fascinating to the human mind; certainly it is to those who experiment with oscillator synchronization. It is also interesting that the coupling of Huygens' clocks was phase-repulsive: they tend to oscillate with a 180 degree phase gap. This form of coupling is the rarely studied case on which our work is focused. Had Huygens added a few more clocks to his beam, he might have encountered some of our results! Today, the synchronization of two oscillators is essentially a solved problem. This is the result of the fact that motion on a two-torus (T^2) is highly constrained, in a topological sense. Much of the more recent work on larger oscillator systems will be discussed below.

1.1.3 Statistical Mechanics

The third area to which our work is connected is statistical mechanics. This is necessarily so, since we are studying a collection of oscillators rather than two or three. While the fifteen oscillators used in our experiments only barely justifies the use of the term 'statistical', much of the recent work in oscillator systems and nonlinear dynamics has focused on the case of very large N. Winfree [Winfree, 1967] was probably the first to make the fundamental observation that there is a close connection between the temporal coherence of synchronization in a population of oscillators and the spatial coherence of a phase transition in, for example, a population of spins. The variation in the natural frequency, from oscillator to oscillator, plays the role that thermal energy plays in the spin system. He concluded (and observed experimentally) that oscillator systems could undergo phase transitions, spontaneously becoming ordered (phase-locked) when the coupling

between oscillators was sufficient to overcome the 'thermal' effects. The connection with statistical mechanics has since been put on a solid formal footing by Kuramoto & Nishikawa [Kuramoto & Nishikawa, 1988], who showed that the critical behavior found in globally coupled oscillator systems is analogous to the critical behavior in a system of spins coupled by a mean field. The mathematical tools of statistical mechanics, such as the order parameter and the self-consistent equation also have analogs in oscillators systems. Since then, the theoretical work on systems of oscillators has grown substantially. It now includes systems coupled locally via lattices of various dimensions [Strogatz & Mirollo, 1988], systems that include frustration and exhibit spin-glass behavior [Daido, 1992], [Omata *et al.*, 1988], discrete-time systems [Daido, 1987], [Kaneko, 1991], [Kaneko, 1992], systems with delays [Niebur *et al.*, 1991], and systems with neuron-like impulsive interactions [Tsodyks *et al.*, 1993]. It appeared however that there was almost no experimental connection associated with this theoretical work. It was into this gap that we directed our efforts. It is worth noting here that there is also a fundamental connection between the relatively new theory of neural networks and the theory of Ising spin systems. It is with this in mind that we will speculate in the concluding section on the possible link between our work on oscillator systems and neural networks.

1.2 Survey of Coupled Oscillator Systems

We turn now to a review of some the important and interesting applied work done on oscillator populations. We focus first on physical systems such as Josephson junctions and laser diodes. Then we will turn to biological systems. The field is, of course, is much too large for this survey to be rigorous or complete. However, our purpose is twofold. It is first to convey a sense of the broad applicability and richness of this field, and second to provide a context of real-world systems against which our system of electronic oscillators will not seem so abstract.

1.2.1 Physical Systems

There are several technological applications of synchronization in oscillator populations. The problem arises typically in connection with Josephson junctions and laser diodes when one wishes to scale up the power output of a single oscillator. One way to accomplish this is to use many oscillators. It is clear, however, that they must be made to oscillate in synchrony (and in phase) for that strategy to be effective. Owing to the considerable practical value of Josephson junction oscillators, extensive theoretical and experimental work has been performed and has led to a relatively complete understanding

of the dynamics of arrays of these oscillators. The work until 1984 is well reviewed by A. K. Jain [Jain *et al.*, 1984] with slightly more recent developments discussed by Hadley [Hadley *et al.*, 1988a,b].

As with Josephson junctions, there is a practical interest in making one large laser out of many small semiconductor lasers. To do so, necessitates making the individual lasers coherent with respect to each other. This is done typically by coupling the lasers together with normal or evanescent electromagnetic waves. Experimental work has been performed by Elliot [Elliot, 1985] and others; and theoretical work was done by Wang and Winful [Wang & Winful, 1988], [Winful & Wang, 1988].

Another technological example of an oscillator synchronization problem is in the generation of electrical power, where generators are coupled together by an electrical power distribution network [Kopell & Washburn, 1982].

Finally, perhaps the most recent example of oscillator synchronization comes from the world of computer networks. In this unusual case [Floyd, 1993], [Treese, 1992] the synchronization is inadvertent and undesirable. Various nodes on a computer network are often programmed to emit packets of information at precisely timed intervals (hence they are oscillators). It has been observed that when coupled through a network, the nodes, which would normally be independent of each other, can become synchronized. The result is an inefficient and destructive pattern of traffic flow, characterized by huge bursts of information flow across the network.

1.2.2 Biological Systems

We have discussed several examples of technological problems involving oscillator synchronization. Among natural systems, however, the problem of oscillator synchronization finds its broadest applicability in the study of biological oscillators. Undoubtedly the most picturesque example is the synchronous flashing of species of Asian fireflies [Buck & Buck, 1976], [Buck, 1988]. As darkness falls, the background light from the sky decreases, increasing the effective coupling between neighboring fireflies. Over the course of the night, the flashing of the fireflies gradually becomes synchronized, culminating in a spectacle that was described compellingly by Smith [Smith, 1935]:

> "Imagine a tenth of a mile of river front with an unbroken line of trees with fireflies on every leaf flashing in synchronism, the insects on the trees at the ends of the line acting in perfect unison with those between."

Other examples of mutual synchronization among biological oscillators are abundant. The periodic beating of the heart can be modeled [Peskin, 1975], [Torre, 1976], [Honerkamp, 1983] with a system of coupled oscillators. Synchronization of the menstrual cycles of women who live together has also been observed [McClintock, 1971]. Chains of coupled neuronal oscillators can exhibit wave phenomena. Such systems have been used to model swimming types of locomotion [Cohen *et al.*, 1982] and the peristaltic movement of intestines [Brown *et al.*, 1975].

1.3 Statement of Purpose

The experimental approach taken in the work presented here builds directly on the experimental work of Linsay and Cumming [Linsay & Cumming, 1989], [Cumming & Linsay, 1988]. This work extends their use of two and three electronic oscillators into the realm of the statistical by studying larger numbers of oscillators. The technique of performing experiments on an electronic system is unusual and it inverts, to some extent, the traditional roles of theory and experiment. In our case, the experimental system, being constructed of well understood electronic components, is of no *inherent* physical or technological interest. Rather it serves as a prototype of the current theoretical models. Some of the implications of this strategy are discussed more fully in Sec. 6. In contrast, most of the other experimental work on oscillator populations deals with the detailed dynamics of specific applications, such as Josephson junctions or laser diodes discussed above.

The theoretical work with simple oscillator models, such as the one we will describe in Sec. 2, has grown dramatically. This is, in part, due to the recognition that the mathematical tools of statistical mechanics could be elegantly applied to such simplified problems. It is also due to the growing availability of computing power. Yet, while the level of theoretical work has grown, there has been little attempt to test these elegant and general theories with experiment. In addition, while much theoretical work has been done on oscillator populations which tend to attract each other in phase, the case of repulsive interactions studied here has received, by comparison, almost no attention.

This thesis reports the results of experiments on a collection of as many as fifteen electronic relaxation oscillators, coupled with a simple mean-field type coupling. The absence of a well developed theory applicable to the case of repulsive interactions makes the results somewhat phenomenological. However, a simple geometrical model of the structure of the system's phase space will be presented which will aid in understanding the

novel transient behavior of the system. In addition, a simple, discrete numerical model will be developed which captures some of the essential features of the dynamics without resorting to a full-blown simulation of the electronics. The electronic oscillators used in these experiments serve, hopefully, as generic models of the 'real world'. They permit a rapid and intuitive exploration of large regions of parameter space while including all the vagaries and difficulties of any 'real' system. The ultimate aim is to uncover generalities about the dynamics of such systems.

1.4 Layout of the Thesis

The remainder of this thesis will be structured as follows. We will embark in Sec. 2 on a review of the applicable theory. This will include a rather cursory overview of some important general ideas in the field of nonlinear dynamics, followed by a more detailed discussion of the current theory as it relates to our experimental system. In Sec. 3, the details of our particular experimental system will be discussed. This will include both the basic functioning of the oscillators themselves, as well as a relatively detailed description of the associated control and data acquisition electronics, and software. In Sec. 4, the results of the experiments will be presented, focusing primarily on the unusual transient behavior of the system. Section 5 will contain a discussion of the results. A simple model of the geometry of the phase space will be presented as a way of understanding the results from the preceding section. This will be followed by a crude and rather incomplete mathematical model of the system. Finally, Sec. 6 will conclude with a summary of the important results and a discussion of possible future directions for this research.

2. THEORY

We turn here to a review of the relevant theory of oscillator synchronization. Before doing so, however, we will touch briefly upon some of the important concepts and tools of nonlinear dynamics; especially those used in our primarily experimental work. The approach will initially be somewhat tutorial, for those less familiar with the subject. No attempt is made to be rigorous in the development of these ideas. Nor can it be claimed that what follows is complete. Indeed, large areas of nonlinear dynamics, and much of the prolific recent work on oscillator populations will be left out. Rather, the goal is to establish the theoretical context which is typically used in understanding systems of the type studied here. As shall be seen later, the theory falls well short of what is needed to understand the behavior of our system.

2.1 Simple Linear Systems

The most natural place to begin such a discussion is with the most rudimentary of all possible oscillatory systems: one described by the linear second-order differential equation

$$\frac{d^2x}{dt^2} + \gamma\frac{dx}{dt} + \omega^2 x = 0, \tag{2.1}$$

where γ is the damping coefficient and ω is the frequency of undamped oscillations. Of course, many simple physical systems are well modeled by this equation. For example, Eq. (2.1) describes the position of a mechanical system consisting of a mass M, a spring of spring constant κ, and a damper which produces a frictional force, β dx/dt, if one makes the following identification:

$$\omega \leftrightarrow \sqrt{\frac{\kappa}{M}}$$

$$\gamma \leftrightarrow \frac{\beta}{M}$$

Alternatively, the same equation describes the current in a series R-L-C electrical circuit if one makes the following identification:

$$\omega \leftrightarrow \sqrt{\frac{1}{LC}}$$

$$\gamma \leftrightarrow \frac{R}{L}$$

The important point to recognize is not that many systems *happen* to be described by Eq. (2.1), but rather that this equation is the lowest order approximation that one can make to many real world physical systems without destroying their oscillatory behavior.

The field of dynamical systems is naturally divided into two broad categories of problems, depending on how areas of phase space behave under the action of the system's dynamics. Systems in which areas of phase space are a constant of the motion are termed *conservative*. Such conservation of areas of phase space places significant geometrical constraints on how such systems move through phase space. The study of the nonlinear dynamics of conservative systems has important application to many areas of physics including quantum chaos and the chaotic motion of planetary systems. The fundamentally important KAM (Kolmogorov, Arnold, Moser) theorem applies only to conservative systems.

On the other hand, systems in which phase space area is not a constant of the motion are said to be *dissipative*. Dissipative systems are the other 'half' of the field of nonlinear dynamics. The substance of this work will be confined entirely to dissipative systems. In terms of Eq. (2.1), which models many mechanical and electrical problems, the most fundamental of all physical quantities is energy. For such systems the conservation or non-conservation of energy corresponds exactly with the conservation or non-conservation of phase space area. That is, dissipation implies a loss of energy.

At first glance, dissipative systems in which no energy is ever added may appear to hold little interest, in that all energy is eventually lost and the system ceases to move. A particle moving in a potential with friction, for example, will eventually come to rest at the minimum of the potential. If the potential has two minima however, there will be two possible final states and one may then ask: what is the set of initial conditions that leads to each particular final state? Even for relatively simple potentials, these sets of initial conditions, or so called *basins of attraction*, can be profoundly complex. If one permits the addition of energy as well as dissipation (such systems are still referred to as dissipative) the system can exhibit a wide variety of interesting motions.

Let us return now to the simple linear oscillator described above and write down the well known expression for its energy:

$$E(x,\dot{x}) = \frac{1}{2}\dot{x}^2 + V(x) = \frac{1}{2}\dot{x}^2 + \frac{1}{2}\omega^2 x^2 \tag{2.2}$$

where $\frac{\partial V(x)}{\partial x} = \omega^2 x$, and we have chosen m=1. Differentiating Eq. (2.2) yields an expression for the evolution of the energy,

$$\dot{E} = \dot{x}\ddot{x} + \frac{\partial V(x)}{\partial x}\dot{x}$$

Using Eq. (2.1) we get

$$\dot{E} = \dot{x}\ddot{x} + \omega^2 \dot{x}x = -\gamma\dot{x}^2 . \tag{2.3}$$

Clearly, for γ=0, the energy is a constant of the motion and the system is conservative as we expect. For γ>0 the system is constantly losing energy as long as it is in motion. Thus, it will eventually come to rest with x=0. The case of γ<0, though less common physically, is nevertheless useful, in that it corresponds to a continual addition of energy to the system. The result is oscillations of ever increasing amplitude. Figure 2.1 illustrates these three familiar cases by constructing a phase space from the velocity and position of the linear damped harmonic oscillator. The vectors indicate the direction and speed of the flow through phase space. For γ>0, points spiral in to the origin; for γ=0, points travel in ellipses around the origin. (The orbits will be circular, if the axes are chosen with the appropriate scales); for γ<0 points spiral outward toward infinity.

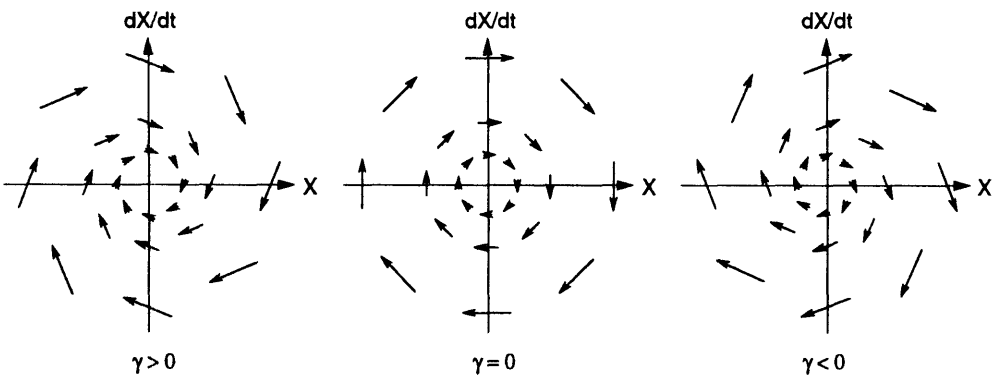

Figure 2.1 Three views of the flow in phase space of a damped linear oscillator. The three cases shown are normal damping (γ>0), undamped (γ=0) and negative damping(γ<0). The axes are scaled such that the motion is circular.

2.2 Simple Nonlinear Systems

The mathematics of Eq. (2.1) (and all higher dimensional linear systems) has long been completely understood. The real interest comes in understanding systems in which the nonlinearities of the real world have not been completely removed. In viewing Eq. (2.1) as a linearization of a more complicated system, we understand the coefficients γ and ω to be merely the zeroth order terms in a Taylor expansion. We may now consider what happens when we perturb the system with a bit of the nonlinearity that had been previously ignored. While not the most general perturbation, we can consider the case where the coefficients γ and ω are functions of position, x:

$$\omega^2 = \omega^2(x)$$

$$\gamma = \gamma(x) = \alpha_0 + \alpha_1 x + \alpha_2 x^2 + O(x^3). \tag{2.4}$$

Clearly, the dependence of ω on x can be represented purely as a modification of the potential, such that the potential now satisfies

$$\frac{\partial V(x)}{\partial x} = x \cdot \omega^2(x)$$

As mentioned above, such problems are interesting, but they properly fall in the realm of conservative systems. Of greater interest here is the position dependence of the damping coefficient. Note that the expression Eq. (2.3) for the evolution of the energy remains valid, except that γ is now a function of position. The constant term in Eq. (2.4) is obviously just the damping coefficient in the harmonic oscillator Eq. (2.1). We neglect the first-order term (and all other odd terms) in the Taylor expansion of γ, since its perturbative effect on the energy is small when Eq. (2.3) is averaged over one cycle of the oscillator. Thus the lowest order term of interest is the second-order term. Discarding higher order terms yields an amplitude dependent damping coefficient which can be written in the form

$$\gamma(x) = -\gamma_0\left[1 - \frac{x^2}{x_0^2}\right].$$

When damping of this form is used, the resulting differential equation is the well known Van der Pol equation. After a suitable change of variables it can be written in dimensionless form as

$$\frac{d^2x}{dt^2} - (\varepsilon - x^2)\frac{dx}{dt} + x = 0. \tag{2.5}$$

For small amplitude oscillations, $x^2 << \varepsilon$, the oscillator behaves like a harmonic oscillator with a *negative* damping coefficient, which causes the oscillations to *grow* in amplitude. For large amplitude oscillations, $x^2 >> \varepsilon$, the damping 'coefficient' becomes positive causing the oscillations to decay in amplitude. As one might expect, there is a trajectory of intermediate amplitude for which these two competing effects cancel each other over the course of one complete oscillation. Thus, for any given ε, there is a single trajectory or *orbit* toward which all initial conditions (except the trivial case of the origin) are attracted.

Such an orbit is known as a *limit cycle*. Like an undamped harmonic oscillator, the system will continue to oscillate forever. In contrast to the undamped harmonic oscillator, however, the amplitude of oscillation is dependent on the parameters of the system, rather than on the initial conditions. All information about the initial condition is destroyed by the compression of phase space that arises from the damping. The limit cycle itself is a feature found only in dissipative dynamical systems. Figure 2.2a shows a schematic view of the phase-space flow in the neighborhood of a limit-cycle. One can approximately decompose the flow near the limit cycle into motion along the limit-cycle (in the θ–direction) and motion normal to the limit-cycle (in the radial direction). Figure 2.2b shows (again schematically) what the differential equation governing flow in the radial direction might look like. The motion in the radial direction can in some sense be regarded as a one dimensional dynamical system with a fixed point attractor at R_0, the radius of the limit-cycle. The larger the magnitude of the slope near R_0, the more strongly points are attracted to the limit-cycle.

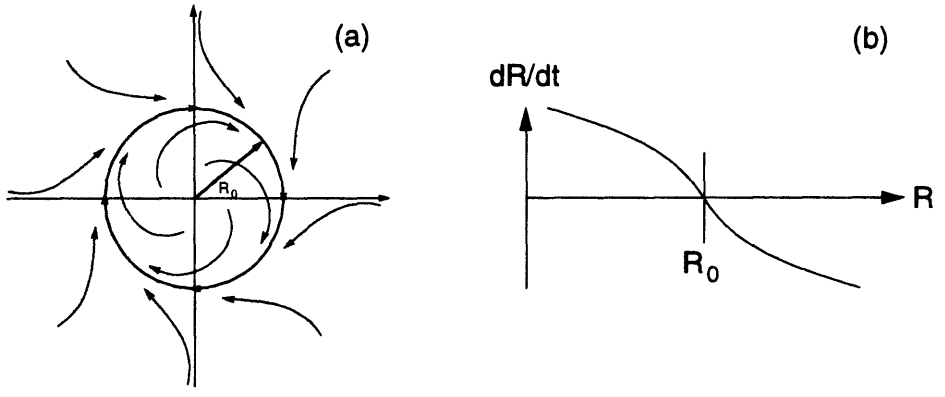

Figure 2.2 Schematic view of limit-cycle dynamics. a) Flow through phase space. b) Dynamics in the radial direction

Figures 2.3a and 2.3b show the actual (numerically computed) phase-space trajectories of the Van der Pol oscillator for small and large initial amplitudes, respectively. In this case ε=0.1, hence the weak nonlinearity produces trajectories that are nearly circular. Figures 2.3c shows x(t) for times sufficiently long that the transients have disappeared. Note the essentially sinusoidal trajectory, again consistent with the fact that the system is a weakly perturbed harmonic oscillator.

Figure 2.4 is analogous to Fig. 2.3, except that ε=4.0; a very strong nonlinearity. Note that the transients in Fig. 2.4 are much shorter: the system typically reaches its stable orbit in less than one oscillation. Furthermore, the trajectories are no longer nearly circular, but are highly distorted as a result of the nonlinearity. For large ε, the graph of x(t) also exhibits another important feature.

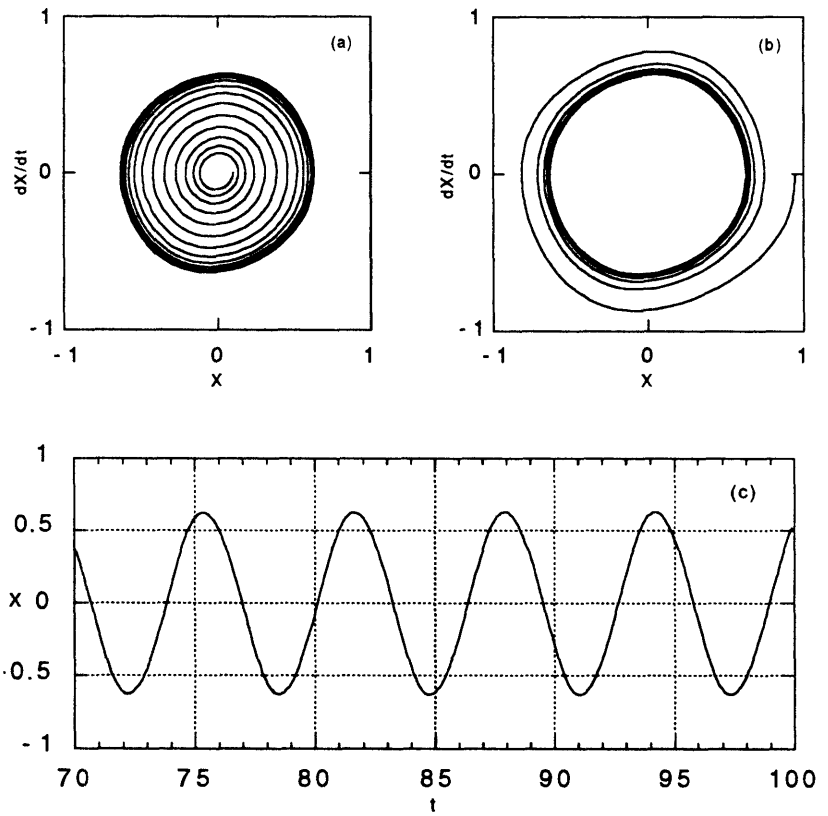

Figure 2.3. Dynamics of a Van der Pol oscillator for ε=0.1. Figures a and b show phase space trajectories for initial condition inside and outside the limit-cycle, respectively. Figure c shows the nearly sinusoidal variation in position after the transient has decayed.

There are two distinct time scales associated with the motion: a slow drift followed by a rapid movement. Oscillations with separate fast and slow time scales are known as *relaxation oscillations*. The corresponding oscillators are called *relaxation oscillators*.

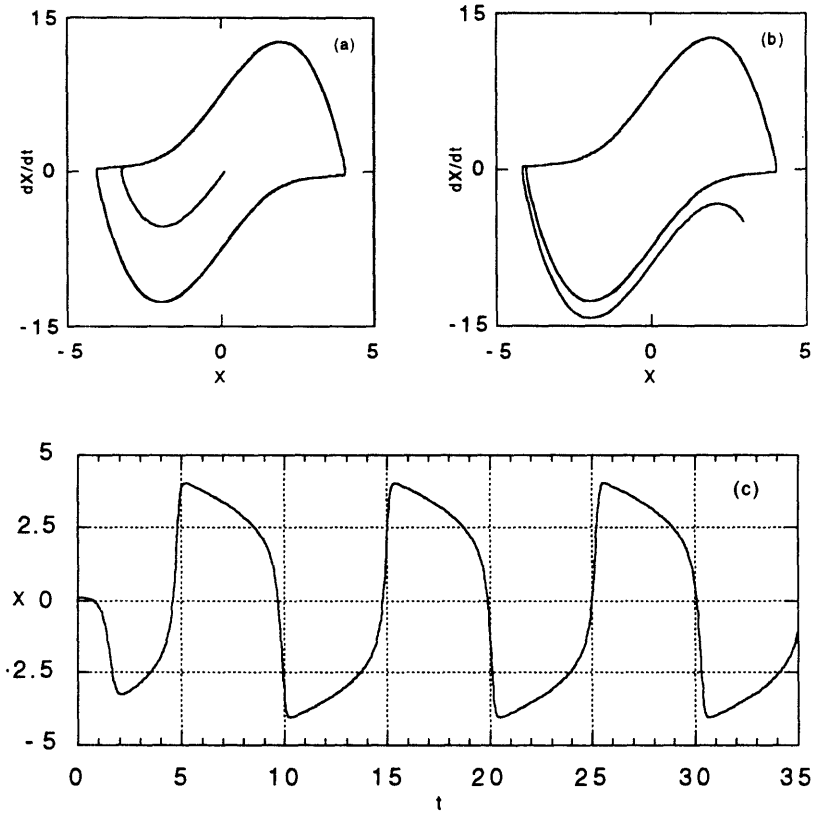

Figure 2.4. Dynamics of a Van der Pol oscillator for ε=4.0. Figures a and b show phase space trajectories for initial conditions inside and outside the limit-cycle, respectively. Figure c shows the variation in position as a function of time. Relaxation oscillations are evident from the two time scales visible in the motion. Note also how quickly the transient decays compared to the case ε=0.1.

2.3 Dynamical Systems

Taking a broader view, let us consider *dynamical systems* in general. Virtually any dynamical system, including the simple ones discussed above can be described by a system of N first order differential equations

$$\frac{d\bar{x}}{dt} = \bar{F}_{\lambda}(\bar{x})$$

where λ represents a parameter (or possibly several parameters) of the system. The N-dimensional phase space of the system is simply the space formed by the components of $\vec{x}$. $\vec{F}_\lambda(\vec{x})$ is a vector field which determines the trajectory of any point $\vec{x}$, in phase space.

Dissipative systems are characterized by flows which tend to contract (N-dimensional) areas of phase space. Geometrically, this means that under the action of the dynamical system, an initial area of phase space will gradually be compressed until it has no area. Formally the condition for dissipation can be written:

$$\sum_{i=1}^{N} \frac{\partial F_i}{\partial x_i} < 0.$$

Conservative systems, on the other hand, are characterized by a flow through phase space which, as required by Liouville's theorem, preserves areas. Thus,

$$\sum_{i=1}^{N} \frac{\partial F_i}{\partial x_i} = 0.$$

It is possible and often very useful to reduce the dimension of a continuous dynamical problem by cutting the phase space with an N-1 dimensional plane. One records on the plane the set of points of intersection between the plane and a trajectory in phase space. This set of points is a *Poincaré section* and is illustrated in Fig. 2.5. By additionally recording the temporal ordering of the points on the Poincaré section, dynamical information is retained.

The transformation that takes one point into the next is known as a *map*: a discrete version of a dynamical system. In fact, a map is more general in that it need not derive from any differential dynamical system. The map describes the 'new' state of a system given its current state according to $\vec{x}' = \vec{f}(\vec{x})$.

For dissipative dynamical systems there are invariably transients which decay away given sufficient time. However, there is often a set of phase space points called an *attractor* such that a trajectory begun on the attractor, will remain on it forever. An attractor is said to be dynamically stable if trajectories perturbed away from the attractor return to it. If the perturbations are amplified it is a dynamically unstable attractor, sometimes called a repeller. The general types of attractors are well cataloged. The simplest are, of course, fixed points. The limit-cycle, which has already been discussed, is another common type of attractor. Strange or chaotic attractors, which were mentioned

in Sec. 1 and play a fundamental role in the modern theory of dynamical systems, posses unusual properties. Stable chaotic attractors are attractors in the truest sense, in that a trajectory perturbed *off* the attractor will return to it. Yet, perturbations *along* the attractor tend to grow exponentially in time, giving rise to the well known property of strange attractors: *sensitivity to initial conditions.* As one varies a parameter of a dynamical system an attractor may undergo a sudden, discontinuous change known as a *bifurcation.* A typical example of a bifurcation involves a fixed-point attractor becoming a limit-cycle or the two-torus, T^2, becoming a chaotic attractor.

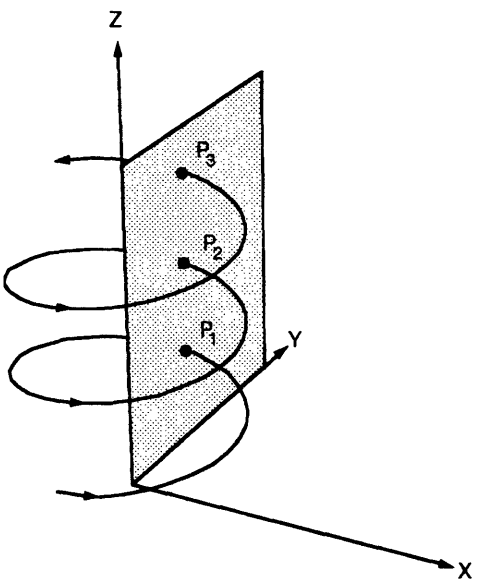

Figure 2.5. Schematic view of phase space showing the construction of a Poincaré section. An orbit is shown as it intersects the Y-Z plane at points P_1, P_2, P_3.

In general, dynamical systems reside in a phase space consisting of R^N, where N is the total number of canonical phase space dimensions. An important simplification (which we shall later make explicitly for our particular system) of the limit-cycle oscillator problem can be made for systems where phase space points are strongly attracted to the limit-cycle. This simplification assumes that the motion of each oscillator is confined to the limit-cycle itself, allowing the *state* of a single oscillator to be completely described by an angular variable. The *state* space of each oscillator is then a circle or T^1, a 1-torus. For a system of N oscillators, the *state* space of the entire system consists of the product of the *state* spaces of each oscillator, or the N-torus, T^N. The term phase space will henceforth refer to this *state* space consisting of the set of angle variables necessary to specify a system of oscillators. (In fact, we will often only be interested in the *relative* motions of the N oscillators, in which case the term phase space

will refer to T^{N-1}; one dimension having been eliminated by ignoring the average motion of the system). Figure 2.6 shows the trajectory of a system of two oscillators on T^2.

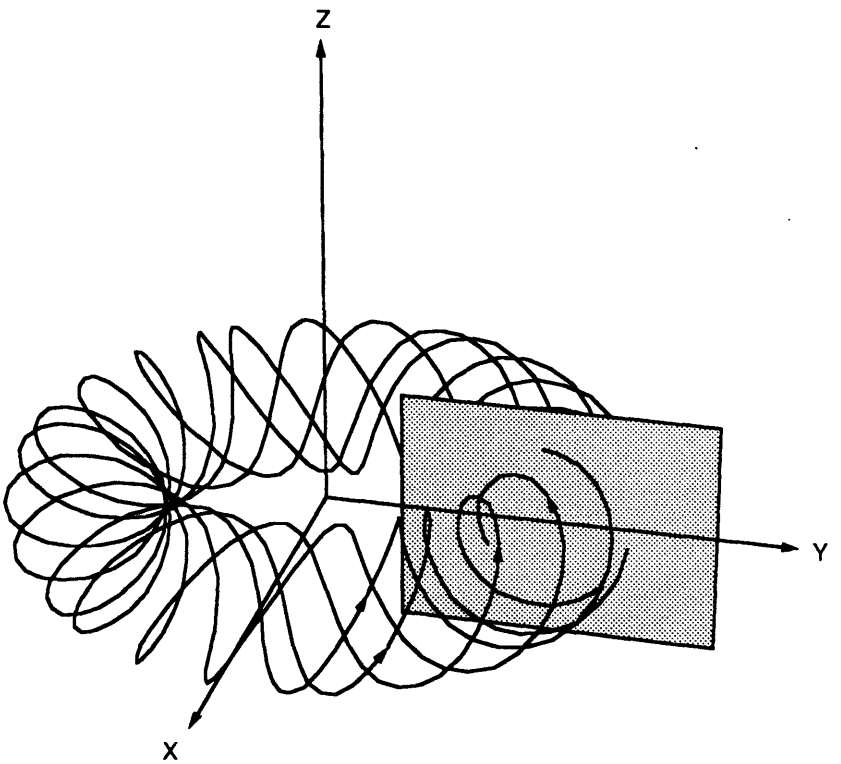

Figure 2.6. A single trajectory of a system of two oscillators on T^2. The beginning of a Poincaré section is also shown in the y-z plane.

It can be seen from the diagram that a differential system residing on T^2 can be reduced to a map of the circle, T^1, onto itself. If the ratio, ρ, of the natural (uncoupled) frequencies of two oscillators is a rational number, such that $\rho=p/q$, where p and q are integers, then the behavior of the two uncoupled oscillators will be periodic (marginally). This ratio is known as the 'bare' (uncoupled) winding number. For irrational winding numbers, the phase space trajectory on T^2 never falls back upon itself, but rather explores the entire surface of the torus. Such a system is said to be quasi-periodic, since although it is not strictly periodic, there are nevertheless two (or in general N) distinct frequencies present. Coupling will often cause the two otherwise incommensurate oscillators to lock together in a periodic motion. Figure 2.7 shows a schematic view of a classic phase diagram for the problem of two coupled oscillators. The phase diagram shows the parameter space of the system, with coupling strength plotted versus the *bare* winding number. The shaded areas show the so-called *locking tongues*: regions of parameter space for which the locked system has a particular winding number. It can be seen, for

example, that as coupling strength increases, the range of frequencies for which locking in a 1:1 ratio occurs, also grows larger.

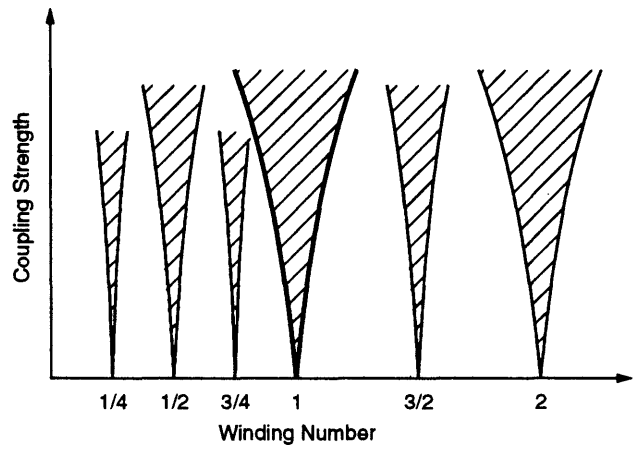

Figure 2.7. Typical phase diagram for two coupled oscillators. Several locking tongues are shown (hatched) for several rational winding numbers. The case of 1:1 frequency locking is shown with a heavy line.

2.4 Transient Lengths

For many dynamical systems, and particularly for systems of oscillators which tend to phase lock to each other, an important feature of the dynamics is the initial transient. Indeed, for phase-locking oscillators, there is usually little to be said about the system after phase-locking has occurred. The most interesting part of the dynamics is *how* the oscillators arrived at synchronization. An obvious question is how long does the initial transient last? In the case of phase-locking oscillators the time required for the system to evolve from an initial state to a phase-locked state is called the *locking time*. In general, the transient of a system will consist of trajectories which involve a decay toward a limit cycle. In our case, however, the off-limit-cycle transient decays virtually instantaneously. The dynamics of interest will be exclusively the motion of each oscillator along its limit-cycle.

2.4.1 Transient Lengths Near a Fixed Point

Consider a simple one dimensional system with an attracting fixed point. In the neighborhood of the fixed-point the dynamics of the system will be governed by

$$\frac{dx}{dt} = -kx, \quad (k > 0)$$

with the elementary solution $x(t) = x_0 e^{-kt}$. While this model of a transient is about as elementary as one can possibly find, it is not unreasonable to use it in an attempt to understand locking times. One difficulty of this model is that there is no clear 'end' of the transient; the length of the transient is, mathematically speaking, infinite. One possible approach is to associate the duration of the transient with the characteristic decay time, or some multiple thereof. For example, if we define the transient length, τ, to be the time required for the system to fall within a small 'locking' radius, ρ, of the origin then τ, is given by

$$\tau(x_0) = k^{-1} \ln(x_0/\rho).$$

If we further assume that the initial state x_0 is chosen from a uniform random distribution in some finite range $[0,x_{MAX}]$, then it can easily be shown that the distribution of transient times, $h(\tau)$ is given by

$$h(\tau) = \begin{cases} \dfrac{\rho}{x_{MAX}}\left[\delta(\tau) + ke^{k\tau}\right], & \tau \le \tau(x_{MAX}) \\ 0, & \tau > \tau(x_{MAX}) \end{cases} \qquad (2.6)$$

where the delta function is the result of initial conditions which lie inside the locking radius.

2.4.2 Transient of Unstable Chaotic Attractors

As will be shown later, the preceding results do not agree with our experimental results. Seminal studies [Grebogi & Ott, 1983], [Grebogi *et al.*, 1985], [Grebogi *et al.*, 1988] of boundary crises and unstable chaotic attractors have demonstrated the existence of an exponential distribution of transient lengths in simple, low dimensional systems. Since our high dimensional experimental system also displays an exponential distribution of transient lengths, it is worthwhile to discuss briefly the theoretical work. On the other hand, the underlying connection, if any, between the two systems is unclear.

The logistic map, given by $x' = f(x) = \lambda x(1-x)$, is probably the most widely studied and well understood nonlinear dynamical system. It is well known that as the parameter λ is increased from zero, the stable attractor undergoes a series of period-doubling bifurcations, eventually becoming chaotic as λ is increased past a critical value. Figure 2.8 shows the logistic map for $\lambda=4+\varepsilon$.

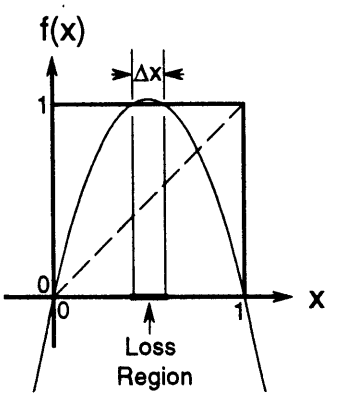

Figure 2.8. The logistic map, $x' = f(x) = \lambda x (1-x)$, for $\lambda>4$. Also shown (dashed) is the line $f(x) = x$. The loss region is a range of values of x for which $f(x) > 1$. Orbits which fall into the loss region are mapped to $x>1$ and then to $x<0$ and then accelerate toward $-\infty$. The width of this region is Δx.

As λ approaches $\lambda=4$, the maximum of f(x) approaches f(x)=1, hence the chaotic trajectory explores a wider and wider band, until that band covers the entire range [0, 1]. At $\lambda=4$, the chaotic band collides with the unstable fixed point at x=0. The collision is known as a *boundary crisis*. For $\lambda>4$, the chaotic behavior becomes unstable. Trajectories which fall in the small central 'loss' region that satisfies $f(x)>1$ will necessarily be mapped to $x>1$ on the next iterate. On the following iterate, the trajectory will then be mapped to $x<0$ and will then diverge rapidly toward $x \to -\infty$. Thus, for a loss region which is sufficiently small, a trajectory may orbit chaotically on [0, 1] (excluding the loss region) for a long time. In this case the motion is not true chaos, but is rather a chaotic transient which lives for a while on what remains of the chaotic trajectory after it has become unstable.

Suppose we define the length of the transient, τ, to be the time (number of iterations) required for an initial condition to be mapped into the loss region. Since the orbit prior to falling into the loss region is essentially chaotic, the orbit will ergodically explore the region [0,1]. It is clear then, that for a loss region of width $\Delta x \ll 1$, initial conditions chosen from a uniform random distribution on [0, 1] will have an exponential distribution of transient lengths given by

$$h(\tau) = \frac{1}{\tau_0} e^{-\tau/\tau_0},$$

where τ_0 is the mean length of a transient. This exponential is simply the result of Poisson statistics, since the probability of falling into the loss region is constant in time. The probability per iteration that the trajectory will fall into the loss region is simply Δx,

hence, we expect that τ_0 will scale as $1/\Delta x$. It is simple to show that $\Delta x = (1-4/\lambda)^{1/2}$. Writing the parameter $\lambda = 4+\varepsilon$ as a perturbation near the point λ=4, we get

$$\tau_0 = 2\varepsilon^{-1/2}. \tag{2.7}$$

Clearly, this logistic map dynamics differs from the case of phase locking of oscillators, since in the latter case, the end of the transient corresponds to the arrival at a fixed point of the system. In the case of the logistic map, the end of the transient corresponds to a diverging of the state, x: $x \to -\infty$, as $t \to \infty$. In fact, it has been shown numerically [Grebogi & Ott, 1983] that the well known Hénon map also exhibits a boundary crisis in which one attractor loses its stability, allowing orbits to live for long times on the unstable attractor, before escaping suddenly to a different, stable attractor. As with the case of the boundary crises in the logistic map, there is an exponential distribution of transient lengths and the average transient length scales as in Eq. (2.7).

2.5 Limit-Cycle Oscillator Theory

The preceding discussion has been elementary and rather general in that it included a quick tour of some of the important ideas and terminology of nonlinear dynamics, as well as a discussion of the basics of low-dimensional oscillator systems. We will now focus on a specific oscillator model and eventually apply that model to the problem of oscillator populations, which is of central interest to our experimental work.

As mentioned earlier, one of the important simplifications employed in studying systems of limit-cycle oscillators is to assume that phase-space trajectories are strongly attracted toward the limit-cycle. This assumption permits us to consider only the motion of points *along* the limit-cycle. This approximation is important since the dynamics of each oscillator is reduced from an n-dimensional problem to a 1-dimensional problem. The motion of points along the limit-cycle can be described by a single variable, ϕ, the phase of the oscillator. If we consider a system of N independent limit-cycle oscillators, it is always possible to choose ϕ_i for each oscillator, such that the motion along the limit-cycle is of uniform velocity, $d\phi_i/dt = \omega_i$. Perturbing the system with interactions that are a function only of the phase differences yields

$$\frac{d\phi_i}{dt} = \omega_i + \sum_{j=1}^{N} \Gamma_{ij}(\phi_j - \phi_i), \quad i = 1,2,\ldots,N. \tag{2.8}$$

In fact, Eq. (2.8) can be derived [Kuramoto, 1984] perturbatively from the much more general system:

$$\frac{d\bar{X}_i}{dt} = \bar{F}(\bar{X}_i) + \sum_{j=1}^{N} \bar{G}(\bar{X}_i, \bar{X}_j), \quad i = 1,2,...,N. \tag{2.9}$$

The first term on the right hand side of Eq. (2.9) governs the unperturbed dynamics of each oscillator, while the summation represents a perturbative interaction.

Returning to Eq. (2.8), clearly we must require $\Gamma(\phi + 2\pi) = \Gamma(\phi)$. If we assume that each oscillator is coupled equally to all others then $\Gamma_{ij} = \Gamma$. If we further assume that $\Gamma(0) = 0$, then it is natural to choose $\Gamma(\phi) = \frac{-K}{N}\sin\phi$, since it is the leading term in the Fourier expansion of Γ. This yields a simplified model which is tractable and is frequently used in studies of oscillator populations:

$$\frac{d\phi_i}{dt} = \omega_i + \frac{K}{N}\sum_{j=1}^{N} \sin(\phi_j - \phi_i), \quad i = 1,2,...,N. \tag{2.10}$$

It will be shown below that this system can be written as a system of N independent equations coupled together via a mean-field. For now, suppose K>0. Suppose additionally that the jth oscillator has a phase slightly ahead (larger) of the ith oscillator. Then the effect on the ith oscillator due to the jth will be to increase i's rotation frequency, bringing it closer to j. Thus, the oscillators are attracted to each other. For K<0 the opposite is true: there is a pair-wise repulsion between two oscillators.

2.5.1 N=2 Limit-Cycle Oscillators

A system of only two such oscillators is particularly easy to analyze. The oscillators are described by the following pair of equations:

$$\begin{aligned} \frac{d\phi_1}{dt} &= \omega_1 + \frac{K}{2}\sin(\phi_2 - \phi_1), \\ \frac{d\phi_2}{dt} &= \omega_2 + \frac{K}{2}\sin(\phi_1 - \phi_2) \end{aligned} \tag{2.11}$$

Taking the difference between the two equations conveniently yields a single equation which governs the phase difference, $\psi \equiv \phi_1 - \phi_2$. Defining $\Delta\omega \equiv \omega_1 - \omega_2$, we get

$$\frac{d}{dt}\psi = \Delta\omega - K\sin(\psi) \tag{2.12}$$

Figure 2.9 shows $f(\psi) \equiv \Delta\omega - K\sin(\psi)$ plotted versus ψ. The system can only have a fixed-point if $|K| \geq |\Delta\omega|$, that is if the coupling is sufficient to overcome the tendency of the oscillators to drift apart due to the difference in their natural frequencies. If that condition is satisfied, then there will be two fixed points, at the zeroes of $f(\psi)$. The stable (S, solid circle) and unstable (U, open circle) fixed-points will satisfy $f'(\psi_s) < 0$, and $f'(\psi_u) > 0$, respectively. As we would expect, for K<0 the oscillators are repelled from each other causing the stable fixed point to occur near $\psi=\pi$. For K>0 the fixed point occurs near $\psi=0$. Also shown on the diagram are arrows on the abscissae indicating the direction of the flow.

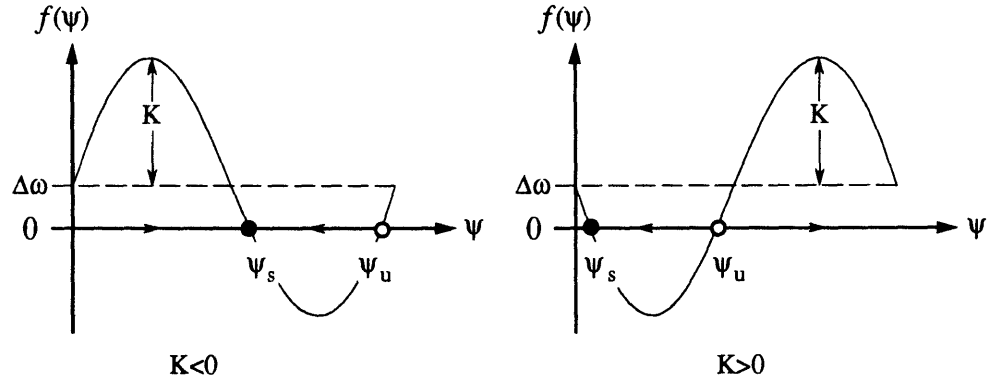

Figure 2.9. Dynamics of two limit cycle oscillators. The repulsive case (K<0) and attractive case (K>0) are shown. The rate of phase separation, f, is plotted versus the phase separation between the oscillators. The stable fixed point (solid dot) and unstable fixed point (open dot) is indicated for each case.

2.5.2 Limit-Cycle Oscillator Populations

We now return to the more interesting case of a large population of N oscillators with mean-field coupling, as modeled by Eq. (2.10). The goal is first to discover the fixed-points of this system, and then to understand its dynamics. The key point to recognize is that for large N, the problem is amenable to the well known tools of statistical mechanics. We expect that, at least for attractive (K>0) coupling, the system will exhibit a phase transition in which a substantial fraction of the population becomes synchronized. We wish to determine the critical coupling strength, K_c, necessary for this to occur.

The mathematical formulation of this problem in terms of the well known mean-field theory tools of statistical mechanics was developed by Kuramoto and Nishikawa [Kuramoto & Nishikawa, 1987]. Their approach, which we follow here, is first to describe the macroscopic state of the system with an *order parameter*, which is simply

the strength of the mean-field. A self-consistent equation for this order parameter may then be formulated; its solution subsequently determining K_c.

We begin by assuming that the natural frequencies of the oscillators are described by some distribution $g(\omega)$, which is symmetric about the mean frequency, ω_0. The next step in many problems of this sort is to transform the system into an appropriate rotating frame. This eliminates the motion of the mean and allows us to focus on the drift of the oscillators relative to the mean. Define the relative phase of an oscillator to be $\psi_i \equiv \phi_i - \omega_0 t$ and *redefine* ω so that it becomes the frequency of an oscillator *relative* to the mean, hence $\omega_i \leftarrow \omega_i - \omega_0$. We also redefine $g(\omega)$ so that it is now symmetric about zero. Substituting these definitions into Eq. (2.10) yields

$$\frac{d\psi_i}{dt} = \omega_i + \frac{K}{N}\sum_{j=1}^{N}\sin(\psi_j - \psi_i). \tag{2.13}$$

We now define a complex order parameter, Z, for this system:

$$Z(t) = |Z(t)|e^{i\Theta(t)} \equiv \frac{1}{N}\sum_{j=1}^{N} e^{i\psi_i(t)}. \tag{2.14}$$

Note that when all N phases are aligned $|Z| = 1$, and when the phases are distributed uniformly around 2π then $|Z| = 0$. An equivalent expression for $|Z|$ is

$$Z(t) = \int_{\psi=0}^{2\pi} n(\psi,t)e^{i\psi}d\psi \tag{2.15}$$

where $n(\psi, t)$ is the number density of oscillators with phases in $[\psi, \psi+d\psi]$ at time, t. Combining Eq. (2.13) and Eq. (2.14) yields a set of N differential equations for the phases, which are now coupled together only through their interaction with Z(t). Thus, we get

$$\frac{d\psi_i}{dt} = \omega_i - K|Z|\sin(\psi_i - \Theta). \tag{2.16}$$

We would like to consider states in which Z(t) is constant in time. Recall that since we are in a rotating frame, such states correspond to a system that exhibits a macroscopic rotation at uniform angular velocity, ω_0, in the 'laboratory' frame. For some fixed Z, Eq. (2.16) divides the population of oscillators into two distinct sub-populations. Those oscillators whose natural frequencies satisfy $|\omega_i| \le |KZ|$ will become synchronized with

each other and with the collective oscillation embodied by Z. We refer to this sub-population, which synchronizes, as the S group. The remaining oscillators satisfy $|\omega_i| > |KZ|$, thus they remain unsynchronized and we refer to them as the U group (The subscripts s and u now refer to the synchronized group and the unsynchronized group, rather than stable and unstable, as they did before). Figure 2.10 shows the distribution of natural frequencies, g(ω). The central part of the population in the range [-|KZ|, |KZ|] forms the S group (shaded), while the oscillators outside that region form the U group (unshaded).

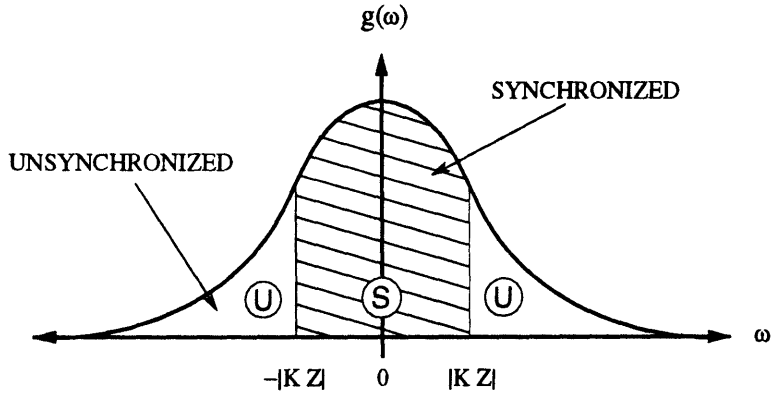

Figure 2.10. Distribution of oscillator natural frequencies. The shaded region indicates the range of oscillator frequencies that spontaneously become synchronized (S). The tails of the distribution (U) remain unsynchronized.

It is convenient at this point to divide the number density, n, the order parameter, Z, and the number of oscillators, N, into their components corresponding to the S group and the U group as follows:

$$n = n_s + n_u,$$

$$Z = Z_s + Z_u,$$

$$N = N_s + N_u.$$

S group. Let us first consider the S group. These oscillators satisfy $|\omega_i| \le |KZ|$, hence there will two fixed points; one stable and one unstable. For a given Z, each oscillator will sit stationary at its stable fixed point. Its phase at that fixed point will be given by the fixed point equation

$$\psi_{i0}(Z) = \Theta + \sin^{-1}(\omega_i / K|Z|) \tag{2.17}$$

These equations imply a one-to-one correspondence between natural frequency ω, and fixed point phase ψ. Hence, the distribution of S group phases is easily determined from the identity

$$n_{s0}(\psi)d\psi = g(\omega)d\omega$$

and the inverse of the fixed point equation

$$\omega = K|Z|\sin(\psi - \Theta). \tag{2.18}$$

Thus the distribution of S group phases is given by

$$n_{s0}(\psi;Z) = g\left[K|Z|\sin(\psi-\Theta)\right]\cdot K|Z|\cos(\psi-\Theta)\,. \tag{2.19}$$

U Group. The oscillators in the U Group are not phase-locked and never come to rest. We wish to discover what contribution do they make toward Z. Their instantaneous angular velocity varies sinusoidally over the course of one cycle and is easily shown to be

$$\frac{d\psi_i}{dt} = v_i(\psi_i) = \omega_i - K|Z|\sin(\psi_i - \Theta)$$

The coupling does have an effect on the (one-cycle) average angular frequency of the U Group oscillators. It is given by

$$\tilde{\omega}_i = \frac{2\pi}{\int_0^{2\pi/\omega_i} dt} = \frac{2\pi}{\int_0^{2\pi} d\psi / v_i(\psi)} = \left[\omega_i^2 - |KZ|^2\right]^{1/2}$$

Assuming that these coupling-modified frequencies are rationally independent, the oscillators will move ergodically over the N_U dimensional torus that forms their phase-space. Thus the probability density of finding a particular oscillator with a given natural frequency at some phase ψ, is given by

$$\rho(\psi) = \frac{\tilde{\omega}(\omega)}{2\pi|v(\psi)|}$$

Thus, the distribution of phases of the U Group oscillators is given by

$$n_u(\psi) = 2\int_{K|Z|}^{\infty} d\omega\ g(\omega)\rho(\psi) = 2\int_{K|Z|}^{\infty} d\omega\ g(\omega)\frac{\tilde{\omega}(\omega)}{2\pi|v(\psi)|}$$

$$n_u(\psi) = \frac{1}{\pi}\int_{K|Z|}^{\infty} d\omega\ g(\omega)\frac{\omega\left[\omega^2 - |KZ|\right]^{1/2}}{\omega^2 - \left|KZ\sin(\psi-\Theta)\right|^2}$$

where we have made use of symmetry of g(ω)=g(-ω). It is now possible to write down a self consistent equation for Z as follows:

$$Z = S(Z) = \int_0^{2\pi} n(\psi)e^{i\psi}d\psi = \int_0^{2\pi}\left[n_s(\psi)e^{i\psi} + n_u(\psi)e^{i\psi}\right]d\psi$$

Note that n_u contributes nothing to Z since $n_u(\psi)=n_u(\psi+\pi)$. Inserting the expression for n_s Eq. (2.19). and making the change of variables y=sin(ψ) yields

$$S(Z) = 2\int_0^1 dyKZg(K|Z|y)\left(1-y^2\right)^{1/2}$$

This integral is an odd function of Z. Expanding it to third order in Z produces

$$S(Z) = (1+\varepsilon)Z - \beta|Z|^2 Z + O\left(|Z|^5\right) \tag{2.20}$$

where $\varepsilon \equiv \left(K - K_c\right)/K_c$ is a dimensionless expression of the coupling strength in units of the critical coupling strength $K_c \equiv 2/\pi g(0)$ and the coefficient for the third order term is given by $\beta \equiv -\frac{1}{16}\pi K_c^{\ 3} g''(0)$. Normally we expect the natural frequencies are described by a unimodal distribution which implies $g''(0) < 0$ and therefore β>0. Figure 2.11 shows the graphical solution to the self-consistent equation Z=S(Z) for this normal case. For $K<K_c$, there is a single solution with Z=0 which corresponds to the incoherent state of the system. At $K=K_c$ the system experiences a bifurcation and as K is increased beyond K_c, a second solution to the self-consistent equation appears at

$$Z^* = \left(\frac{\varepsilon}{\beta}\right)^{\frac{1}{2}} e^{i\Theta}.$$

Since Θ is an arbitrary constant (introduced as a result of the arbitrary choice of initial phase of the rotating frame) we may choose it to be zero yielding

$$Z^* = (\varepsilon/\beta)^{1/2}. \tag{2.21}$$

Figure 2.11 also shows the corresponding solutions to Z=S(Z) for the unusual case of $\beta<0$. Note that in determining these solutions it has been assumed that the system was already in a steady-state. The preceding fixed-point analysis contains no dynamical information, consequently the stability of the solutions is indeterminate.

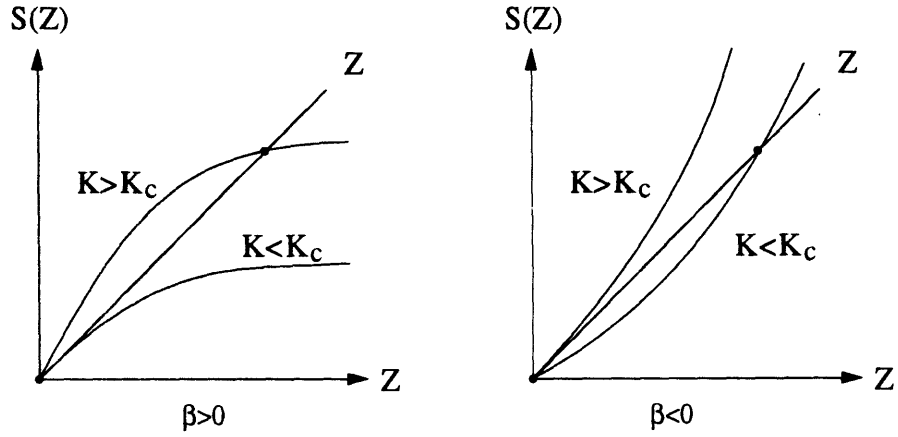

Figure 2.11. Graphical solution of the self-consistent equation S(Z) = Z. Solutions are shown as dots. The normal (g"(0)<0, $\beta>0$) case and the case of a concave upward distribution (g"(0)>0, $\beta<0$) are shown. For each, examples of coupling, K, above and below the critical coupling, K_c, are shown, illustrating the bifurcation.

2.5.3 Dynamics of Limit Cycle Oscillator Population

In order to determine the stability of the fixed-points it is necessary to develop a dynamical form of the self-consistent equation. Rather than reproduce the extensive mathematics of Kuramoto and Nishikawa [Kuramoto & Nishikawa, 1987] we simply present their equation for the dynamics of Z:

$$\xi \frac{dZ}{dt}|KZ|^{-1} \approx \varepsilon Z - \beta|Z|^2 Z$$

where ξ is a constant of order unity. As before, the complex phase factor in Z is arbitrary and can be eliminated from both sides of the equation. Furthermore, we restrict ourselves to the normal case of $\beta>0$. For weak coupling ($\varepsilon<0$), the incoherent state with Z=0 is governed by the dynamics

$$\frac{dZ}{dt} \approx -|\varepsilon|\xi^{-1}KZ^2 .$$

Thus, this state is stable, with Z>0 decaying to zero in time according to

$$Z(t) \approx \frac{1}{|\varepsilon| t}.$$

For strong coupling ($\varepsilon>0$) the Z=0 state becomes unstable and dynamics of Z near the coherent state, Z^*, are governed by

$$\frac{d\eta}{dt} = -\varepsilon^{3/2}\gamma_0\eta, \tag{2.22}$$

where

$$\gamma_0 \equiv \frac{2K_c}{\xi\beta^{1/2}}$$

and $\eta(t) = Z(t) - Z^*$ is the deviation from the fixed-point. Thus the coherent state has become stable, with perturbations about this state decaying exponentially toward zero according to

$$\eta(t) \propto \exp\left(-\gamma_0\varepsilon^{3/2}t\right). \tag{2.23}$$

The dynamics described by Eq. (2.22) are the simple dynamics found near an attracting hyperbolic fixed point. It is to be expected then from our earlier discussion of transient lengths that for a large system of oscillators with excitatory coupling, the distribution of locking times will be finite and relatively short.

2.5.4 Repulsive (Inhibitory) Coupling

The case of repulsive or inhibitory coupling, in which the interactions between oscillators are such that their phases tend to become anti-parallel, has been studied very little indeed. The preceding theory assumed that K>0 (attractive). The results above can be extended to the case K<0. The only change is in Eq. (2.17), in which the phase of a synchronized oscillator is shifted by π. Hence, the new phase for the repulsive coupling case is given by

$$\tilde{\psi}_{i0}(Z) = \psi_{i0}(Z) + \pi = \Theta + \pi + \sin^{-1}\left(\omega_i / K|Z|\right),$$

where K is implicitly negative (that is we redefine K such that $K = |K|$). Pursuing the mathematics as before we find that the only effect of this change is to invert the sign of S(Z), thus the new S(Z) for the repulsive coupling case is given by $\tilde{S}(Z) = -S(Z)$. Clearly, Fig. 2.11 indicates that since the function S(Z) is inverted, there is still the

expected incoherent state at Z=0. On the other hand, S(Z) must increase monotonically with Z, therefore $\tilde{S}(Z) = -S(Z)$ must decrease monotonically with Z. Thus we may conclude that there are no other solutions to the self-consistent equation.

One way of viewing the problem of repulsive coupling is to consider the simpler problem in which all the natural frequencies are identical. In the rotating frame, then, all of the natural frequencies will be zero. Eq. (2.16) yields a fixed point equation

$$0 = K|Z|\sin(\psi_i - \Theta)$$

There are only two solutions to this equation. The first is the coherent solution with all phases aligned with each other and thus with Z. All of the sine factors are zero and the equation is satisfied. The other solution is one where $|Z| = 0$. To accomplish that, we require that the sum in Eq. (2.14) be zero. Figure 2.12 shows a typical set of N=7 phases in the complex plane which graphically satisfy this requirement. Clearly this arrangement, for all N>3, can be smoothly deformed (other than a trivial rotation) into another configuration which also satisfies the fixed point equation. That there are an infinite number of states which satisfy the fixed point equation suggest that none are preferred and none are stable.

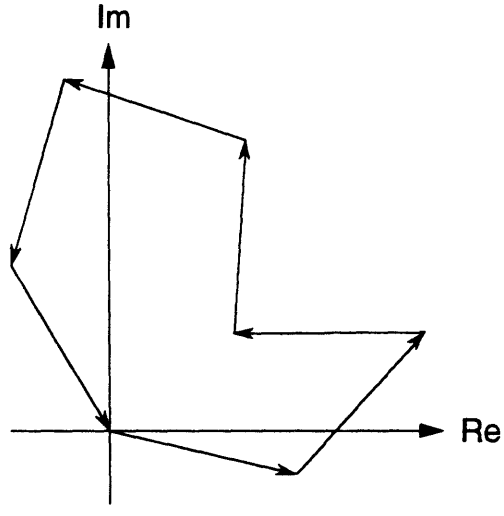

Figure 2.12. Imaginary plane showing N=7 oscillators.

In summary, the foregoing theory of limit-cycle oscillator population makes several predictions:

- For N→∞ and excitatory coupling, synchronization should occur after a short, finite transient.

- For $N \to \infty$ and inhibitory coupling, synchronization cannot occur.
- For $N>3$, identical oscillator frequencies and inhibitory coupling, synchronization cannot occur.

None of these predictions can be tested directly, since it is neither possible to achieve $N \to \infty$, nor is it possible to create a real experimental system with identical frequencies. Rather, these theoretical results will serve as a guide and as points of comparison with the experimental results. Having touched upon many of the important ideas of nonlinear dynamics and having focused on the basic theory of collective synchronization in oscillator populations we are now prepared to proceed with the details of the experimental work.

3. EXPERIMENT

3.1 Overview

This chapter describes the details of the coupled oscillator system used in this experiment. The layout of this chapter is as follows. First the electronic hardware will be described. This will include a discussion of the basic oscillator unit, followed by a description of the manner in which these oscillators are coupled together. Additionally, the data acquisition and control system hardware will be described, along with some considerations of calibration and systematic error. Finally, we will discuss the software system for acquiring and analyzing data. This will include the method of oscillator initialization, followed by the determination of various experimental variables (and their errors) such as trajectories, locking times, fixed-point phases and fixed-point frequencies.

3.2 Hardware

3.2.1 Unit Relaxation Oscillator

As with any experimental apparatus, an idealized mathematical model must eventually be implemented in real and inevitably less than ideal hardware. In the experiments we have performed, the oscillators are electronic, and are constructed using a single operational amplifier (op-amp) as the central element of each oscillator. Electrical engineers and experimental physicists are generally quite familiar with op-amps since they serve as building blocks in a wide variety of circuits. For the less experimentally minded, it is worth describing the operation of this common and useful electronic component. Figure 3.1 shows the schematic symbol for an individual op-amp.

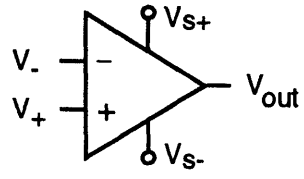

Figure 3.1 Schematic symbol of an op-amp showing two power supply terminals, inverting (-) and non-inverting (+) input terminals and output terminal.

There are five important connections to the op-amp. The terminals labeled V_{s+} and V_{s-} supply power to the op-amp and are typically $V_{s+} = +15v.$ and $V_{s-} = -15v.$ Since these terminals only supply power they are often not shown and are implicitly assumed to be present. The ideal op-amp is little more than differential amplifier, with an infinite

gain. The voltage appearing at the output, V_{out}, is some multiple of the difference between the voltage placed on the non-inverting input, V_+, and that on the inverting input, V_-. That is $V_{out} = G(V_+ - V_-)$, where the gain, G, in an ideal op-amp is infinite. In a real op-amp, G is typically some very large number. For example, the op-amps used in these experiments are the LF357 type made by National Semiconductor and they have a gain, $G \sim 10^5$. In addition, the ideal op-amp has an infinite input impedance (no current may flow into the inputs) and zero output impedance (the output will produce whatever current is necessary to maintain the correct output voltage).

Of course, all real electrical components, including the op-amp, behave in a less than ideal manner. One of these non-ideal effects, *saturation*, is a simple non-linearity found in many physical systems including every amplifier, since no real amplifier can amplify an arbitrarily large input. It is the one non-ideal effect which plays an important role in the operation of the oscillator circuit. In an op-amp, the saturation effect is caused by the fact that voltage output of the op-amp is constrained to lie somewhere between the two power supply voltages. Often however, op-amps saturate at a voltage slightly less than the positive power supply voltage and slightly more than the negative power supply voltage, however we will ignore this effect for now and assume that saturation occurs at the power supply voltages. The huge gain of the op-amp means that saturation will occur as soon as either input exceeds the other by more than a tiny fraction of a millivolt. The input-output characteristic of an op-amp with saturation and a large but finite gain is shown in Fig. 3.2.

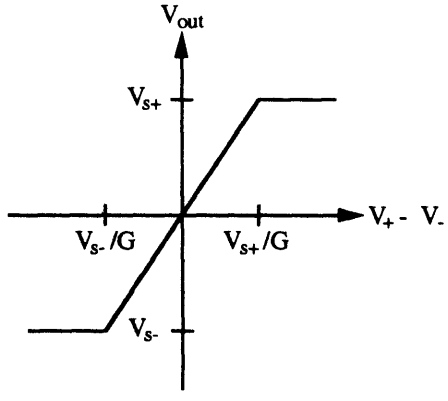

Figure 3.2 Input-output characteristic of an op-amp with gain, G, and saturation voltages Vs+ and Vs-.

When used as an amplifier, an op-amp is connected with some negative feedback, which reduces the gain and widens the central linear region to include the voltages one wishes to amplify. In our oscillator circuits however, the negative feedback is incidental

since there is also enough *positive* feedback to cause instability. Thus, the op-amp behaves essentially as a comparator: its output saturates at V_{s+} for $V_+ > V_-$ and the output saturates at V_{s-} for $V_+ < V_-$.

In addition to the narrow band of voltages over which the op-amp behaves as a linear amplifier rather than a comparator, the op-amp also suffers from other imperfections. The inputs do in fact have a finite resistance and therefore do draw a tiny current. In our apparatus this amounts to a few tens of picoamps. Furthermore the output is capable of sourcing or sinking only a finite amount of current, typically a few tens of milliamps. These effects will be treated essentially as negligible corrections to the ideal op-amp behavior.

The LF357 used in our experiments was chosen specifically for its high speed. Often an op-amp includes internal compensation capacitors so that when configured as an amplifier, it will be stable. Since our circuit is intended to oscillate, stability is of no concern (indeed, the circuit must be unstable to oscillate). The LF357 is a member of a well known family of op-amps which, as a result of its lack of compensation, sacrifices stability in favor of higher speeds. The slew rate, a measure of the switching speed of an op-amp, is the finite rate of change of the output, when a large (saturating) voltage is placed across the inputs. For the LF357, the slew rate is about 50 V/μs, which implies a lower limit of about 0.6μs for the time required to make the 30 volt transition from negative to positive saturation. This time scale is very short, although not necessarily negligible, compared to the roughly 200 ms typical period of oscillation of our oscillators.

Since we use of an op-amp in an unstable configuration that oscillates between positive and negative saturation (as we shall see below), we are lead to consider two other non-ideal effects which normally would be irrelevant for an amplifier in the linear region. As mentioned above, some op-amps, including the LF357, do not saturate cleanly at the power supply voltages. This is due to the use of bipolar transistors in the output stage of the op-amp. This essentially DC effect would not be a problem except that the positive and negative saturation voltages can differ slightly from each other, resulting in slight asymmetries in the oscillator waveform. Additionally, saturation voltages can differ from op-amp to op-amp producing small amplitude variations from oscillator to oscillator. The corresponding AC effect is that after an op-amp has been driven into saturation it requires a finite time to settle at its saturation voltage. During this *settling time*, the output may overshoot the saturation voltage and exhibit *ringing*: small, damped oscillations about the saturation voltage.

Having reviewed the essential properties of op-amps we now turn to a discussion of the oscillator itself. The basic oscillator unit used in this experiment is shown in Fig. 3.3. It is a simple electronic relaxation oscillator familiar to many electrical engineers [Horowitz & Hill, 1989] and is the same basic circuit that has been effectively used in other non-linear dynamics experiments [Linsay & Cumming, 1989]. It is composed of a single op-amp with sufficient positive feedback to produce oscillation.

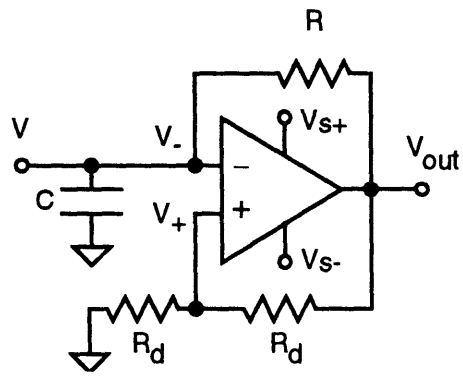

Figure 3.3 Relaxation oscillator circuit schematic. The capacitor, C, charged via resistor, R, has a voltage, V, applied to the inverting (-) input of the op-amp. The output, V_{out}, is a square-wave which also appears, attenuated by a factor of two at the non-inverting input (+).

To understand how the oscillator oscillates, recall that the op-amp is nearly always operating in saturation, thus $V_{out} = V_{s+}$ for $V_+ > V_-$ and $V_{out} = V_{s-}$ for $V_+ < V_-$. The voltage divider formed by the two resistors, R_d (which need not in general be equal) presents the non-inverting (+) input with a threshold voltage $V_T = V_{out}/2$. When V_{out} saturates at the positive supply voltage, the capacitor C, is charged through a resistance R by a constant voltage source of voltage V_{s+}. The voltage on the capacitor, $V = V_-$, increases until the upper threshold voltage is reached: $V = V_{T+} = V_{s+}/2$. At this point V_- will just exceed V_+ causing V_{out} to switch sign and saturate at the negative supply voltage. The capacitor is then discharged by a constant voltage source of voltage V_{s-} in a similar fashion. When the negative threshold is reached, $V = V_{T-} = V_{s-}/2$, the output switches to the positive supply voltage again and the cycle repeats. Figure 3.4 shows, on identical time scales, the idealized waveforms $V_{out}(t)$ and the capacitor voltage, $V(t) = V_-(t)$. Clearly, between switches of the oscillator, V(t) decays toward the corresponding supply voltage with a simple exponential form. The period of oscillation, T, is thus determined by the RC time constant as well as the threshold voltages. For a relaxation oscillator with $V_T = V_s/2$, it is easy to show that $T = 2RC \ln 3 \approx 2.2\ RC$.

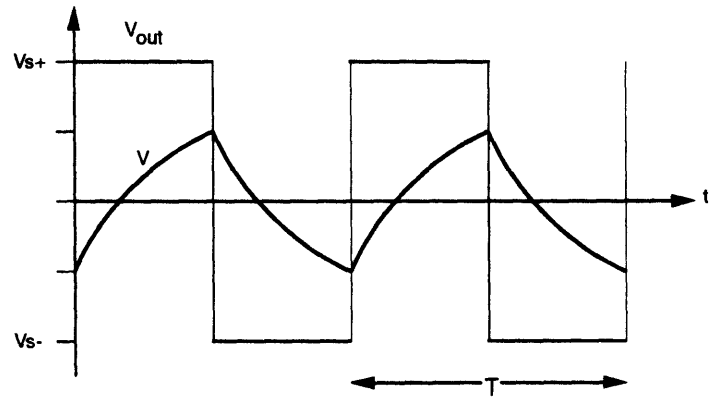

Figure 3.4 Waveforms of a single relaxation oscillator. The capacitor voltage, V(t) and output voltage, $V_{out}(t)$, are shown on the same time scale

The capacitor voltage between switches of the op-amp can be written simply as

$$V^{\pm}(t) = \pm V_s\left[1 - \tfrac{3}{2}e^{-t/\tau}\right], \quad t = [0, T/2] \tag{3.1}$$

where $V_s \equiv V_{s+} = |V_{s-}|$. V^+ describes the charging phase, and V^- describes the discharging phase of oscillation, and t is the time since the last switch of the op-amp. The derivative of V(t) between switches is thus given by

$$\dot{V}^{\pm}(t) = \left(-V^{\pm} \pm V_s\right)/\tau \tag{3.2}$$

Using this latter expression it is simple to construct a phase portrait of the individual ideal relaxation oscillator. The limit-cycle of the oscillator is shown in Fig. 3.5. It is nearly impossible to perturb the system away from the limit-cycle shown. In that sense, the strength of attraction to the limit-cycle is infinite. That the system exists on an essentially one-dimensional curve is not surprising since the oscillator contains only one capacitor. Other than the single bit of state information stored by the op-amp itself, the one capacitor contains all information needed to describe the system. The system traverses the solid curve in the direction shown by the arrows, moving relatively slowly over the sloped segments of the limit-cycle and traversing the vertical, V=const. segments instantaneously. The dashed segments of the curve indicate the only permitted perturbation away from the limit-cycle of the ideal relaxation oscillator. Points on these branches correspond to transient states in which the capacitor is charged to a voltage above the upper threshold ($V > V_{T+}$) or below the lower threshold ($V < V_{T-}$). Clearly, in initializing a relaxation oscillator to known state, it is not sufficient to simply charge the capacitor to a known voltage. For any given voltage in the normal range of oscillation, there are two possible states that the system may take: charging or discharging. In

initializing the oscillators in our experiments we make use of the transient branches of the phase-portrait. By setting $V > V_{T+}$ the system is forced onto the lower (discharging) branch of the limit-cycle. Similarly, by setting $V < V_{T-}$ the system can be forced onto the upper (charging) branch of the limit-cycle. A subsequent setting of the desired initial capacitor voltage between the two thresholds uniquely determines the state of the system.

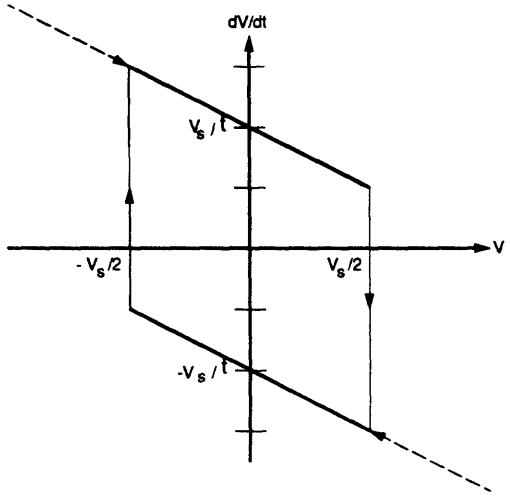

Figure 3.5 Phase space trajectory of an ideal relaxation oscillator. Solid line indicates limit cycle associated with normal oscillation. Vertical segments at threshold voltages correspond to sudden switches in direction. Setting the capacitor voltage outside the thresholds produces initial conditions lying on the dashed segments.

The actual electronic implementation of this experiment used *oscillator elements,* shown in Fig. 3.6. These building blocks are a slightly more complicated version of the preceding circuit. First, each oscillator element includes an LM311 comparator on the output of op-amp oscillator. This comparator serves a dual purpose. It electronically isolates and buffers the oscillator from noise that might introduced by the data acquisition system. It also converts the op-amp output voltage, which swings between the analog power supply voltages into suitable digital logic levels (of GND=0v and V_{CC} = 5v). We call the digital logic signal output of the comparator, S. When the oscillator capacitor is charging, S=1, when it is discharging, S=0.

Each oscillator element also includes two solid-state FET (field effect transistor) switches under digital control. The two switches come in a single DG300ACJ integrated circuit made by Intersil. When open, the 'RUN' switch breaks the oscillator's negative feedback path and isolates the capacitor from the rest of the oscillator circuit. Since the capacitor is still connected to the (very high impedance) inverting (-) input of the op-amp, the 'RUN' switch does not disturb the state of the system. When opened, it merely freezes

the system in its current state. When the switch is closed, the system will begin oscillating from wherever it was left.

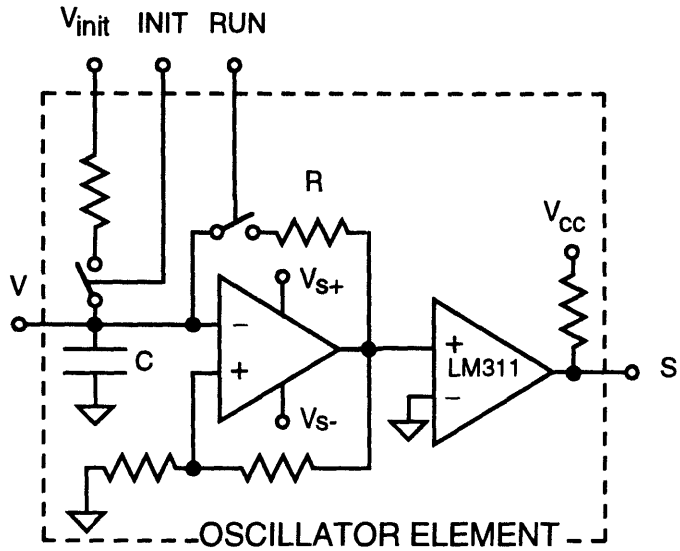

Figure 3.6 An oscillator element consisting of a relaxation oscillator followed by an LM311 comparator which buffers and conditions the oscillator output. Also shown are the FET electronic switches. The switch controlled by the RUN signal starts and stops the oscillator and the switch controlled by the INIT signal charges the capacitor to the voltage applied to the V_{INIT} input. The signal S is the digital output and V is the node which provides a connection to the coupling network.

The other switch is the 'INIT' switch. If the 'RUN' switch is open, the 'INIT' switch may be closed so as to allow the capacitor to be charged to any desired voltage applied at the input V_{INIT}. Thus the oscillator may be initialized in the following way. First, 'RUN' is opened and 'INIT' is closed. The oscillator is then forced on to the desired branch of its hysteresis curve by setting V_{INIT} to charge the capacitor to a voltage outside the range of threshold voltages. Next, V_{INIT} is set so as to charge C to its desired initial voltage and finally, 'INIT' is opened. When 'RUN' is closed, the oscillator will begin its trajectory from the initial condition to which it has been set.

The signal V, on the oscillator element allows the oscillator to be coupled to other oscillators through a coupling network which will be discussed below. Two digital inputs, RUN and INIT control their respective switches, and a single digital output, S, describes the state of the oscillator. It should be noted that this one bit of information is insufficient to completely describe the state of the oscillator. It merely tells us whether the capacitor is charging or discharging. At the time of a $0 \rightarrow 1$ transition in S (that is when an oscillator begins the charging part of its cycle) the phase is determined *by definition* to be zero. Between switches of the oscillator we have no way of measuring

the phase of an oscillator. For a system of weakly interacting oscillators such as ours, however, it is reasonable to assume that perturbations in phase are small. Thus, the phase of an oscillator during a cycle is approximated by interpolation. Its phase at any time is approximately the time since the last switch as a fraction of the oscillator's local period.

Each oscillator element was made on a separate miniature printed circuit board which was plugged into a larger 'motherboard'. The purpose of this approach was to separate the specific oscillators from the data acquisition system. In this way oscillators could easily be removed, interchanged, modified, and replaced as necessary. Should we wish to use a different type of oscillator for example, a new oscillator element could simply be plugged in. The connector between the motherboard and each oscillator element supplied power, switch control signals INIT and RUN, and initialization voltage V_{INIT}. In addition, the output signal S and the capacitor voltage V are connected through the connector to the motherboard.

There is another element of the construction of the oscillator, shown in Fig. 3.3, that is worth noting. The charging resistor, R, was actually a variable 5 kΩ resistor built from a trimmer potentiometer. This allowed the natural frequency of each of the oscillators to be adjusted by hand. The two resistors, R_d, which comprise and the voltage divider in the positive feedback path were also actually implemented using a single 5 kΩ trimmer potentiometer. The potentiometer was connected between ground and the output of the op-amp. The center tap of the potentiometer was connected to the non-inverting (+) input of the op-amp allowing the threshold voltage to be set by this variable voltage divider. Thus, it was also possible to vary the amplitude of oscillation manually.

Figure 3.7 shows a typical time series and phase space trajectory for a single relaxation oscillator. As can be seen from the straight lines in the phase space motion, the behavior of an individual oscillator is very close to that of an idealized op-amp relaxation oscillator.

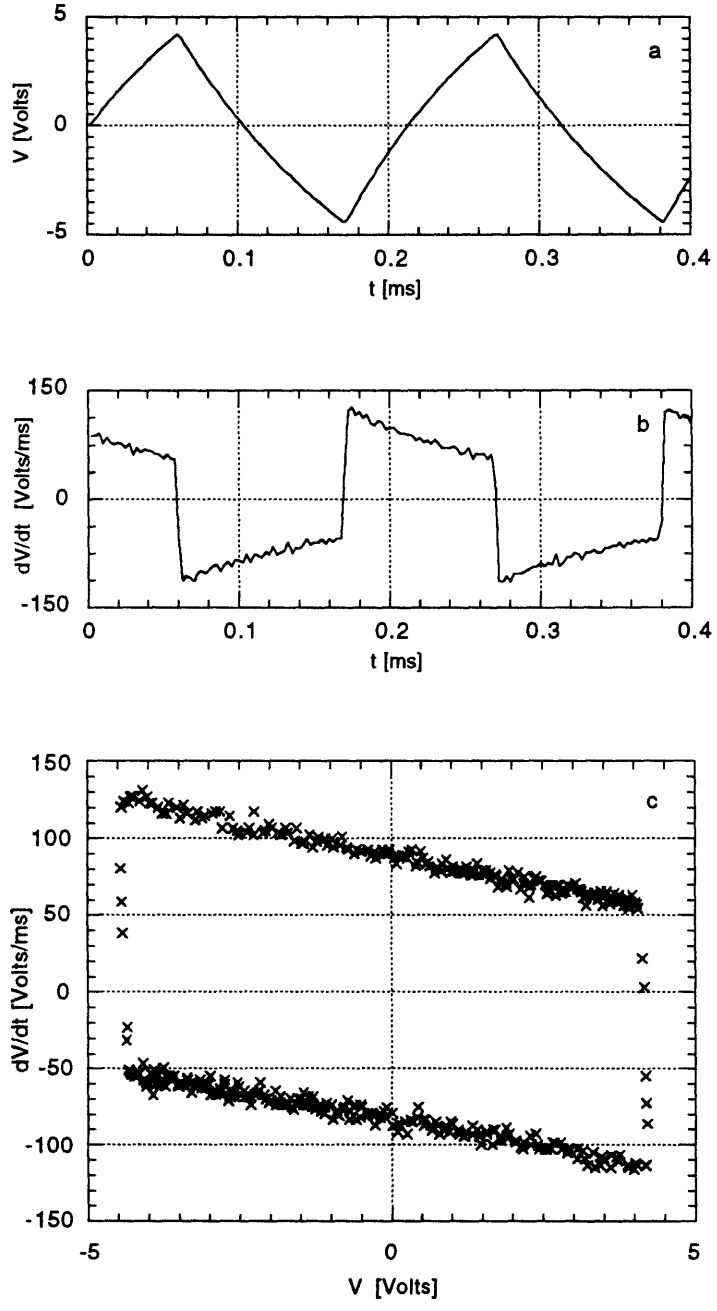

Figure 3.7 Figure a shows the capacitor voltage, V(t), for a single oscillator, measured with a 12 bit resolution A/D converter at a rate of 2 MHz. Figure b shows dV(t)/dt computed numerically from V(t). Figure c shows the phase portrait of the oscillator, dV(t)/dt versus V(t). The 'noise' on dV/dt is the result of the numerical differentiation. The differencing operation effectively amplifies the small digitization errors associated with V(t).

3.2.2 Coupling of the Oscillators

The oscillators in this experiment interacted with each other via a mean field coupling. That is, each oscillator was perturbed by essentially the same signal derived from a sum over all of the oscillators. Figure 3.8 shows a schematic representation of the way the oscillator elements were coupled together. The input, V, of each oscillator element was connected through a coupling capacitor, C_c, to a single common node. The voltage at this node, V_c, is the variable that plays the role of the mean field in this system. This common node is then connected through a variable resistor, R_c, to ground. This resistor controls the strength of mean field coupling. When R_c is zero, the coupling signal, $V_c(t)$, is also zero, hence there is no coupling between oscillators. As R_c increases, the amplitude of $V_c(t)$ increases, hence, the oscillators become more strongly coupled together.

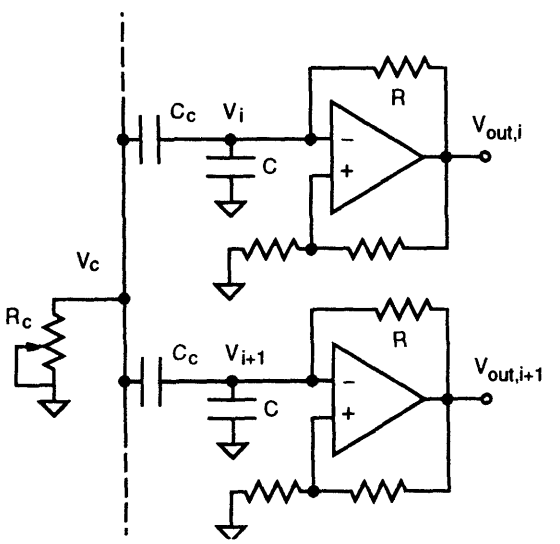

Figure 3.8 Schematic of the mean field coupling showing oscillators i and i+1.

The equation governing the voltage, V_i, on the ith oscillator is easily determined to be

$$\frac{dV_i}{dt} = -\frac{1}{RC_T}V_i + \frac{1}{RC_T}V_{OUT,i} + \frac{C_C}{C_T}\frac{dV_c}{dt}, \tag{3.3}$$

where $C_T \equiv C + C_C$. The first term on the right-hand side describes the well known dynamics of a simple RC circuit. The second term is the driving term. The third term is the coupling term. The equation describing the coupling voltage, V_c, is found by summing the currents flowing through the C_c and into the R_c.

$$\frac{dV_c}{dt} = -\frac{1}{N\tau_c}V_c + \frac{1}{N}\sum_{j=1}^{N}\left(\frac{dV_j}{dt}\right) \tag{3.4}$$

where $\tau_C \equiv R_C C_C$.

Since the output voltage takes on only two possible values we may write V_{OUT} in terms of the constant supply voltage $V_{OUT,i}(t) = \sigma_i(t)V_s$, where $\sigma_i(t) = \{+1, -1\}$. The threshold voltage, which is some fraction, k, of V_{OUT}, is then given by $V_{T,i}(t) = k\sigma_i(t)V_s$. The equations above describe only the dynamics of the oscillator system between switches, during which period V_{OUT} is constant. To complete the picture they must be supplemented by the rule governing the switch that occurs when an oscillator reaches threshold. Hence,

$$\text{If} \quad \sigma_i(t)V_i(t) \geq kV_S, \quad \text{Then} \quad \sigma_i(t^+) = -\sigma_i(t) \tag{3.5}$$

The purpose of the coupling capacitors is to prevent any DC flow of current from the oscillator's internal capacitors, C. Without them, the charge on the internal capacitors would tend to simply drain off. It was noted after the experiments had been performed that the capacitor, C, could be eliminated from the oscillator circuit entirely. This causes a substantial simplification in the governing equations. It is important to note that the coupling capacitors effectively differentiate the signal V(t) produced by each oscillator. Consequently, the contribution to the signal, V_c, due to a single oscillator is approximately a square wave, since the signal at V(t) is approximately triangular.

Figure 3.9 shows the effect of the coupling network on the waveform of a single oscillator. Figure 3.9 shows V(t) and $V_c(t)$ for the single oscillator. Note the distortion in the V(t) waveform relative to the unperturbed waveform of Fig. 3.7a. This is a 'self-coupling' effect: the oscillator contributes a roughly square-wave coupling signal to the mean-field, $V_c(t)$, shown in Fig. 3.9b. This mean-field signal is then (approximately) superposed on V(t) itself.

In our implementation of this circuit, the important circuit elements had the following values: R = 1 kΩ, C = 0.01μF, C_c = 0.1μF, and R_c was typically varied up to roughly 1000 Ohms. Figure 3.10 is a calibration curve showing the nearly linear variation of the amplitude of $V_c(t)$ with the coupling resistance, for values of $R_c < 300\ \Omega$.

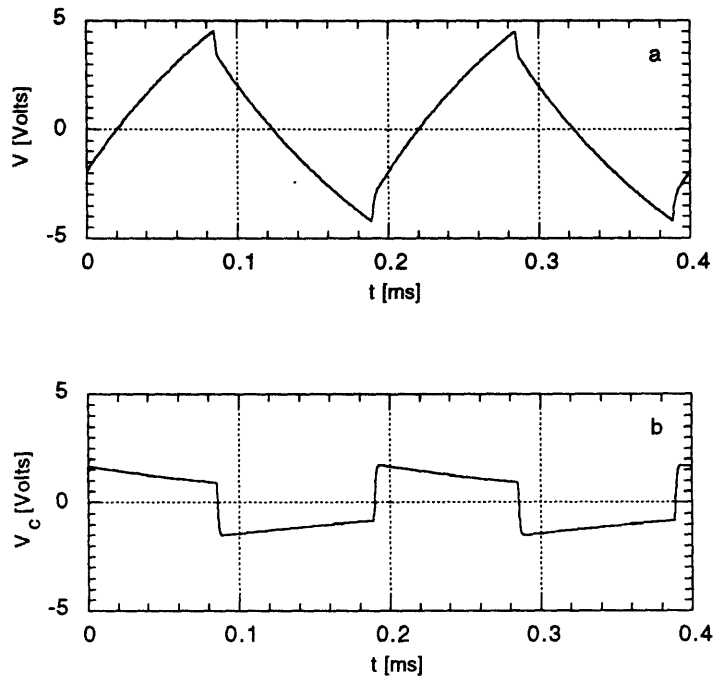

Figure 3.9. Waveforms of a single oscillator coupled to the coupling network with Rc=68 Ohms. Figure a shows the oscillator voltage, V(t). Figure b shows the coupling voltage, $V_c(t)$.

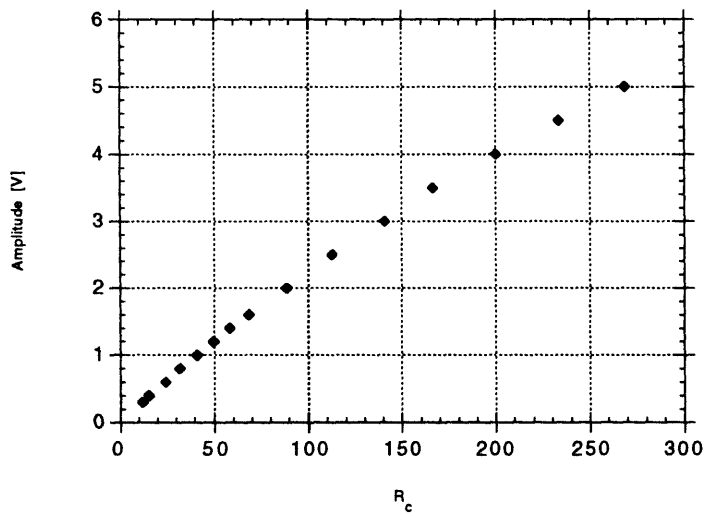

Figure 3.10 Coupling signal calibration curve. Amplitude of coupling signal, V_C, is plotted versus the coupling resistance, R_C.

Like the oscillator elements, the details of coupling were segregated to a separate printed circuit board. The capacitor voltage V_i of each oscillator is passed through to the

motherboard and then to a ribbon cable that could be plugged into a coupling board. The separate coupling board provides prototyping space and flexibility to allow experimentation with different coupling topologies and different circuits. The separate coupling board approach makes it possible, for example, to change coupling schemes merely by plugging in a different circuit board.

3.2.3 Data Acquisition and Control system

We now turn toward a discussion of the data acquisition and control system for this experiment. In addition to the coupling which was discussed above, Figure 3.11 also shows a schematic of the digital electronics used in the experiment. The most important part is the Macintosh IIx computer which was used to control the entire system and to store and analyze the data. The computer contained two specialized cards which plug in to the Macintosh NuBus bus. The first was a National Instruments NB-DIO-32F card for doing 32-bit digital input and output. The NB-DIO-32F contains four 8-bit ports, each of which was separately programmable for reading or writing out digital data. The board also contains a set of programmable clocks which coordinate the reading and writing of information by the ports. By deriving timing signals from the clock, the state of the system can be measured at evenly spaced and precisely defined intervals. Without such a clock, rate of measurements would depend critically on the rate of software execution and any branching in the software could easily produce a time series with a non uniform sampling rate. To obtain a master clock frequency, the 10 MHz NuBus clock is in effect divided down to 2.5Mhz. The clock signal used for sampling data from the oscillator system (the sampling clock) is then produced by dividing the 2.5MHz master clock frequency by a software programmable number. It was found by testing the system with a signal generator that data cannot be sampled at a rate higher than approximately 400 kHz.

The other NuBus card was an NB-DMA-8-G card also made by National Instruments. This card performs direct memory access (DMA) in conjunction with the NB-DIO-32F. Its purpose is to allow the DIO card to quickly move data in and out of the computer's memory, bypassing the Macintosh processor. Since it works almost transparently, and since it is not connected directly to the experiment, we need not discuss it further.

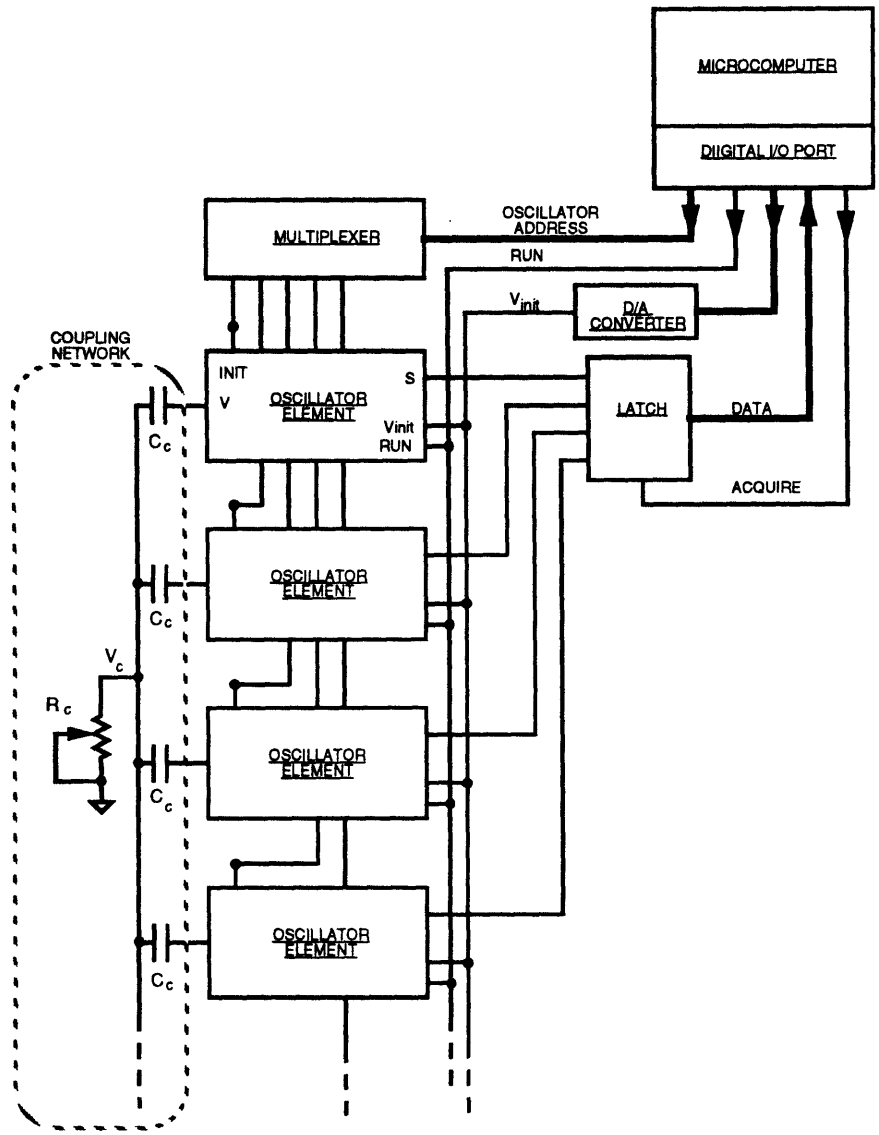

Figure 3.11 Schematic diagram of oscillator elements (four are shown) connected to the coupling network and to the data acquisition system. The coupling network (broken line) consists of a set of coupling capacitors, C_C, connected to the V input of each oscillator element and connected to ground through a common variable resistor. A microcomputer controls the data acquisition system via a plug-in digital I/O port. The oscillators are enabled for initialization by a multiplexer that decodes the oscillators' address. A D/A converter sets the initialization voltage and the oscillators are instructed to start oscillating by the RUN signal. Finally, the ACQUIRE signal latches the output state, S, of each oscillator simultaneously into the latch where it is read by the computer.

The state, S, of each oscillator element was input to a 16-bit latch. The computer periodically sampled the state of the system by strobing the latch and then reading out its contents. The system permitted data to be sampled a variety of different rates, although in these experiments, a rate of 100 kSamples/s was used almost exclusively. With typical

oscillator frequencies of about 5 kHz, this produced roughly 20 samples per oscillator cycle.

The RUN signals of all the oscillators were connected together and driven by a single bit of the I/O port. Thus, the oscillators could be started and stopped collectively, but not individually. Four more output bits of the I/O port were used as inputs to a 16-bit multiplexer, the outputs of which were connected to the INIT signal of each oscillator element. In this way, the computer could address an individual oscillator for initialization. Finally, the addressed oscillator was initialized to its desired voltage by the V_{INIT} signal which was common to all oscillators. The V_{INIT} signal was produced by a 8-bit digital-to-analog converter which was also under computer control. Although the V_{INIT} signal is connected to all oscillator elements, only the addressed oscillator is initialized.

The total number of oscillators, N, in use at any one time in the experiment was not under computer control. Rather, N was controlled manually by simply inserting or removing oscillator elements (each of which was on its own separate, pluggable, circuit board) from the system.

3.2.4 Experimental/Systematic Considerations

We now consider some details of the experimental system regarding calibration, errors and various systematic details. First, as shown in Fig. 3.12, the oscillator system requires some time to warm-up and come to equilibrium after being initially powered up. The figure shows the variation in the natural frequencies of 15 uncoupled oscillators as a function of time after power is applied. This variation is undoubtedly the result of thermal effects in the individual oscillator op-amps, as well as a variation in the power supply voltage as the power supply itself warmed up. The figure shows that after about 20 minutes several thermal time constants of the system have elapsed. Additionally, there was some long term variation in the frequencies which we believe does not significantly affect our results. At large times, the frequency drift of the oscillators is estimated to be less than 0.3% per hour. After the N=15 system had reached equilibrium, the natural frequencies had a mean of 4.80 kHz and a standard deviation of approximately 0.198 kHz. This corresponds to a frequency spread of about 4.1%. One of the weaknesses of this experiment was the poor control over the oscillators' natural frequencies. While the frequencies could be measured to relatively high precision, they could only be set by manually adjusting a potentiometer. Thus, in this experiment, the

natural frequencies were adjusted by hand to be within about 10% of each other and the data was collected without further changes, except the unavoidable long-term drifts mentioned above.

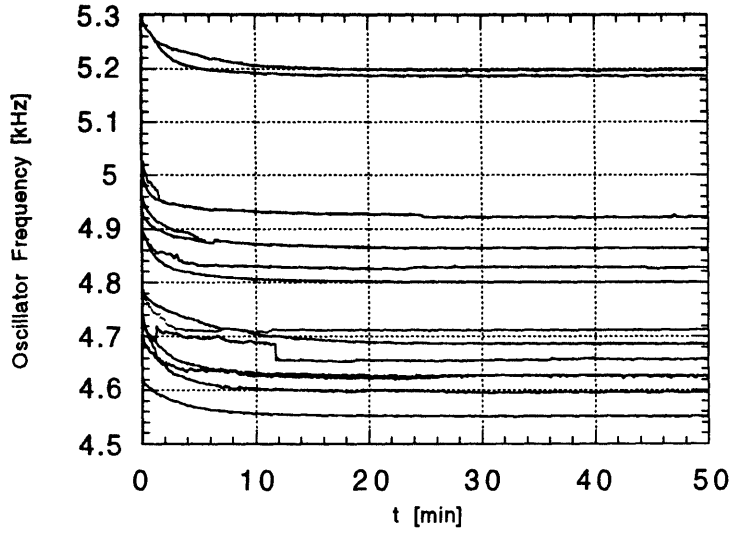

Figure 3.12 Oscillator frequency drift during initial warm-up. Frequencies of N=15 oscillators are plotted versus time after system power-up.

Another source of oscillator-to-oscillator variability arises from differences in the oscillator thresholds. This parameter could also be changed manually by adjusting a potentiometer and an effort was made to minimize this variability. The typical variation in threshold voltage is roughly 5%. Clearly, two otherwise identical oscillators with different thresholds will have different natural frequencies. Since the natural frequency is also an adjustable parameter, much but not all of the effect of differing thresholds can be corrected for in setting the natural frequency of each oscillator. Even when the first order effect of frequency variation is corrected for, differences in threshold do cause a very slight change in the shape of the oscillator waveform. Also, a reduction in oscillator amplitude means that the coupling signal presumably has a larger relative effect on that oscillator. This would lead in principle to a system that is not purely mean-field coupled, but rather has slight variations in the strength of coupling between oscillators. We expect that both these effects are quite small. Another source of inhomogeneity in the coupling strength is the manufacturing variability in the coupling capacitors which are rated to a tolerance 5%. As before, this variability can largely be absorbed into variability in natural frequencies. No attempt was made to eliminate the relatively small differences in

coupling strength. Nor were they included in our models of the system which will be discussed later.

As in any real system of oscillators, our ability to understand these electronic oscillators is limited by uncertainty in their initial conditions as well as random (in this case, electronic) noise that is essentially additive as the state of the system evolves.

3.3 Software

This section is concerned with the relatively straightforward method of initializing the coupled system of oscillators. It will be followed by a discussion of the various quantities measured in this experiment and the algorithms used to determine them. The computer program "AcquireDMA.c", which is the main data acquisition and analysis program, is reproduced in the Appendix.

3.3.1 Oscillator Initialization

In initializing the oscillators, note that since they are coupled together, setting the voltage on one oscillator affects the voltage on all of the others. This presents a difficulty, since the oscillators must be initialized sequentially rather than simultaneously. If V_1 is set to its desired value, subsequently setting V_2 to its desired value will alter V_1. This difficulty was overcome by repeatedly initializing the entire set of oscillators. It was found that the system relaxes exponentially to the desired initial state. After roughly 50 full initializations, the system of 15 oscillators appears to essentially reach equilibrium. As discussed previously, the state, S, is set by first initializing each oscillator to a voltage either above its upper threshold or below its lower threshold. Only then are the oscillators set to their desired initial voltages. It is necessary, therefore to perform the entire relaxation procedure twice: once to set the entire set of S_i, then once again to set the entire set of V_i.

3.3.2 Determination of Transition Times

The basic quantity measured in this experiment is the value of S for each of the oscillators, as a function of time. Fig. 3.13 shows the basic timing relationships involved in the experiment. Let τ be the index into the vector of sampled data, thus we are measuring $S_i(\tau)$, the state of the ith oscillator at time τ, where i=1,N and τ=1,$N_{SAMPLES}$. We will use τ henceforth as the most convenient unit of time (in samples). The time of

the τth sample, in seconds, is then simply $t_\tau = t_s\tau$, where t_s is the sampling period in seconds.

While nothing is measured directly about the state of an oscillator during most of its cycle, a transition in S from S=0 to S=1 indicates that the oscillator has passed, by definition, through ϕ=0. Thus, we are essentially making a measurement of the transition times, $\tau_i(n)$: the time at which the ith oscillator makes its nth switch from discharging to charging. The maximum uncertainty in each transition time is simply the time between measurements of S, that is the sampling period t_s. The first step in the data analysis was to simply examine each array, $S_i(\tau)$, as a function of time, and recording the transition time of each transition encountered, in a new array $\tau_i(n)$.

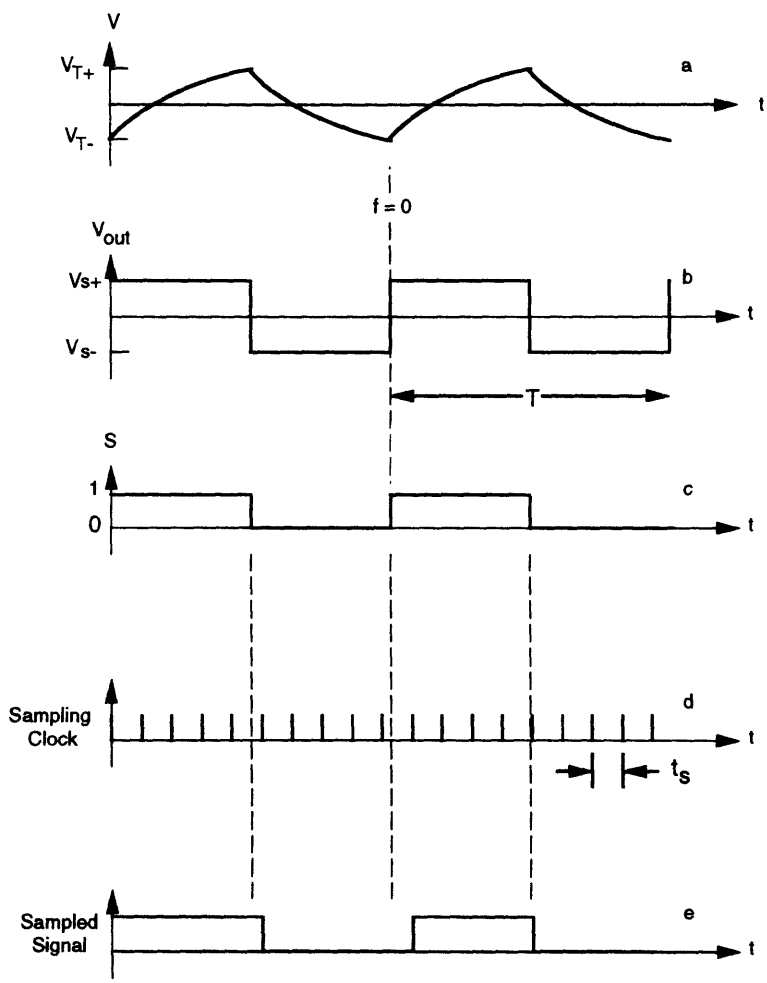

Figure 3.13 Timing relationships of the data acquisition system. A typical single oscillator waveform is shown in a. The definition of f=0 is taken arbitrarily to be the start of a charging cycle. Figure b shows V_{OUT}, the corresponding output of the op-amp with the period, T. Figure c shows S, the digital state signal which is sampled at regular intervals, t_s, by the sampling clock shown in Fig. d. The sampled signal with its corresponding time-quantization errors (exaggerated) is shown in Fig. e.

3.3.3 Determination of Phase & Error

The instantaneous period of the ith oscillator, at the nth cycle, $T_i(n)$ (actually it is not quite instantaneous since it is averaged over a single cycle) is then $T_i(n)=\tau_i(n+1)-\tau_i(n)$. Since, ϕ, the fractional part of the phase is simply the fraction of the current cycle that has been completed, the phase of an oscillator at any time may be estimated by linear interpolation between $\phi=0$ at the nearest preceding transition and $\phi=1$ at the nearest subsequent transition. Thus we may write the fractional part of the phase of oscillator i at time τ.

$$\phi_i(\tau)=\frac{\tau-\tau_i(n)}{T_i(n)} \quad \text{for} \quad \tau_i(n)<\tau<\tau_i(n+1) \tag{3.6}$$

The total phase, Φ, of each oscillator can be written as a sum of the fractional part, given above, and the integral part, ν, which is simply the number of complete cycles, or transitions, completed by the oscillator at any given time. Thus

$$\Phi_i(\tau)=\nu_i(\tau)+\phi_i(\tau) \tag{3.7}$$

The second step in the data analysis was to calculate the total phase of each oscillator as a function of time. Note that the oscillator transitions do not occur simultaneously. The preceding interpolation made it possible to approximate the phase of an oscillator at any arbitrary time, and in particular, it is important for measuring the phase of the oscillators simultaneously. Since the interpolation adds no new information beyond what was present in $\tau_i(n)$, it is really unnecessary to record the $\Phi_i(\tau)$ for all τ. It is sufficient to record the phase roughly once per cycle, and because the periods of all oscillators were very nearly the same, we chose oscillator #1 arbitrarily as a reference and recorded the phase of each oscillator only when oscillator #1 made a transition. That is we computed $\Phi_i(n)=\Phi_i(\tau_1(n))$ for $n=1,n_{MAX}$, where $\Phi_i(n)$ is the total phase of the ith oscillator at the time of the nth transition *of oscillator #1*. Thus, the phases of the oscillators are being strobed every time $\phi_1=1$. In most cases, n_{MAX} was typically about 2500 cycles.

3.3.4 Determination of Locking & Locking time

Having determined the phase of each oscillator as a function of time, it is relatively straightforward to determine when they are phase locked. For the purposes of this work,

the oscillators are said to be phase-locked when their *relative* phases remain unchanged after one complete cycle of any oscillator.

A weaker condition known as frequency-locking permits a cycle-to-cycle variation in the relative phases of the oscillators. The long-time average of these variations must be zero, however, such that the average frequencies of the oscillators are all equal. Since frequency-locking without phase-locking was not observed in our system, we will not consider the possibility further. In some work on oscillators systems, the term phase-locking implies the stronger condition that the relative phases of the oscillators remain fixed *throughout* the entire cycle of any oscillator. As will be seen later, there are some oscillator systems, namely those that interact discrete 'events', where this type of strong phase-locking is not possible or relevant. Our experiment is an example of one such system.

The time at which the system phase-locks is determined as follows. Oscillator #1 is again used as a reference and we ask whether the remaining oscillators are locked to oscillator #1. When all oscillators are locked to this reference, the system is said to be locked. This somewhat asymmetrical locking condition will be justified later when we show that, in practice, the oscillators lock together almost simultaneously, rather than in groups, making the choice of reference oscillator irrelevant.

In order to determine whether two oscillators (specifically, the ith oscillator and the reference, oscillator #1) are phase-locked, we begin by *assuming* that locking has occurred by the last (n_{MAX}th) cycle of data. We then scan through the data backwards, from end to beginning until the phase difference between the oscillators has changed from its final value by some amount δ. Thus $n_{LOCK,i}$, the cycle at which the ith oscillator locks to the reference, is the *largest* value of n which satisfies

$$\left\|\left[\Phi_i(n)-\Phi_1(n)\right]-\left[\Phi_i(n_{\max})-\Phi_1(n_{\max})\right]\right\|>\delta. \tag{3.8}$$

The value of δ was typically a fraction of one cycle, normally taken to be $\delta = 0.2$. Note that n and $n_{LOCK,i}$ count cycles of the reference oscillator only. Thus pair-wise locking time, $\tau_{LOCK,i}$, of each oscillator with the reference, is determined easily from the stored array of transition times: $\tau_{LOCK,i}=\tau_1(n_{LOCK,i})$. Furthermore, the cycle at which the whole oscillator system is locked, n_{LOCK}, is taken to be the largest value of $n_{LOCK,i}$, hence

$$n_{lock} = \mathrm{MAX}_i\left(n_{lock_i}\right) \tag{3.9}$$

and locking time for the whole system is $\tau_{LOCK}=\tau_1(n_{LOCK})$ Finally, if $n_{LOCK} > (0.95)\, n_{MAX}$, then this was taken to mean that locking had occurred suspiciously close to the end of the data set and that in fact the system had not locked at all during the time data was being acquired.

3.3.5 Determination of Fixed Point phases, Frequencies & Errors

Once the locking time has been determined, the trajectory of the system is of course naturally divided into two regimes: the transient regime for $\tau < \tau_{LOCK}$ and the large τ regime for $\tau > \tau_{LOCK}$. Note that in the N-1 dimensional state-space comprised of the *relative* phases of the oscillators (with respect to the reference), the phenomenon of phase locking corresponds to a fixed-point, since we are in a frame rotating with the oscillators. Clearly the integer part of the phase, which is relevant in analysis of the locking transient, is not relevant in understanding the fixed points. This fixed point is characterized, obviously, by its location in state-space: that is the set of relative phases. In addition, each fixed-point is characterized by one additional number: the frequency of oscillation of the system at that fixed-point.

It is possible to make good use of the many measurements of phase and frequency taken at the fixed-point after the system has locked in order to significantly reduce the cycle-to-cycle sample errors through averaging. There are often hundreds or thousands of cycles of data taken after the system has locked allowing measurement of relative phases to within 0.5% or better and measurement of fixed-point frequencies to within 10^{-4}. The average frequency of oscillation (in cycles per sample, or cycles per time step) at the fixed point is easily computed by finding the change in total phase between two widely separated times:

$$\langle f_i \rangle_{AB} = \frac{\Phi_i(\tau_B) - \Phi_i(\tau_A)}{\tau_B - \tau_A}, \tag{3.10}$$

while the average fixed point phase is given by

$$\phi^*_{i,1} = \frac{1}{\tau_B - \tau_A} \sum_{\tau=\tau_A}^{\tau_B} [\phi_i(\tau) - \phi_1(\tau)] = \frac{1}{\tau_B - \tau_A} \sum_{\tau=\tau_A}^{\tau_B} \phi_i(\tau) \tag{3.11}$$

where $\tau_A = \tau_1(n_{lock})$ and $\tau_B = \tau_1(n_{\max})$.

3.3.6 Counting Fixed Points

The method used to count the number of fixed points, N_{fp}, was relatively simple. Consider two fixed points, 1 and 2, each described by a set of N-1 relative phases:

$$\{\phi_i^1\},\ \{\phi_i^2\},\quad i=1,\ N-1$$

The two fixed points were considered identical if they satisfied the following condition:

$$MAX_i\left[\left|\phi_i^1-\phi_i^2\right|\right]\le\varepsilon,\quad i=1,\ N,$$

where ε is a characteristic 'confusion radius', and was chosen to be ε=0.004 based on the typical error associated with our measurements of fixed point phases. The Appendix contains the computer code "FixedPtCluster.cp" used to count the number of fixed points.

Having described the experiment itself, as well as some of the basic data analysis, we now proceed in the next section, to a discussion of our main experimental results.

4. RESULTS

So far, we have presented a common theoretical model of systems of limit-cycle oscillators, followed by a presentation of our simple experimental system of electronic relaxation type limit-cycle oscillators. Although the mathematical model is a highly idealized and does not suffer from many of the complexities of the electronic oscillators, it is not unreasonable, at least in the absence of experimental results, to expect the model to capture the essential features of our system of relaxation oscillators. This is especially true for weak coupling, since the model is a perturbative treatment of a much more general system.

In this section we discuss the results of our experiments. Of particular interest are the fixed points of the oscillator system and the unusually long transients that occur before the system reaches its fixed point. As with most many-body problems, the appropriate place to begin is with an understanding of the two-body interactions. Thus, in order to understand the behavior of a system of N oscillators, we turn first to a consideration of the simplest possible system: two oscillators.

4.1 Behavior of Two Oscillators.

The behavior of N=2 oscillators is neither complicated, nor particularly interesting in and of itself. We are interested in the N=2 system primarily to understand the sign of the interaction between the oscillators and to verify that our mathematical model works well in this simplest of cases. One of the first observations one makes of the N=2 system is that when the coupling is sufficient to cause the oscillators to phase lock, they invariably do so with 180 degrees of phase difference between them. This holds true for oscillators started in any arbitrary set of initial conditions. This 'phase repulsion' simply means that the pair-wise interaction of two oscillators is such that any phase difference between the two tends to grow until it reaches its maximum value at ϕ=0.5. This repulsive interaction is purely the result of our choice of coupling. Figure 4.1 shows the unique final state of the N=2 system. We see in Fig. 4.1a the (capacitor) voltage, $V_1(t)$, on one of the oscillators *after* the system has phase locked. The trajectory for the other oscillator, which is not shown, is essentially identical, except that it is phase shifted by 180 degrees ($\Delta\phi$=0.5). Note that at each peak and trough of the trajectory there is a small negative 'spike'. This spike is due to the coupling signal, $V_C(t)$, which is superposed upon each of the otherwise unperturbed oscillator trajectories. This coupling signal, shown on

an expanded vertical scale in Fig. 4.1b, consists of small negative-going spikes which occur each time an oscillator switches state.

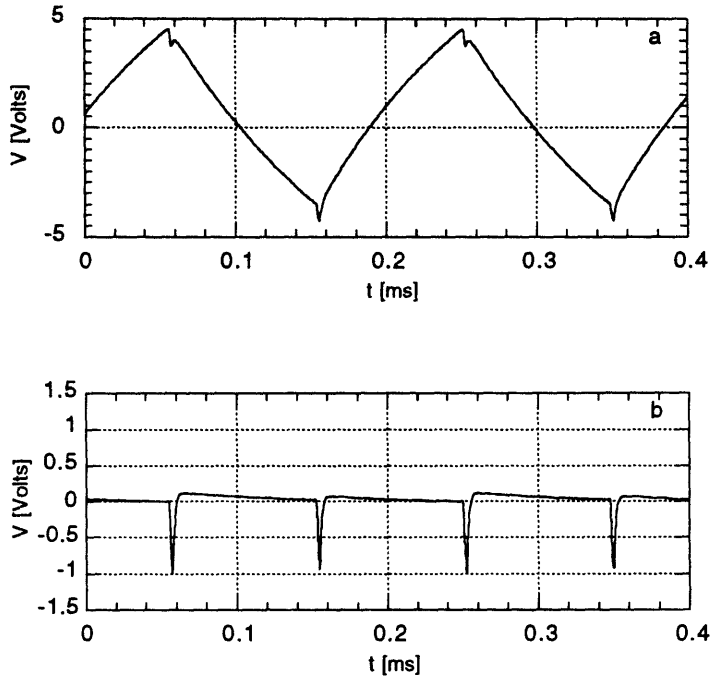

Figure 4.1. A time series for N=2 oscillators locked together with a coupling resistance of R_C=68 Ω. The voltage on one of the oscillators is shown in (a). The voltage of the other oscillator is similar, but is phase shifted by $\Delta\phi$=0.5. The mean-field coupling voltage, V_C is shown in (b), on an expanded scale.

In order to understand what is occurring in this locked state recall from Fig. 3.9b that the coupling signal produced by a single oscillator is, roughly speaking, a square wave. Since the net coupling signal is the sum of these square waves, and since the oscillators are out-of-phase with each other, the coupling signals, tend to cancel out. Hence the oscillators, in finding their locked state, have arranged themselves so that the total mean-field signal is very nearly zero, except twice every cycle when the oscillators are switching. During these brief periods, one oscillator has switched but the second has not. This delay is the result of the finite frequency difference between the two oscillators which requires that one oscillator must switch in advance of the other. The resulting incomplete cancellation of the square-wave coupling signals produces a net coupling signal with pulses which occur every half-cycle.

In the case shown, we can understand the asymmetry of V_C (the spikes are always negative in the example shown) as follows: Oscillator 1 reaches its upper threshold first, and switches, causing V_C to suddenly decrease. The decrease in V_C promptly *induces*

oscillator 2 to cross its lower threshold and it then also switches states, thus returning V_C to zero. One half cycle later, the roles of the oscillators are switched and oscillator 2 reaches its upper threshold first and induces oscillator 1 to switch, thus producing another negative spike.

Consider now a third oscillator coupled to a locked pair of oscillators. It will essentially 'see' no coupling signal due to the locked pair, except during those brief periods when the pair of oscillators is switching. This pulse type of interaction is believed to be important to the transient behavior of the larger system of oscillators which will be described below.

Although the N=2 system is not central to our results, but is rather more important as a basis for understanding the interactions, it is worth digressing further from a formal presentation of the main results in order to understand the dynamics of phase locking for the N=2 system. As a crude (but sufficient) model of the N=2 system consider single isolated oscillator (say oscillator 1) coupled weakly to the coupling network. Although the shape of V_1 will be slightly modified by the coupling, it will behave essentially as it did without the network. That is, it will have a periodic, roughly triangular waveform which we call $V_{01}(\phi)$ where the phase, $\phi=\omega t$, increases uniformly in time. If we now add a second oscillator of essentially equal frequency but different phase, it will modify the voltage on oscillator 1 such that $V_1(\phi) = V_{01}(\phi) + C(\phi+\psi)$, where ψ is the phase difference between oscillators. As has been discussed, the shape of C(t) is roughly a square-wave. As oscillator 1 nears a threshold, the effect of the additive coupling term, C, will be to advance or retard the time at which the oscillator switches. Thus, when oscillator 1 switches, it will have experienced a phase shift, $\Delta\phi$, relative to where it otherwise would have been had C not been present. What happens when an oscillator switches may compactly be described by the function $\Delta\phi(\psi)$. The assumption that $V_{01}(\phi)$ is triangular is valid to first order, since all phase shifting occurs when the oscillator is near its threshold.

Now let us construct $\Delta\phi(\psi)$ by considering the situation near the ψ=0.5 fixed point in more detail. The situation is shown in Fig. 4.2 for several different values of ψ, where ψ is now assumed to be a *perturbation* around the fixed point. Since the oscillations are nominally out of phase with each other, we expect a positive-going transition in C(t) to occur near the time that oscillator 1 reaches its upper threshold. If the positive-going transition in C(t) from oscillator 2 is perturbed toward earlier times by a sufficiently large amount as in Fig. 4.2a, oscillator 1 will be raised toward threshold by a constant amount,

independent of ψ. When it switches, oscillator 1 will then be phase shifted by a constant $\Delta\phi=\Delta\phi_0$, which tends to reduce the perturbation.

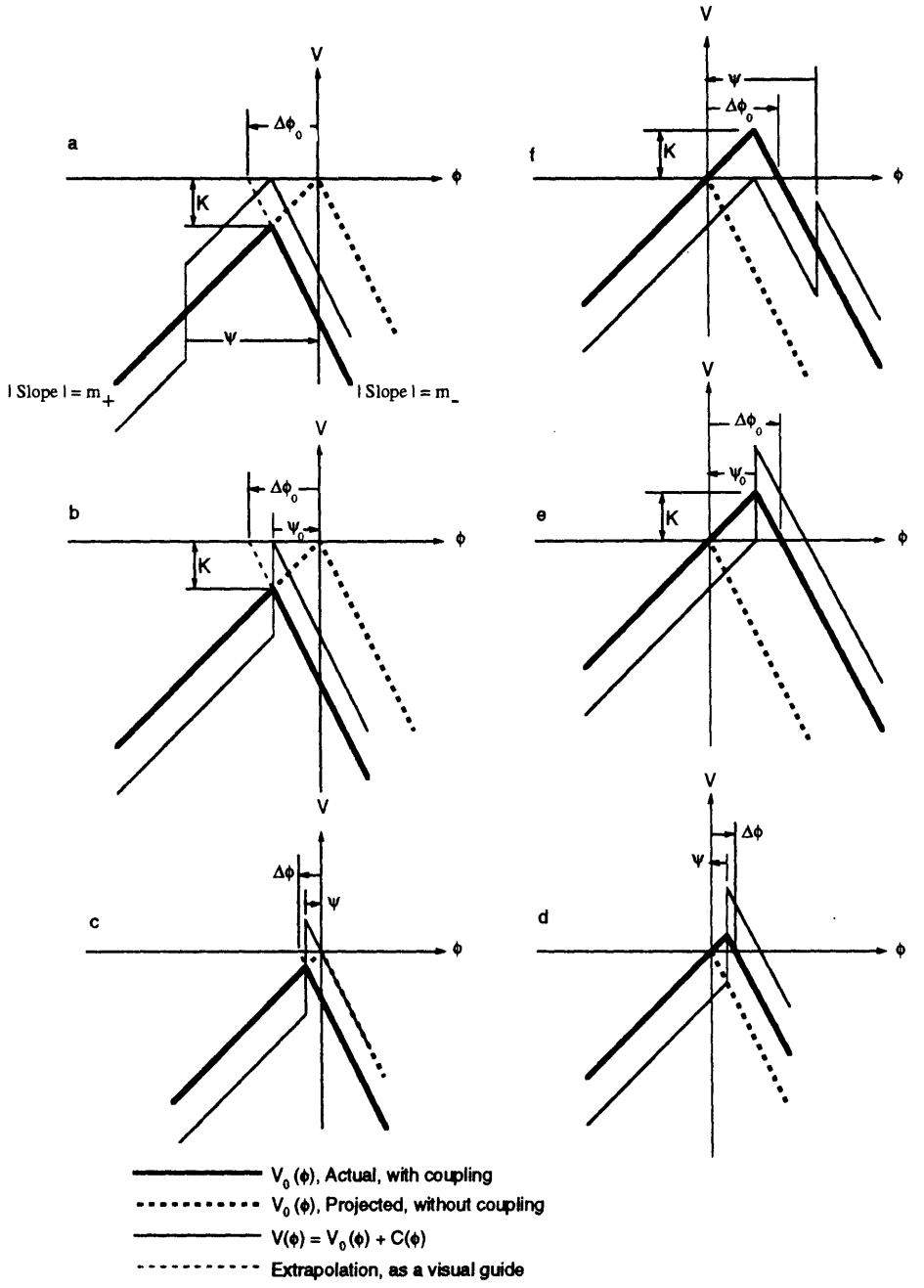

Figure 4.2 Diagram showing several cases of the N=2 oscillator dynamics near the fixed point of the system. The effect on oscillator 1 of a switch in the state of oscillator 2 is shown for a sequence of different relative phases. The peak-to-peak amplitude of C(t) is K. For convenience, the horizontal axis is also used to indicate the upper switching threshold.

Similarly, if the positive-going transition of C(t) is perturbed toward later times by a sufficiently large amount, as in Fig. 4.2f, oscillator 1 will be depressed below threshold by a constant amount, independent of ψ. When it finally switches, oscillator 1 will then be phase shifted by a constant $\Delta\phi=\Delta\phi_0$, tending to increase ψ. The change in phase difference at a switch, $\Delta\phi(\psi)$, is plotted in Fig. 4.3, with the letters a-f corresponding to those in Figs. 4.2a-4.2f.

For sufficiently small perturbations, ψ, it is possible for the switching of oscillator 2 to immediately force oscillator 1 above threshold from its previously depressed state. In this regime, the restoring phase shift, $\Delta\phi(\psi)$, is proportional to ψ. The leading and lagging cases for this regime are shown in Figs. 4.2c and 4.2d. The boundary cases, which occur at $\psi = \psi_0$ and $\psi = -\psi_0$, are also shown in Figs. 4.2b and 4.2e with their corresponding points indicated in Fig. 4.3. An analysis of the system near the negative threshold of oscillator 2 produces identical results. Furthermore, since the two oscillators are essentially identical, interchanging their roles in the preceding analysis will also produce identical results. Thus, the mapping implicit in $\Delta\phi(\psi)$ is applied not once, but four times during each cycle of the system: once for each switch of each oscillator.

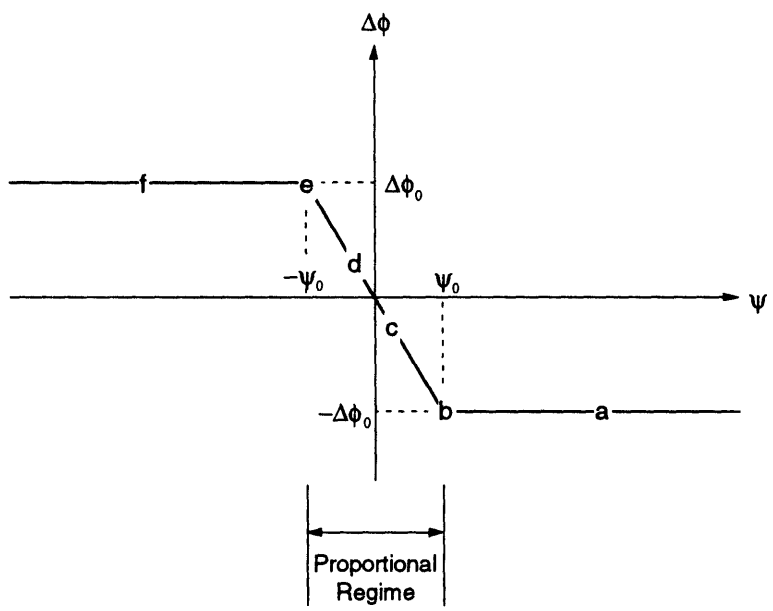

Figure 4.3 Approximate map of the N=2 oscillator system about the point ψ=0.5. The shift in the relative phases of the two oscillators is shown as a function of their relative phase. The regions marked by letters (a-f) correspond to the cases shown in the previous diagram. The origin is at ψ=0.5.

Let us assume, as shown in Fig. 4.2, that C(t) has a amplitude of K, which is a measure of the coupling strength. Assume also, that near its upper threshold $V_1(t)$ has

rising and falling slopes of magnitude m_+ and m_-, respectively. It can then be seen by examining Fig. 4.2 that

$$\Delta\phi_0 = K\left(\frac{1}{m_+} + \frac{1}{m_-}\right) \text{ and } \psi_0 = \frac{K}{m_+}.$$

Clearly, $\Delta\phi_0 > \psi_0$. We note that since m_- is invariably larger in magnitude that m_+, it is also true that $\Delta\phi_0 < 2\psi_0$. Thus, the slope of the proportional regime in Fig. 4.3 is given by $-2 < -\Delta\phi_0/\psi_0 < -1$. The return map for a single switching event describes the relative phase of the two oscillators after a switch as a function of their initial relative phase. It may be easily constructed by writing $\psi'(\psi) = \psi + \Delta\phi_0(\psi)$. Figure 4.4 shows the return map. It shows a fixed point at ψ=1/2 where the map intersects the diagonal. Furthermore, the central proportional region of this map has a slope m, which satisfies the well known condition for stability: $-1 < m < 0$. Thus, it can be seen from the return map that all initial phase differences between the two oscillators are attracted toward the fixed point. For most initial conditions, phase differences tend to change at a constant rate since most of the map has unity slope. As the system approaches its fixed point, it enters the proportional regime where the dynamics are hyperbolic. There, the deviation from the fixed point decays away exponentially.

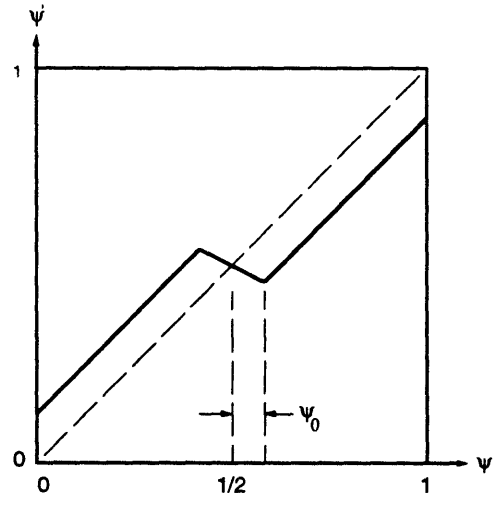

Figure 4.4 Approximate return map of the N=2 oscillator system, for a single switch of one oscillator.

There is also a fixed point at ψ=0, however it is a hyperbolic repeller, so it is not shown in the figures. The effect of a small frequency difference between the oscillators will be the accumulation of a small constant phase shift during each cycle. This will be in addition to the effects of coupling described above. Thus, the return map will be

shifted up or down by an amount proportional to the difference in frequency of the oscillators. For small frequency differences, there will be small shifts in the position of the fixed point. Eventually, however, the return map will be shifted up or down so far that the fixed point disappears entirely. We have also assumed that C(t) is a square-wave. In fact ,this is not quite true. The curvature of C(t) between switches of the oscillator means that the phase shift map shown in Fig. 4.3 is not quite constant in the regions a and f outside the proportional region. For small frequency differences, however, these regions do not contain the fixed point, hence small amounts of curvature will only cause small variations in the speed at which the system phase-locks.

4.2 Phase Trajectories.

We now focus on the more interesting case of N>2. Figure 4.5 shows a typical time-series for the case of N=15 oscillators in a fully phase-locked state.

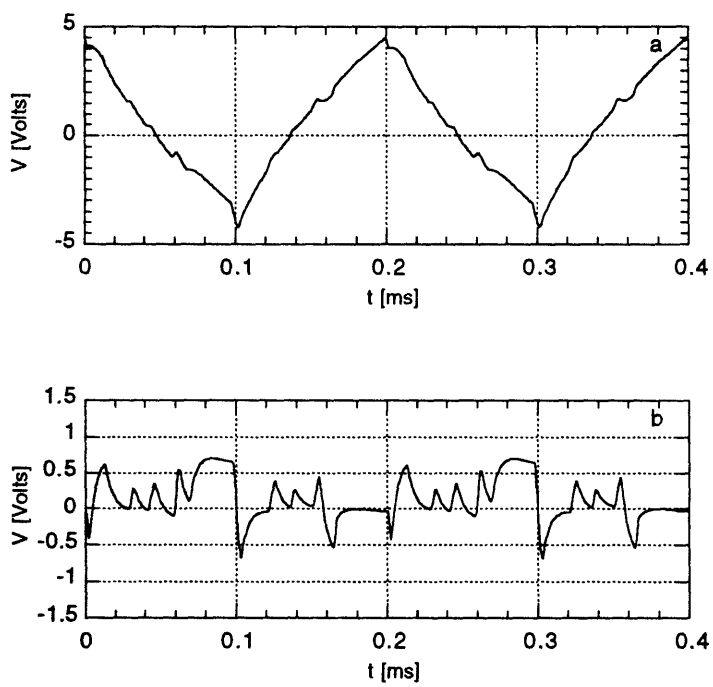

Figure 4.5. Time series for the case of N=15 oscillators in a typical locked state. The oscillators are coupled with a coupling resistance R_C=48 Ω. The voltage on oscillator #1 is shown in (a). The mean-field coupling signal V_C is shown in (b) on an expanded scale.

In this case, the coupling strength was adjusted so that it was just enough (R_C=48Ω) to cause the system to phase-lock. Figure 4.5a shows the typical waveform for the voltage on oscillator 1, $V_1(t)$. The perturbations due to the coupling are visible, but are small compared to the overall amplitude of the waveform. The associated coupling

voltage, $V_C(t)$ is also shown on expanded scale in Fig. 4.5b. This signal, which is clearly periodic, shows the typical behavior of the system at a phase locked state. The spikes in $V_C(t)$ are due to the switching of the other oscillators in the system, and are spread out over a broad range of phases relative to oscillator 1.

Before turning to a more complete treatment of the fixed points of the N=15 system, let us examine the unusual dynamics of the transient that occurs prior to the system reaching a fixed-point.

A typical set of phase trajectories is plotted in Fig. 4.6a for the case N=15. The oscillators were coupled with a relatively strong coupling resistance of $R_C = 562\ \Omega$. In this figure a single oscillator (oscillator 1) is arbitrarily chosen as a reference oscillator. The total accumulated phase difference between each of the other oscillators and the reference oscillator is plotted as a function of the total phase (in cycles) of the reference oscillator. In this way we have transformed the problem into a frame rotating with the reference oscillator. Note that the system has an exceptionally long transient followed by an apparently abrupt arrival at the phase locked fixed point. The transient lasts for approximately 1100 cycles of the reference oscillator. (At approximately 20 samples per cycle of the oscillators, this transient required roughly 22,000 data samples before locking. Sampled at a rate of 100 kHz, the transient lasted for about 0.22 seconds of real time). After approximately 1100 cycles the relative phase trajectories become flat indicating that the oscillators have ceased accumulating phase relative to each other. By the end of this particular transient, the fastest oscillators have accumulated about 73 cycles more than the reference, while the slowest oscillators have fallen behind by about 18 cycles. A close inspection of the transient part of the phase trajectories reveals another interesting feature. At different times the trajectories of different groups of oscillators appear to have small plateaus of nearly zero slope, indicating that for short periods, small groups of oscillators can become phase locked together. After some period the coherent behavior of the group of oscillators, is destroyed.

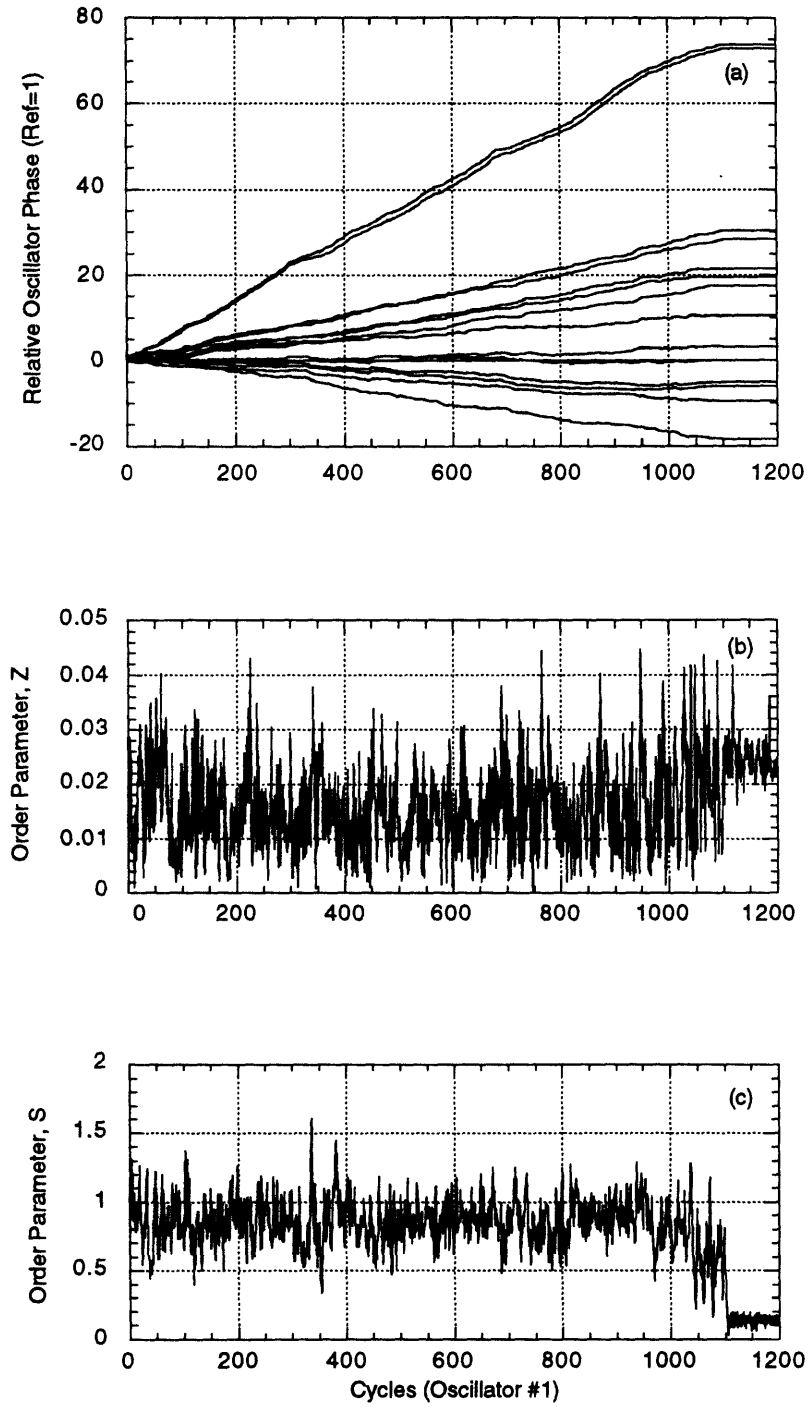

Figure 4.6. Typical phase trajectory for the system of N=15 oscillators at a coupling resistance of $R_C = 562\ \Omega$. The relative phase of each oscillator (relative to the phase of oscillator #1) is plotted (a) versus the overall phase of oscillator #1. Also shown on the same horizontal scale are the order parameters Z (b) and S (c). Phase locking occurs around 1100 cycles of oscillator #1.

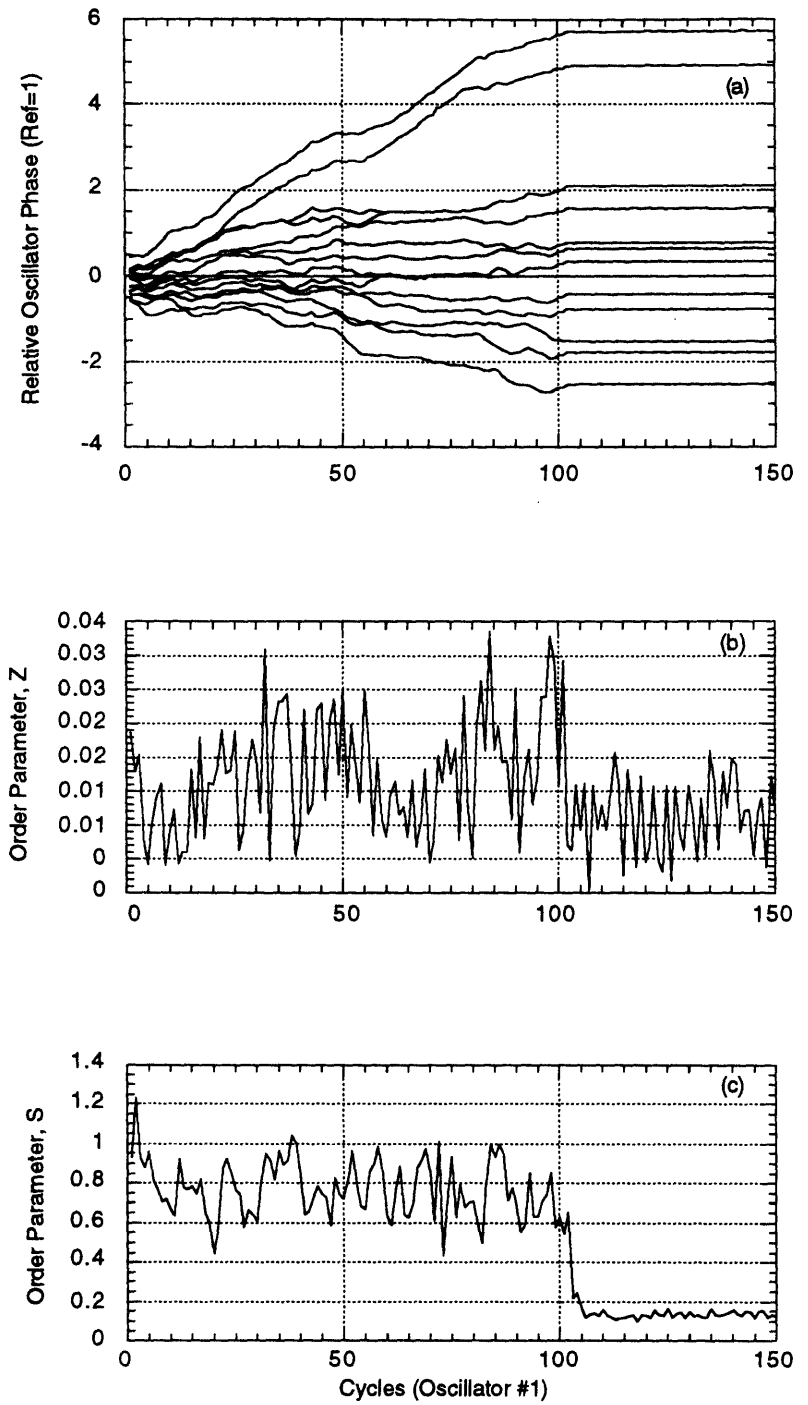

Figure 4.7. Another typical phase trajectory for the system of N=15 oscillators at a coupling resistance of R_C = 562 Ω. The plots correspond to those in Fig. 4.6. Phase locking occurs much earlier here than in the previous case.

It is also important to note that the frequency of each oscillator (relative to the reference oscillator) is given by the slope of its trajectory. Thus, the average behavior of

each oscillator during the transient involves short term frequency fluctuations about a mean frequency. The oscillators are essentially drifting apart in phase at a uniform average rate. This mean frequency is a characteristic of the oscillator and remains substantially constant during the entire transient. Clearly, for a system of uncoupled oscillators, the trajectories would simply be smooth diagonal lines with a slope precisely equal to the oscillator's natural frequency. Indeed, the average frequency of each oscillator corresponds closely to its natural frequency, as one would expect the weak coupling limit. The question raised by this data is how is it that the coupling is both strong enough to cause phase locking, yet weak enough to produce nearly linear trajectories which do not seem to be approaching a fixed point until they actually do?

Shown in Fig. 4.6b is the experimentally measured order parameter, Z, associated with the trajectories shown in (a). It can clearly be seen that phase locking of the oscillators corresponds to an increase in Z, from an average of roughly Z = 0.015 to an average of about Z = 0.025. In the fully locked state, the phases of the oscillators are fixed with respect to each other. We therefore expect that locking will cause the inherent fluctuations in Z to disappear. Indeed, Fig. 4.6b shows this reduction in the fluctuations in Z. Of course, the fluctuations are not identically zero since there are still measurement errors present. In a system of oscillators with attractive interactions one expects to find a stable states in which the phases of all the oscillators are approximately equal. Under such conditions, Z is clearly a useful order parameter since the stable state corresponds to values of Z near unity. On the other hand, our system of oscillators exhibits stable states with the phases spread over a wide range of values. For, example, one can imagine a stable state in which a group of oscillators rotate together rigidly, but whose phases are spread uniformly around the circle. In such a case, the parameter Z is almost useless, since both complete order and complete disorder correspond to Z=0. The two states are distinguished only by a decrease in the fluctuations in Z. In our case the change in Z as the system phase-locks is evident, but relatively subtle, at least in comparison to the magnitude of the fluctuations.

To remedy this deficiency, we introduce a more appropriate order parameter, S, which measures the degree of uniformity of oscillator *frequencies*, rather than phases. We define

$$S = \frac{\left[\sum_i \left(\dot{\phi}_i - \langle \dot{\phi} \rangle\right)^2\right]^{\frac{1}{2}}}{\left[\sum_i \left(f_i - \langle f \rangle\right)^2\right]^{\frac{1}{2}}}$$

where the $\{f_i\}$ are the natural (uncoupled) frequencies of the oscillators. The quantity, S, is then simply the standard deviation in the oscillator frequencies, scaled by the standard deviation in the uncoupled oscillators frequencies. As the coupling approaches zero, S approaches unity. Conversely, when the oscillators are phase locked and rotating rigidly, all the frequencies become identical, hence S approaches zero. In this sense it might be more appropriate to call S a 'disorder parameter'. Figure 4.6c shows S as a function of the absolute phase of the reference oscillator. Prior to phase locking, S fluctuates around an average value of about 0.9. After locking has occurred, S fluctuates about a mean of roughly 0.15, which results from sampling noise. Clearly, S is a more useful quantity for describing the overall state of the system.

4.3 Exponential Locking-Time Distribution

Another example of phase trajectories is shown in Fig. 4.7. This figure is identical to Fig. 4.6 and was produced under identical coupling conditions, but with different, randomly chosen, initial conditions. In this case the transient is strikingly shorter. The system becomes phase-locked after only about 100 cycles of the reference oscillator. Of course, the total phase accumulated by each oscillator is correspondingly reduced as well. Because of the expanded scale, this figure also illustrates well, the partial phase locking plateaus that occur, in this example, between cycles 60 and 80.

By examining many trajectories, such as those in Figs. 4.6-4.7, starting from randomly chosen initial conditions, we can obtain a more complete picture of the transient behavior, as well as global picture of the structure of the phase space of this system. To this end we construct probability distributions of the locking times, shown in Figs. 4.8a–4.8f. Each histogram is for a different coupling strength. These histograms are based on the locking times of 1000 different phase trajectories with initial conditions chosen randomly from a uniform distribution over the space of all initial conditions. Shown on a semilog scale, the distribution clearly appears to be well fit by exponential over much of the data.

The important implications of an exponential distribution are that locking times can be arbitrarily large and that the probability that locking will occur during any short interval of time is a constant. This latter observation is in accord with the observation in the previous section that the system shows no signs of evolving toward a fixed point: the system's dynamics just prior to locking are essentially indistinguishable from the dynamics at the beginning of the trajectory. The distribution of locking times remains essentially exponential for as few as N=8 oscillators. For N<8, the locking time distributions begin to have a complex peaked structure and the long exponential tail of the distribution disappears. For N=2, the distribution is very narrow, with most transients lasting only a few cycles.

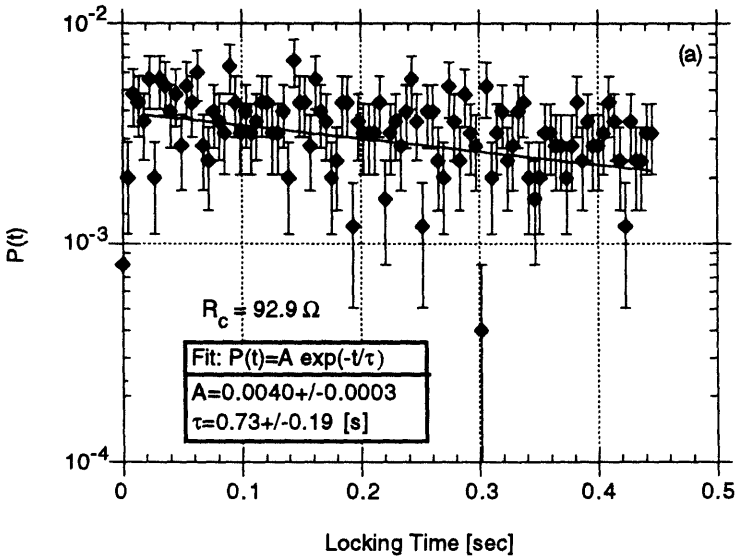
(a)
10^{-2}
10^{-3}
10^{-4}
P(t)
R_c = 92.9 Ω
Fit: P(t)=A exp(-t/τ)
A=0.0040+/-0.0003
τ=0.73+/-0.19 [s]
0
0.1
0.2
0.3
0.4
0.5
Locking Time [sec]

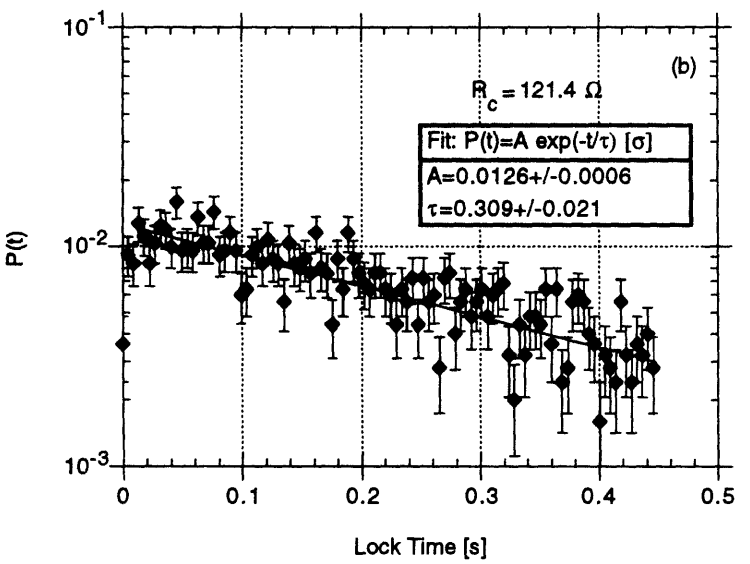
(b)
10^{-1}
10^{-2}
10^{-3}
P(t)
R_c = 121.4 Ω
Fit: P(t)=A exp(-t/τ) [σ]
A=0.0126+/-0.0006
τ=0.309+/-0.021
0
0.1
0.2
0.3
0.4
0.5
Lock Time [s]

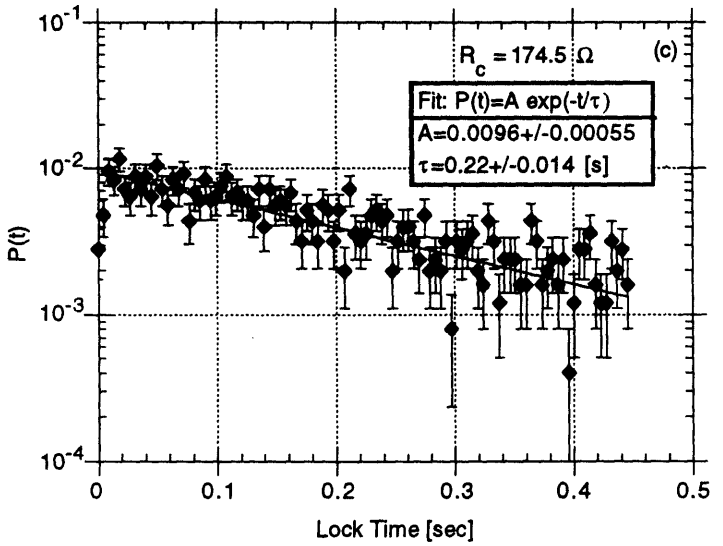
$R_c = 174.5\ \Omega$
(c)
Fit: P(t)=A exp(-t/τ)
A=0.0096+/-0.00055
τ=0.22+/-0.014 [s]
P(t)
Lock Time [sec]

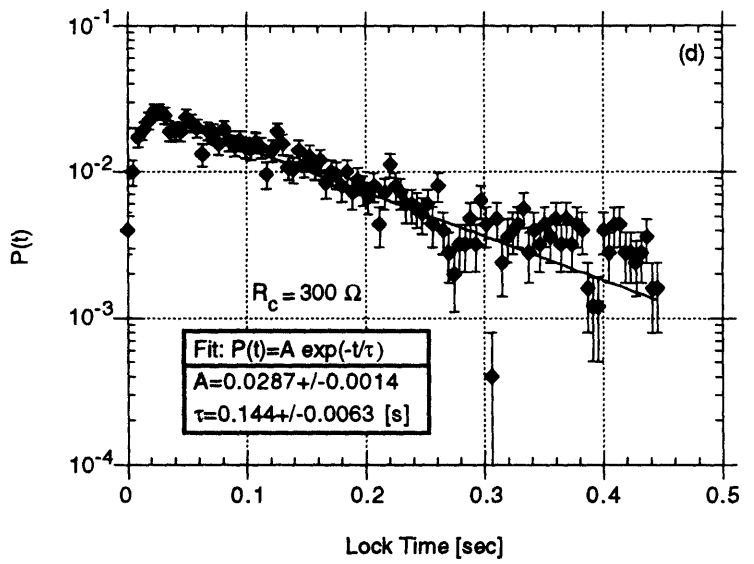
(d)
$R_c = 300\ \Omega$
Fit: P(t)=A exp(-t/τ)
A=0.0287+/-0.0014
τ=0.144+/-0.0063 [s]
P(t)
Lock Time [sec]

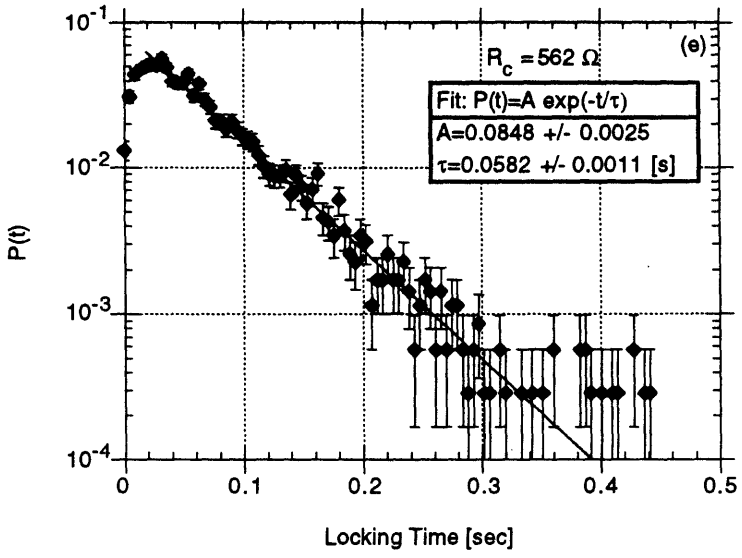

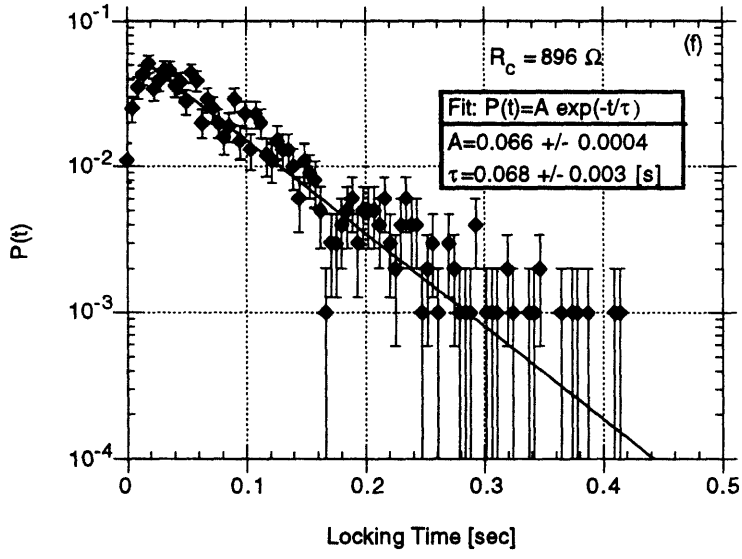

Figure 4.8. Locking time distributions for several different values of R_C are shown in Figs. a-f. Also shown on each is a least-squares fit of an exponential and the values of the fit parameters.

As one might expect, stronger coupling between the oscillators increases the likelihood of phase-locking and consequently leads to shorter locking-times. The slope of the exponential, therefore, becomes increasingly negative. Figure 4.9 shows the decay

constant, τ, as a function of the coupling strength, R_C. A least-squares fit shows that the data are well fit by a function of the form

$$\tau(R_c) = \frac{A}{R_c - R_{CRIT}}$$

where A and R_{CRIT} are parameters of the fit. The critical coupling strength, R_{CRIT}, represents the coupling strength below which no phase locking can occur.

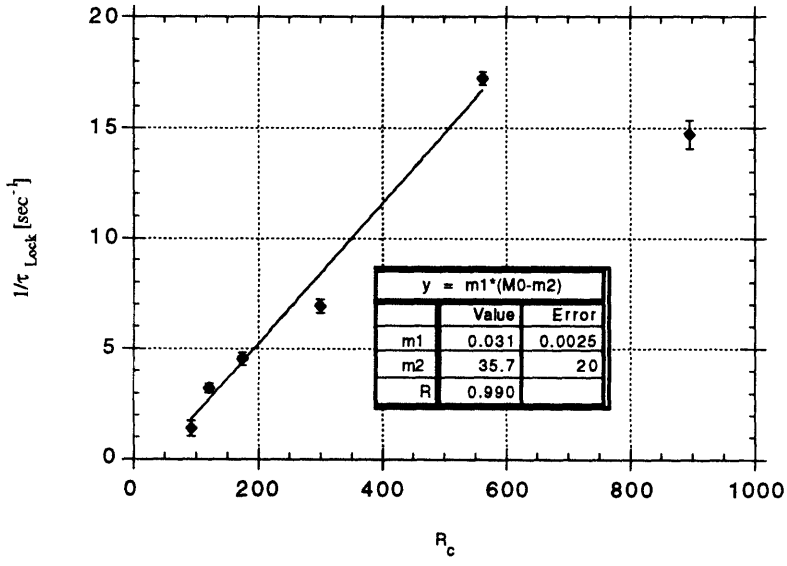

Figure 4.9. Plot of the inverse of the measured locking time constant, $1/\tau$, versus the coupling resistance R_C. A linear relationship is apparent extending to roughly 600 Ω. A linear fit is shown. The x-intercept of the line is the critical resistance R_{CRIT} at which the locking time approaches infinity.

For our system, with its particular distribution of natural frequencies, the value of the critical coupling, R_{CRIT}, at which the system underwent a phase transition to the phase-locked state, ocurred at R_{CRIT} = 35.7 +/- 20 Ohms.

4.4 Numbers of Fixed Points

So far we have only considered the transient behavior of the oscillator system. After the system has phase locked we can examine the relative phases of the oscillators as they rotate rigidly at a fixed frequency. For N=2 we have already seen that the system possesses the single, unsurprising final state in which the oscillators are separated by $\Delta\phi$ = 0.5 (180 degrees). For N=15, there appears to be a very large number of different final

states. Indeed, the number is so huge that our apparatus cannot come close to exploring them all. Figure 4.10 shows several typical final states of the N=15 system. Note that, in a crude approximate sense, the oscillators appear to prefer to phase lock in diametrically opposed pairs with the pairs distributed around the circle at roughly equal intervals.

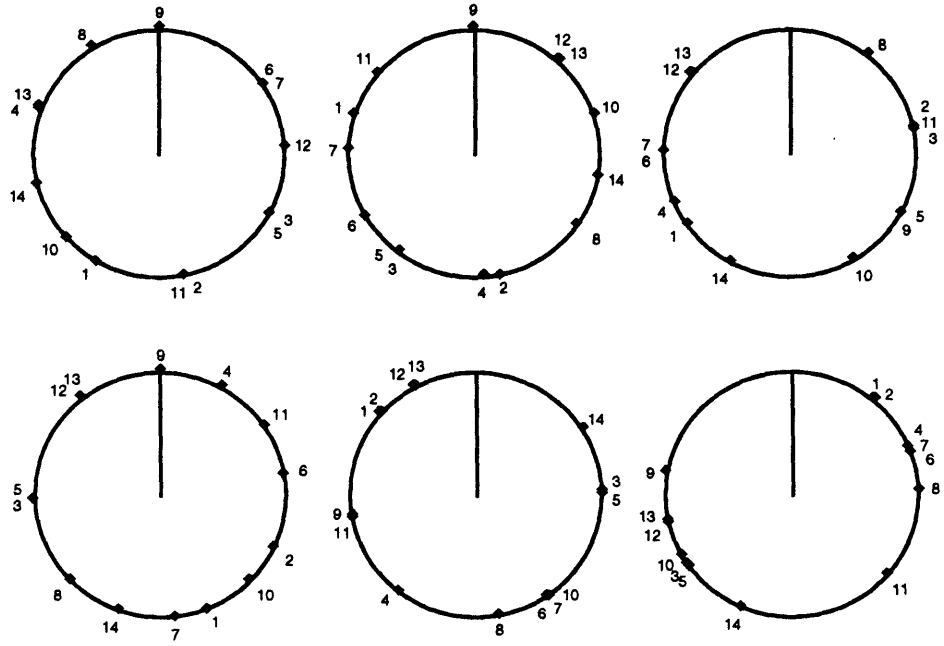

Figure 4.10 Diagram showing several typical examples of the final states of the N=15 system. The phase of each oscillator, relative to oscillator #1, is plotted as a point on the circle. Oscillator #1 is shown as a vertical line with phase increasing clockwise. The number of each oscillator is also shown.

For $N < 9$ we are able to count the number of distinct fixed-points, N_{fp}, that the system possesses. In order to count the number of fixed-points that the system possesses it is necessary to initialize the system many times and record the fixed-point configuration of the phases. To obtain statistically accurate estimates of N_{fp} it is clearly important to initialize the system many more times than there are fixed points so that each fixed-point is 'discovered' more that once. Since N_{fp} grows so quickly with the size of the system, N, it becomes prohibitively difficult to obtain N_{fp} for N>8. The results of the counting of fixed points is shown in Fig. 4.11. The data are well fit by the function $N_{fp}=(N-1)!$ which is also plotted. These data were taken with up to 10,000 separate runs or random initializations of the system when necessary. That the N=8 point is perhaps lower than expected may be due to the fact that at N=8, N_{fp} is approaching the number of runs, causing the space of fixed-points to be less than fully explored.

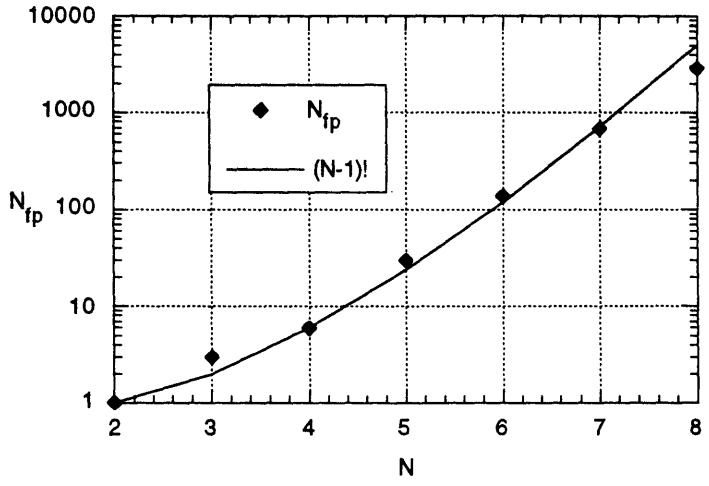

Figure 4.11 Plot of the experimentally determined number of fixed points as a function of the number of oscillators, N. Also plotted is the function (N-1)!. Data are measured at R_C=32 Ohms.

The quantity (N-1)! is simply the number of unique ways of ordering N items around the perimeter of a circle. The reduction of N by 1 avoids counting configurations which are related to other configurations by a rigid rotation. That N_{fp} scales as (N-1)! tends to confirm our belief that there is approximately only one fixed-point state for each sequential ordering of the oscillators.

4.5 Errors Growth

We can take a closer look at the transient behavior of the oscillators by asking how the dynamics of the system transform small perturbations in the initial conditions. Experimentally, we can repeatedly initialize the oscillator system to a particular state. Electronic noise will insure that there is some variation in the actual initial conditions established for the system. As the system evolves in time these variations will also evolve, in a manner determined by the dynamics of the system. Figure 4.12 shows the run-to-run RMS variation in each of the relative phases of the oscillators, versus the number of cycles of the reference oscillator. The case where the oscillators are uncoupled serves as a reference. When the oscillators are coupled the error ellipsoid grows much more quickly: perhaps 100 times faster for this case where $R_C = 562\ \Omega$.

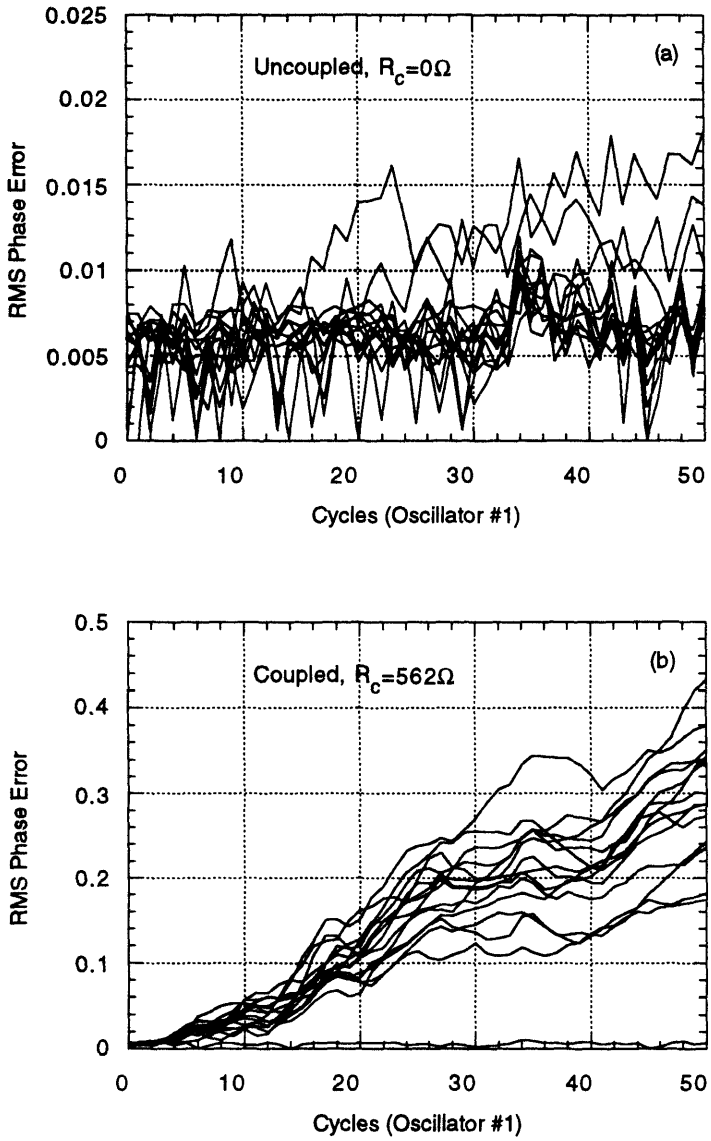

Figure 4.12 Plot showing the growth of the dispersion in run-to-run dispersion of error growth. FIg. (a) shows the uncoupled case. Fig. (b) shows the coupled case with R_C=562 Ohms.

There are several factors that make this measurement quite difficult and the results rather crude. First, there is the continual and presumably constant addition of electronic noise during the evolution of the system will tend to produce a linear increase with time in the size of the uncertainty ellipsoid. Second, it is obviously impossible to simultaneously start the system in several different conditions and directly observe the evolution of the dispersion: the experiments must be performed sequentially. This introduces the possibility of run-to-run variations (such as thermal drift) in the dynamics.

5. DISCUSSION

5.1 Geometrical View of Oscillator Locking

Recall that the important results from the last section were that our electronic oscillators exhibit a multitude of distinct phase-locked states, each of which is represented as a fixed point in the frame rotating along with the phase-locked system. Furthermore, during the transient which precedes phase-locking, points in phase space move almost uniformly (at constant velocity), perturbed about their trajectories by the apparently random fluctuating forces of the coupling field. These nearly free trajectories terminate abruptly when the oscillators phase-lock. The duration of the transient or the locking time is unpredictable and widely variable, but is well described by an exponential distribution.

We wish now to attempt to construct a simple geometrical model which will help us to understand what is occurring during the transient. In many systems of oscillators, such as that described in Sec. 2, the interaction between two oscillators is non-zero for almost all possible configurations of the two oscillators. For example, the simple theoretical model of Eq. 2.10 contains an interaction term proportional to the sine of the phase difference between the two oscillators. Figure 5.1a shows in a crude schematic manner how the phase space (in the rotating frame) might look for that type of interaction. Only two dimensions are shown, although the diagrams are intended to represent the N-1 dimensional space of relative oscillator phases (relative to the reference oscillator, for example). The trajectory of a point is shown as it spirals in toward a fixed point. The shaded area indicates the region where individual oscillators are subject to a 'force'. In this case that region covers essentially all of phase space.

Recall the behavior of two of our electronic relaxation oscillators. When two such oscillators phase-lock they form a diametrically opposed oscillator pair which approximately minimizes the net coupling field they produce. As we have seen, the net coupling field produced by a locked pair of oscillators is zero, except for short pulses that occur twice during each period, when the oscillators switch.

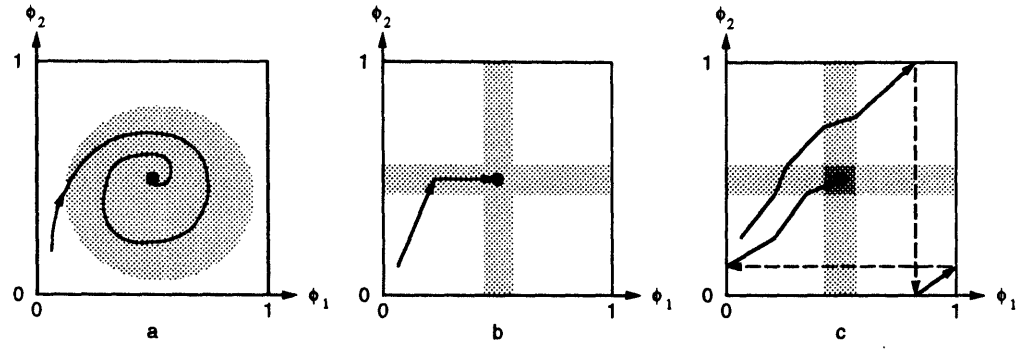

Figure 5.1 Schematic views of three basic types of transient dynamics associated with a fixed point. The figures show the space formed by the relative phases of the oscillators. The regions of attraction are shown shaded and the regions where the dynamics are those of a nearly free particle are unshaded. The diagrams are applicable to higher dimensions although only two representative dimensions are shown. Figure a. shows a trajectory in a region of hyperbolic dynamics (shaded) which fills a substantial portion of phase space. Figure b. shows a case in which oscillators lock together whenever a condition between *any* two oscillators is satisfied. Figure c. shows a case in which oscillators lock together whenever a condition between *all* oscillators is simultaneously satisfied.

Although less frequently studied, systems of oscillators that interact via pulses have been examined experimentally [Winfree, 1967] and theoretically [Bélair, 1986], [Mirollo & Strogatz, 1990], [Keener *et al.*, 1981]. In the latter two references, the integrate-and-fire oscillator is used to model biological oscillators with pulsatile interactions. In this model, pulses from one oscillator are *integrated* into the state of the other oscillators as a pulse of current is integrated by a capacitor. In this way, pulses from one oscillator cause permanent shifts (advancements) in the phase of the other oscillators.

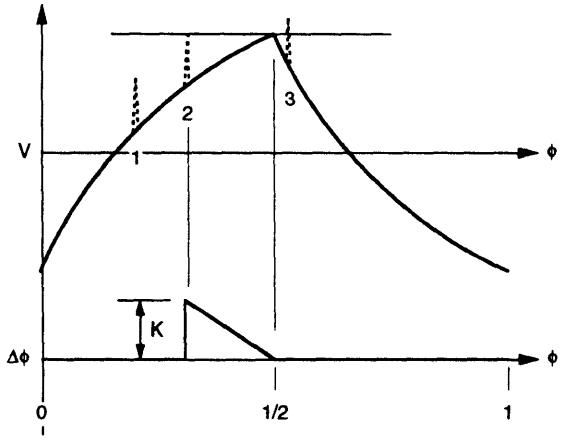

Figure 5.2 Voltage waveform of an oscillator coupled to a locked pair of oscillators. Three superposed pulses from the locked pair are shown at different relative phases. The pulse at 1. is insufficient to kick the oscillator over threshold, hence it has no effect. Pulses occurring between 2 and the peak of the waveform will cause phase shifts shown on the lower axis, with those at 2 causing the maximal shift and those at the peak causing no shift. Pulses such as 3 occurring after the peak also have no effect on phase.

A very general alternative type of pulsatile interaction is one in which the pulse is simply additive. For systems which contain thresholds, a pulse that occurs sufficiently close to the threshold will kick the oscillator above its threshold causing it to switch and shift its phase. Otherwise, the pulse will have no lasting effect at all. Figure 5.2 shows pulses superposed on the waveform of our relaxation type oscillators. The pulses are shown at several different possible relative phases. Clearly, interactions only occur over a limited range of relative phases.

For oscillators which interact in this manner, another mechanism by which the phase locking of a group of oscillators might occur is illustrated schematically in Fig. 5.1b. Consider a collection of oscillators each rotating at an approximately constant angular velocity. Eventually two oscillators will arrive at some phase relationship (shown shaded in the figure) which permits them to phase-lock to each other. We might hypothesize then that these two become permanently locked together and henceforth behave, at some level, as a single oscillator rotating at some new natural frequency. As the system evolves, other oscillators will arrive at some correct phase relationship that allows them to phase-lock with individual oscillators or locked clusters. In this way, locked clusters of oscillators grow in size by 'absorbing' or 'sticking' to others. Eventually the system consists of a single locked-cluster, and has therefore reached its fixed point. In this view, a trajectory moving uniformly through an N-dimensional phase space encounters an N-1-dimensional hyperplane onto which it 'sticks'. The trajectory henceforth remains confined to this N-1-dimensional subspace, drifting almost freely until it encounters an N-2-dimensional hyperplane which further divides that space, and so on, until it is confined to a zero-dimensional space which is the fixed point. The key assumption behind this view is that a permanent phase-locking can occur if *any* pair-wise locking condition is satisfied.

While this type of route to phase-locking has been observed, it clearly fails to adequately describe the transient behavior observed in our experiments. This 'absorption' model clearly would predict a finite and relatively short locking time. Assuming that phase space points drift along their trajectories at a velocity given (approximately) by their average relative frequencies (in cycles/sec)

$$\vec{\nu} = (f_1 \quad f_2 \quad \cdots \quad f_{N-1}) \tag{5.1}$$

then the maximum time required for the system to become confined along the ith dimension is $1/f_i$. Thus, the maximum locking time is simply

$$\tau_{MAX} = \sum_{i=1}^{N-1} \frac{1}{f_i}.$$

In fact, this ignores any cooperative effects among the oscillators. In many systems such as those cited above, the strength of attraction between locked clusters of oscillators increases with the size of the clusters. Such cooperative effects tend to cause the locking process to accelerate over time, thus shortening an already short and finite locking time. In addition to the exponential locking time distribution which this model fails to predict, our results show many examples of groups of oscillators that lock for a while and then come apart.

Now consider the dynamics of *two* locked pairs of oscillators, separated in phase by some amount $\Delta\phi$. The situation is shown in Fig. 5.3. It is clear that for most values of $\Delta\phi$ the pair-to-pair interaction will be zero. This is because the small pulses produced by one pair of oscillators will have no effect on either of the other oscillators unless those pulses occur sufficiently close to the point at which the other oscillators are switching. If the phase difference between the pairs is small enough, then the pulses from one pair will 'kick' one of the other oscillators over its threshold sooner than would otherwise have occurred. Such an event might be described as a 'collision' between oscillator pairs. It is not at all clear what happens during and after a collision of pairs of oscillators, however, we can easily envision that one or both pairs might be broken apart, becoming unlocked from each other. In addition, it is quite possible that one or both oscillators might promptly become phase-locked again, but to an oscillator from the other pair. This process might be called 'stealing' in that it involves one oscillator capturing the partner of another after a collision. In general, each locked pair will have its own unique frequency. Since these frequencies will inevitably be different for each pair, we expect the pairs to gradually drift toward each other until they collide.

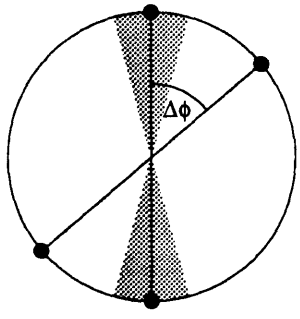

Figure 5.3 Diagram of four oscillators locked together in pairs, with an angle $\Delta\phi$ between the pairs. The shaded region indicates the values of $\Delta\phi$ for which the pairs can interact.

The important point here is that, at some level of abstraction, the range of interaction is limited, rather than extending over all of phase space. In this case we are in some sense referring to interactions between pairs of oscillators, rather than oscillators themselves.

We propose a better geometric model of the transient behavior of our oscillator population by assuming that a permanent phase-locking can occur only if *all* pair-wise locking conditions are simultaneously satisfied. In this view, which is illustrated in Fig. 5.1c, locking occurs only when the phase space trajectory happens to arrive at a state very near the fixed point.

Suppose that throughout most of phase space, trajectories move with constant average velocity as described above in Eq. 5.1. Only in small regions around each fixed point are the trajectories strongly attracted to the fixed point. Elsewhere, the trajectories behave like free particles, albeit perturbed randomly by the field that couples the oscillators together. The situation is shown schematically in Fig. 5.4a.

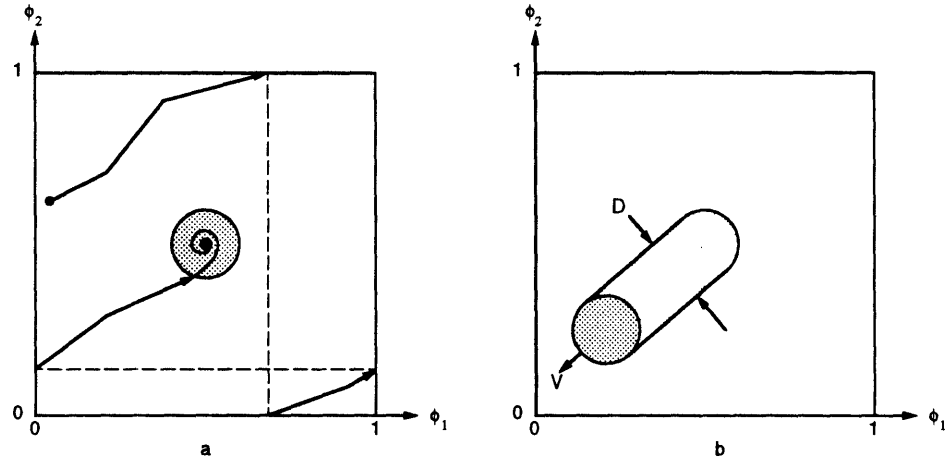

Figure 5.4 A schematic view of the space formed by the relative phases of the oscillators. Figure a. shows a trajectory of a typical point in phase space. The trajectory moves approximately as a free particle, perturbed slightly by the mean-field coupling until it enters a small region (shaded) around a fixed point. The dynamics are hyperbolic in the shaded region. Figure b. shows the system in a frame moving *with* the phase space point. In this frame, the attracting region appears to move at a speed v in the opposite direction, sweeping out areas of phase space of diameter, D.

In this figure the shaded area represents the region of attraction (shaded) surrounding the fixed point (solid dot). Between the random perturbations of the trajectory and the generally irrational ratios of each of the natural frequencies, we may assume that a single phase space trajectory will ergodically explore the entire phase space; at least until phase-locking occurs. When, after a time t_{LOCK}, the trajectory encounters an attracting region it

will be drawn toward the fixed point in a time short compared to the average value of t_{LOCK}.

To understand why this model produces an exponential distribution of locking times, we must compute the probability, A(t), that a randomly chosen initial condition, under the action of the phase space dynamics, will have *not* encountered the attracting region. One way of viewing the problem is to treat it as a classical scattering problem in N-1 dimensional space. The intensity of the unscattered (or unabsorbed) 'beam' will depend on the density of scatterers and their cross-section, and will decay exponentially with distance. Alternatively, we can imagine the attracting region moving across phase space with a velocity, -v, exactly opposite that of the phase space flow as shown in Fig. 5.4b. As the attracting region moves it sweeps out areas of the phase space at a rate of vD where D is the (N-2 dimensional) volume of the attracting region projected onto the N-2 dimensional hyperplane normal to the direction of motion. If A(t) is the fraction of phase space that has not been 'swept up' by the attracting region, then it is also the probability the a particular initial condition has not phase-locked at time t. Clearly, A(t) is governed by

$$\frac{dA}{dt} = -\nu DA ,$$

which can be solved trivially to yield

$$A = A_0 e^{-\frac{t}{\tau}},$$

where $\tau = \frac{1}{\nu D}$ is the characteristic lifetime of an initial condition.

For clarity, we have so far assumed that there is a single fixed point. In fact, if D is the result of n_{fp} fixed points of average size $d = D/N_{fp}$ then

$$\tau = \frac{1}{\nu N_{fp} d}.$$

Since the transformation to the rotating frame has removed the average motion, the velocity through phase space may be approximated

$$\nu = \left(\sum_{i=1}^{N-1} \left\langle \dot{\phi}_i \right\rangle^2 \right)^{\frac{1}{2}} \approx \sqrt{N-1}\,\sigma_f .$$

Using our experimental result that N_{fp} =(N-1)! and the formula for the volume of an N-2 dimensional sphere of radius, r,

$$d_{N-2} = \frac{\pi^{\frac{N-2}{2}}}{\left(\frac{N-2}{2}\right)!} r^{N-2},$$

we obtain

$$r = \left[\frac{\left(\frac{N-2}{2}\right)!}{\pi^{\frac{N-2}{2}}} \left(\frac{f}{\sigma_f}\right)\left(\frac{T}{\tau}\right) \frac{1}{\sqrt{N-1}(N-1)!} \right]^{\frac{1}{N-2}}$$

where T=1/f is the average period of oscillation. Taking N=15, and $\tau/T \approx 500$, $\sigma_f/f \approx 0.10$ gives the approximate mean radius of the attracting regions to be r=0.097. This value, although very crudely calculated, seems to be reasonable. It is about 10% of the length of one cycle, which is comparable to the amplitude of the coupling signal as a fraction of the total amplitude of the oscillator waveform.

The preceding view of the transient dynamics is not the only one possible. As was discussed in Sec. 2, systems with unstable chaotic orbits can also produce transients that have an exponential distribution of transient lengths. It is not clear from our data how to distinguish between the two models. It is possible that the two explanations are simply two different way of understanding the same phenomenon and that in fact they both are correct. Perhaps the very notion of orbits is only useful for systems of relatively low dimension and that as the dimension of the system becomes larger, the transition to a statistical description necessitates a model like the one introduced above.

A related question concerns the basins of attraction of the phase-locked states of the system. A basin of attraction includes, by definition, all initial conditions which ultimately arrive at some phase-locked state. Clearly every point along a particular trajectory through phase space is part of a single basin of attraction. Since, even in the rotating frame, points in phase space move at a uniform average velocity, we may conjecture that the basins consist of long, thin filaments which run parallel to each other. At one end of each filament is the attracting region surrounding a fixed-point. There, the diameter of the filament is of the same order as the attracting region. As one moves along a filament away from the attracting region (toward more distant initial conditions), the filament grows narrower as it is 'eclipsed' by other attracting regions. One can envision

taking a cross section through this bundle of filaments. Although still unclear from our data, it is plausible that when viewed in this way, the basins form a fractal structure.

5.2 PRO Model

The preceding discussion was concerned entirely with describing the geometry and dynamics of the phase space of the experimental oscillator system. It was only weakly motivated by the details of any particular oscillator model. In this section we will discuss our attempts to develop a simple mathematical oscillator model which is, nevertheless, capable of displaying the important exponential distribution of transient lengths.

5.2.1 Overview

Undoubtedly, a differential equation based model of the oscillator system would behave as the real system did, assuming that the model was sufficiently detailed. Such an approach would probably yield little insight into the dynamics of the oscillator population as it would merely be a slavish copy of the real system. Such models are also computationally rather costly.

Instead, we propose a map-like model called a *pulse response oscillator* (PRO) model. The PRO model makes some bold simplifying assumptions in the hope of capturing the essential features found in the real oscillator system. The relative simplicity of the model compared to a system of differential equations opens up the possibility that it might, in the future, be studied theoretically for its own sake.

The first and most important assumption of the PRO is that oscillators interact only via pulses of negligible duration. Each oscillator is completely described by a phase which, in the absence of interactions, grows linearly in time at a rate set by the oscillator's natural frequency. At some point in each oscillation (which we arbitrarily take to be when the fractional part of its phase is zero) each oscillator emits a pulse. All the oscillators coupled to the first have their phases, ϕ_i, instantaneously changed or 'kicked' by an amount $KF(\phi_i)$, where K is the strength of the coupling and F is a periodic function of the phase of the oscillator being kicked. A more mathematical description of the model is given in pseudocode below:

Pulse Response Oscillator Model

1. INPUT: Initial Phases $\{\phi_i(0)\}$, and Natural Frequencies $\{f_i\}$, for i=1,N

2. Propagate all oscillators forward in time using $\frac{d\phi_i}{dt} = f_i$ until one satisfies $\phi_i \bmod 1 = 0$
3. Modify all phases according to $\phi_j' = \phi_j + KF(\phi_j)$ where F is a periodic function which satisfies $F(\phi + n) = F(\phi)$ for all integers, n.
4. Go to step 2.

This can be written even more compactly as

$$\frac{d\phi_i}{dt} = f_i + KF(\phi_i)\left[\sum_{j=1}^{N} \oint \delta(\phi_j) d\phi_j\right].$$

It should be noted that once an oscillator has emitted a pulse it is prevented doing so again immediately without first moving away from ϕ=0. Unlike the model discussed in Sec. 2, in which the interactions between oscillators depended only on their relative phases, the PRO is not rotationally invariant. The interaction depends on the oscillators' absolute position rather than simply their phase differences. In addition, the PRO system captures the sequential nature of many oscillator systems, including that of the experimental system. The oscillators do not interact simultaneously, but rather one after another, such that their positions are coupled to the order in which pulse events occur. Although it is still unclear, it is probably these general properties, as well as the limited range of interaction, that account for the novel transient behavior that has been observed.

5.2.2 Numerical Results

The results of numerical experiments with the pulse response oscillator indicate that it reproduces the exponential locking time behavior of the electronic relaxation oscillator experiments quite well. The function, F, was chosen to be identical to the function $\Delta\phi$ shown in Fig. 5.2. The slope of the interacting region was fixed at m=-1.5, while its peak height, K, served as the coupling strength parameter. The long term coherence of a system of 20 pulse response oscillators was studied as a function of the coupling strength as shown in Fig. 5.5. It can be seen that given sufficient coupling, the system will undergo a spontaneous phase transition in which all oscillators become mutually synchronized.

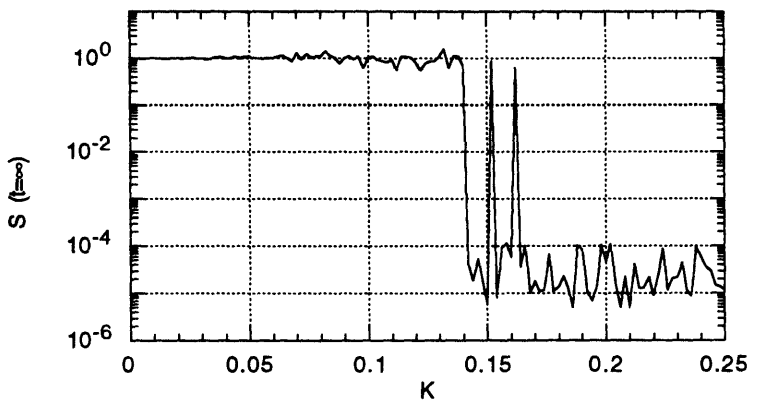

Figure 5.5 A phase diagram showing a phase transition in a population of 20 pulse response oscillators. The order parameter S (the normalized frequency dispersion) at asymptotic times is plotted as a function of the coupling strength, K. At approximately K=0.14 the coupling is strong enough that the population will spontaneously synchronize. The pulse response function is described in the text. The oscillators were drawn from a Gaussian parent distribution with a 5% standard deviation in their natural frequencies. The non zero points after the phase transition are due to insufficiently long calculation times.

By choosing a coupling strength at K=0.15, just above the critical coupling strength, we can qualitatively compare the temporal behavior of the PRO system, as shown in Fig. 5.6, with the analogous experimental Figs. 4.6c and 4.7c. As with the electronic system, the phase trajectories appear to drift at nearly constant average frequency for many cycles before abruptly phase locking.

Additionally, transient or partial phase locking is evident from the occasional plateaus which are visible in the trajectories. Furthermore, the time history of the (dis)order parameter, S(t), which reflects the overall coherence of the system, behaves similarly to its experimental analog. As before, it fluctuates about unity for hundreds of cycles before suddenly falling off to zero.

Finally, for the PRO system, there is the locking time distribution itself. Figure 5.7 clearly shows that the distribution is well fit by an exponential over a range of locking times extending from perhaps 50 to 1000 cycles.

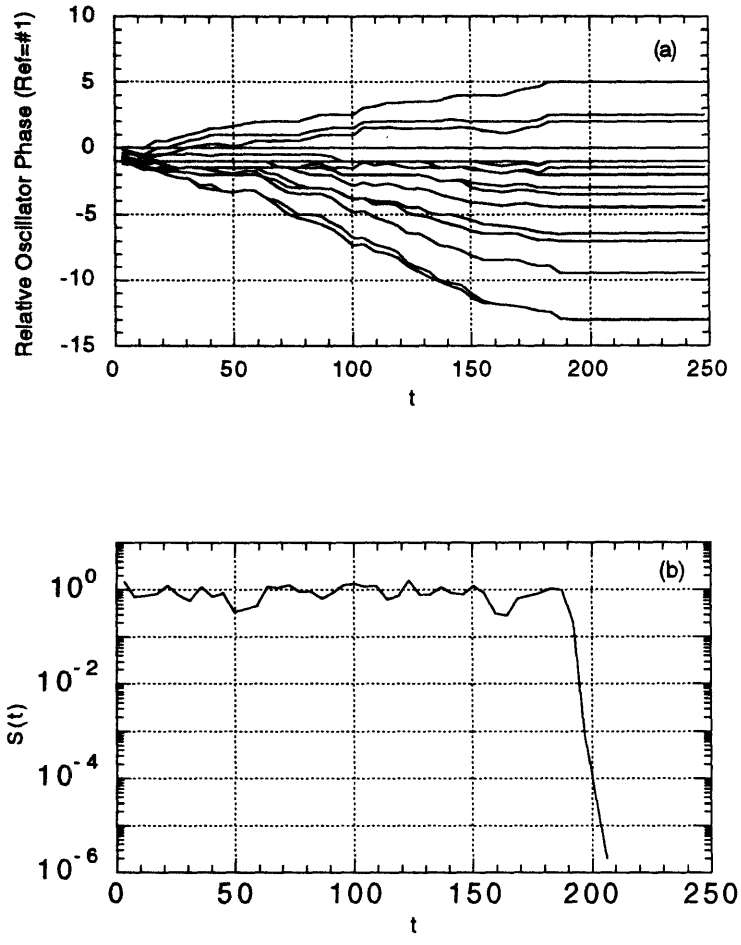

Figure 5.6 A plot of the trajectories of 20 pulse response oscillators (a). The conditions are described in the text. The phase of each oscillator relative to a reference oscillator is plotted as a function of time. Since the oscillators were chosen to have a mean natural frequency near 1.0, the horizontal axis is also approximately in units of cycles. The system can be seen to synchronize abruptly after approximately 200 cycles. Figure b shows the order parameter, S(t). The coupling was K=0.15.

It should be noted that the PRO system fails to reproduce the fixed point states of the electronic relaxation oscillator system. While the PRO system does indeed have a multitude of distinct final states, the fixed-point phases of the oscillators are not spread out over a range of angles, as they are in the electronic system. The PRO oscillators invariably end up divided into two diametrically opposed groups separated by 180 degrees. Although the reason for this difference is not clear, we conjecture that the fixed-point phases in the electronic system are spread over a range of angles as a result of capacitive and other electronic delays which are not modeled at all by the highly simplified PRO model.

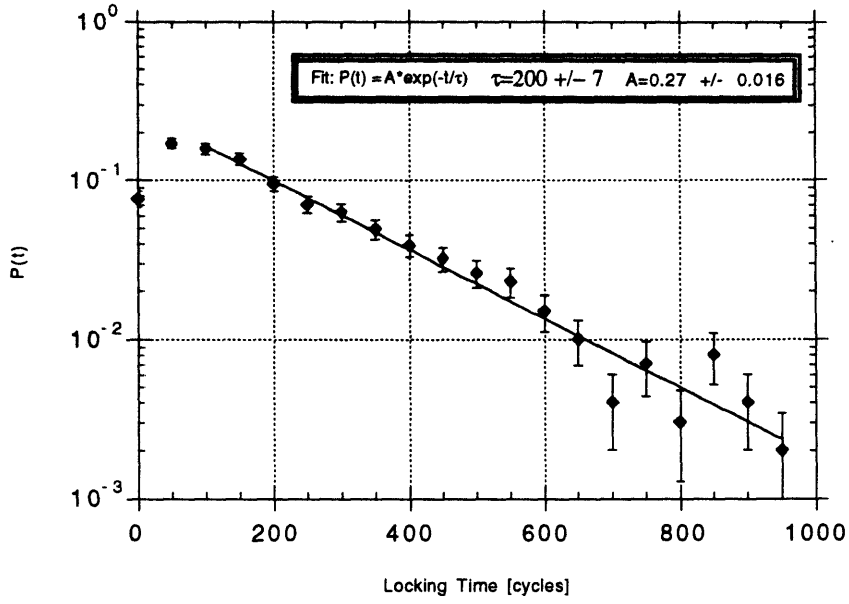

Figure 5.7 A plot of the distribution of locking times for the system of 20 pulse response oscillators described in the text. A least-squares fit to all but the first two data points is shown, indicating a good fit to an exponential distribution. The characteristic transient length in this case is about 200 cycles. The coupling was K=0.15.

5.2.3 Failure at Small Locking Times

It should also be noted that both the experimental results and the results of the PRO simulation indicate that for very short locking times, the distribution of locking times is not well described by an exponential. Both systems are less likely to exhibit short locking times than is predicted by the exponential distribution. One possible explanation for the failure at short times is that there are in fact two separate time scales associated with each transient. This is not unexpected according to our model since, as shown in Fig. 5.4a, the phase space is divided into two distinct types of regions: the regions of essentially free particle dynamics, and the regions of strongly attracting hyperbolic dynamics. At the end of each transient there is presumably a finite length of time associated with the attracting region. This could produce a relative reduction in the number of transients of short length. Another possibility, is that the reduction is essentially computational. The algorithms used to determine the point at which locking occurs are biased in that they find an upper bound on the locking time. They will always determine that locking has occurred on or after the point at which it has actually occurred, which would tend to suppress the reporting of very short locking times.

6. CONCLUSION

We conclude now, first with a brief summary of the experiments and the central results. Next, we will delve into the use of electronic systems as experimental systems, followed by a somewhat speculative discussion of the implications our work with regard to neural networks. Finally, we will explore some of the possible future directions for this research.

6.1 Summary of Experiments and Results

6.1.1 Experiment Summary

We have performed a novel set of experiments on the dynamics of oscillator synchronization. In summarizing what has been accomplished let us first recapitulate the important features of the experiments themselves. While many experimental studies have been done of particular systems of oscillators, such as Josephson junctions, such work is typically focused narrowly on understanding the behavior of that particular type of oscillator. On the other hand, the more recent interest and progress in oscillator populations in general has been entirely theoretical, and has relied on highly simplified mathematical models, such as that discussed in Sec. 2. These theoretical results are quite elegant, but often the work is only weakly coupled with experimental information. Without the guiding and focusing effect of experimental results, the theory runs the risk of veering off toward irrelevance.

We contribute to this field some of the rarely seen experimental data. The oscillators we studied are real electronic oscillators. Rather than construct electronic oscillators specifically to duplicate the behavior of the simplified mathematical model, we simply assembled a population of oscillators possessing certain general characteristics. First, the oscillators were relaxation oscillators, which is a type of limit-cycle oscillator. Hence, they are essentially one-dimensional elements. Second, the oscillators were coupled together with a simple mean-field or all-to-all coupling scheme. Third, a natural consequence of the choice of coupling was that the oscillators repelled each other: they preferred to separate from each other in phase. This last feature, in particular, is one that has rarely been studied theoretically and perhaps never before been studied experimentally, in part because it has been assumed that the repulsive case produced no synchronization. We examined the time required for the entire oscillator system to synchronize. In addition, we examined the phase-locked states of the system. In the next section the primary results are summarized.

6.1.2 Results Summary

The central discovery is that the locking time for our oscillator system is well described by an exponential distribution. The system may persist in a disordered state for a very long time before it abruptly reaches a phase locked state. Indeed, it appears that the length of the transient may be arbitrarily large. As might be expected, the decay constant of this exponential distribution becomes smaller with increasing coupling. While increased coupling shortens the average time required for the system to synchronize, there is no guarantee that the system will synchronize within any given finite time. As the coupling is reduced below some critical threshold, the decay constant approaches infinity, which implies that the probability that any trajectory phase locks within a finite time is zero. This result has interesting implications, since in the study of dissipative dynamical systems it is important to distinguish between short term transient behavior and long term steady-state behavior. In our system, it seems that, given finite time, a single trajectory is insufficient to determine whether the system will ever phase-lock. Hence, distinguishing between the ordered and disordered phases of the oscillator population is meaningless, except in a statistical sense.

We have proposed a crude geometrical model of phase-space and a simple map type model of the oscillator interactions. The former model envisions phase space studded with small localized *attracting regions.* Outside these regions phase-space is flat, on average: neither attracting nor repelling. Inside the attracting regions, points in phase-space are strongly attracted to a phase-locked state somewhere inside the region. While far from being a complete or rigorous description of the system, these models seem to adequately capture the transient dynamics of the system mentioned above.

On the other hand, our models are not capable of describing the phase-locked states themselves. We have found experimentally that there are a huge number of phase-locked states of the oscillator system. The number of states appears to closely related to the number of unique ways of ordering N items around the perimeter of a circle. That is, that number of states goes as (N-1)! as far as our apparatus is capable of measuring. While the number of states is not particularly surprising, the models we present do not account for the actual configuration of the states themselves.

6.2 Discussion of Electronic Systems as Experiments

It is worthwhile to take a broader look at the nature and value of experiments performed *on* electronic systems. An experiment performed on some novel and poorly

understood type of element, such as a new type of diode, is of obvious value. What, however, are the implications of an experiment composed of a novel arrangement of elements each of which is well understood on its own? In our case the well-understood elements are the op-amps; indeed they were *engineered* to behave in a predictable manner. While the behavior of an individual op-amp oscillator is not especially interesting, what about the dynamics of the coupled system?

These questions are analogous to the question of collective behavior of systems of well understood particles. For example, plasmas are governed by the well understood microscopic interactions in quantum mechanics and electromagnetism. Yet the collective behavior of a plasma can be very difficult to understand as a result of strong, long-range, nonlinear interactions. In a similar vein, the poorly understood phenomenon of turbulence in a fluid is probably the consequence, in a microscopic sense, of little more than classical mechanics. In such systems, an experiment can be expected to produce fundamentally interesting information regarding the collective processes of a real, although perhaps simplified, physical system. In our case however, the system of op-amps is not of intrinsic interest. That is, one never encounters a collection of coupled op-amps in nature in the same way one does encounter plasmas, fluids or molecules. The value of the op-amp system lies in its similarity to real physical systems.

There are, in fact, cases where one wishes to engineer a system of oscillators for technological purposes, usually to achieve a scaling up in power. As mentioned earlier, this has been done frequently with Josephson junctions and laser diodes. Nevertheless, since there is no direct interest (that we know of) in engineering a system of coupled op-amp oscillators, their value lies again in their similarity to other oscillator systems.

In an experiment in which an electronic system is itself the subject of the experiment, the electronics become a sort of analog computer. The importance of such 'analog computers' should not be underestimated. Seminal work in the field of nonlinear dynamics was done by Lorenz [Lorenz, 1963] using an analog computer to integrate a set of differential equations governing atmospheric transport. While the analog computer Lorenz used was a precision instrument designed to integrate differential equations accurately, the equations themselves involved only three variables: perhaps the crudest model of the atmosphere imaginable. In spite of this radical simplification, the system produced the earliest observation of chaos in a simple dynamical system.

As with the discovery of chaos in the Lorenz equations, the important behavior in many dynamical systems is often a consequence of the presence of nonlinearity, dissipation and the topology of the phase space rather than the detailed rules for propagating the system forward in time. A simple map, difference equation, or analog computation is frequently sufficient to observe interesting dynamical phenomena.

Other work [Linsay & Cumming, 1989] has been done using electronic systems to demonstrate the existence of chaos and the routes to chaos, as well as to measure some specific theoretically predicted quantities. In addition, the experiments by Winfree [Winfree, 1967] used a system of 70 crude integrate-and-fire oscillators made with resistors, capacitors and neon bulbs as the nonlinear element. The electronic circuit provides a convenient platform from which to conduct experiments which are subject to all the vagaries of a real world system (such as noise), yet which is also relatively easy to construct, manipulate and measure compared fluid, chemical or mechanical systems (for example.) An analog electronic system allows the experimenter visualize its dynamics in real time and to easily see the effect of modifying parameters of the system. In a certain sense one can think of the electronic experiment as an experiment *on the mathematics*.

The oscillators in our case, while simple to construct, differ from most relaxation oscillators in that the charging and discharging parts of their cycles are symmetrical. Furthermore, the repulsive coupling, while rarely studied, is also uncommon in nature and rarely of interest in any current technological applications.

As the power of digital computers increased, the relative value of analog computation for obtaining detailed numerical results rapidly diminished. Digital computers have played a key role in the development of nonlinear dynamics. Not only are digital computers useful in the traditional sense, for performing precise numerical calculations, but they have allowed exploration of mathematical models that would otherwise be intractable analytically.

Although they share this latter trait, the two approaches, digital and analog, each have advantages and disadvantages that are worth discussing. One advantage of digital computation is reduced noise. Digital computations suffer from errors due to the finite precision of the variables that can be represented (roundoff), as well as error due to the discretization of time in approximating a differential equation with a difference equation. These errors can generally be well quantified and controlled. An analog computation, in contrast, is plagued by electronic noise of all sorts (fundamental, thermal drifts, radio and

line interference etc.) which can be quite difficult to track down and control. In nonlinear systems such as ours, there is often a *sensitivity to initial conditions*. In such cases, the amplitude of the noise has a devastating effect on the ability to correlate initial and final states.

Another advantage of a digital approach is flexibility and control. In a digital computer changing a parameter such as a natural frequency or a coupling strength is essentially trivial. Even wholesale changes in a model are relatively inexpensive to implement. Furthermore, a digital implementation may approach an idealized model as closely as one wants. An analog system, on the other hand, may contain undesirable features that must simply be lived with. It has much less flexibility, in that gaining computer control of some parameter, such as the natural frequencies of the oscillators, requires a substantial amount of engineering. A change in the basic oscillator behavior would probably mean a costly re-engineering.

Worse still, the engineering challenge rapidly grows more severe as the number of elements increases. Suppose, for example that one wanted to model a system of N elements with an arbitrary coupling between any pair of elements. In a digital model one only needs to fill an NxN matrix with the desired coupling strengths. In an analog system the coupling would be implemented, perhaps using a digitally controlled potentiometer between every pair of elements. For N=100 elements that requires 10,000 digitally controlled potentiometers, each of which must be individually addressable and each of which must be connected to perhaps an 8-bit data bus which determines its resistance. Problems of cost, reliability, power consumption, wire routing and other difficulties make the digital approach very attractive in comparison.

A final, though probably less severe, difficulty with analog systems is the increased failure rate with large N. Assuming that the system does not produce valid data unless all of its constituent elements are working properly (this not necessarily a valid assumption), the overall failure rate of the system increases linearly with N. For sufficiently large N, the system may not be able to operate for periods long enough to acquire the desired data.

On the other hand, the analog approach does indeed have some advantages. Foremost among them are those mentioned above: the analog electronic system allows the experimenter to interact with the apparatus in a way that gives rapid feedback and lends itself to an intuitive understanding of the system, rather than a being a blind exploration of some parameter space. Another advantage of the analog electronic system is speed.

Analog computers of all sorts have the fundamental advantage that they perform their 'computations' in parallel. In many-body physics it is relatively easy to pose problems which greatly exceed the capabilities of even the most powerful digital computers. The number of particle-to-particle interactions typically scales as N^2.

Here again the analog approach has serious limitations. Although an analog system may be very efficient at simulating a system or producing data, the data still must be analyzed, invariably on a digital computer. While the problem of analysis may not be as severe as that of simulation, it is worth considering whether the two are comparable, in which case the analog approach makes little sense from the perspective of computational speed.

6.3 Neural Nets

We turn now to a brief speculation upon the connection between our system of oscillators and neural networks which have become increasingly important technologically. As mentioned in Sec. 1, there is substantial similarity between the statistical mechanics tools used to analyze populations of oscillators, populations of neurons, and populations of magnetically interacting spins. In the usual analogy between neurons and spins [Müller & Reinhardt, 1990] the state of a spin is analogous to the *average rate* at which a neuron is firing pulses. Inputs to the neural net are analogous to initial states of the spin system and outputs are the stable, equilibrium states. The neuronal 'memories' are encoded in the set of weights which couple one spin to another. In this crude equation, the dynamics on the time scale of individual pulses are completely ignored. Indeed, even the firing rate of the neuron is coarsely described with a one bit binary value, high rate or low, corresponding to say, spin up or down.

It is not yet clear, in the field of neurobiology, whether this average neuronal firing rate approximation is appropriate. It may be that important processing is occurring on a pulse-to-pulse time scale. For example, the relative arrival time of pulses from two different neurons may carry information of some sort. Certainly, the proper functioning of the heart depends on the proper timing of individual neuronal impulses. In addition, while artificial neural networks are generally effective for optimization, decision making, and pattern recognition, they find little use in sequential problems such as counting.

The work reported here is part of a growing trend toward looking at oscillator systems which interact via impulses [Tsodyks *et al.*, 1993], [Mirollo & Strogatz, 1990], [Brailove, 1992]. We have already seen that the sequential dynamics and ordering of our

oscillators plays an important role in their fundamental behavior. These oscillators may capture some essential aspect of sequential neuronal processing. If one makes the analogy between the stable phase-locked states of our oscillator system, and neuronal 'memories', the transient dynamics of the oscillator system might correspond to a neuronal system 'searching' for a memory. In addition, a small external perturbation is sufficient to perturb the system away from a stable state, allowing it to resume its transient dynamics and begin 'searching' again. The significance of the exponential locking time distribution is not clear. A comparison with studies of the time required to recall actual memories might prove fruitful.

Another unusual and particularly interesting feature of our system is that a mean-field coupling produces a multitude of distinct stable states. In contrast, a simple spin system coupled with a sufficiently large mean-field possesses only a single trivial stable state (spins aligned). A nontrivial artificial neural network must be capable of recognizing and classifying many different input patterns. Thus it is necessary that the 'spins' to interact locally, and that the interactions be frustrated. In this way, a multitude of stable states of approximately equal energy are created.

6.4 Future Directions

In closing, it is useful to consider some of the possible future directions for this research, as well as some more mundane experimental improvements. One of the great difficulties with the experimental apparatus was the inadequate degree of computer control over many parameters of the system. As the size of a system increases it becomes all the more important, and yet all the more difficult to have computer control over the increasing number of parameters available in the experiment. The most important of these parameters are the natural frequencies of each of the oscillators. The ability to automatically control the frequencies of each oscillator would permit the careful study of the competition between the width of the frequency distribution and the coupling strength. Since most of the recent theoretical work on oscillator populations concentrates on the determination of the phase diagram, such an improvement would allow a more extensive comparison between theory and experiment.

Another obvious improvement, is to extend the experimental results to larger N. The number of oscillators used in our experiments N=15 is just barely large enough to be considered in the realm of the statistical. Ideally, one would like to have N large enough that experimental results could be studied over a broad range of N. In this way it might be

possible to extend the results to the continuum limit $N \rightarrow \infty$. It is difficult to imagine, for reasons we have already discussed, scaling N up by much more than one order of magnitude. Certainly, the problems of parameter control, data acquisition and expense would be horrendous for N=1000. On a practical level, at larger N, it becomes a matter of necessity that N to be treated as a parameter of the system. The experiment should improved so that individual oscillators can be automatically removed from or added to the population, without manual intervention by the experimenter.

A particularly fertile area of future investigation would be to explore different types of coupling. The mean-field coupling employed in our experiments is the simplest coupling scheme possible. It necessarily precludes the existence of spatial effects. There are a great variety of local coupling schemes possible, akin to those studied in statistical mechanics. Considerable theoretical work has been done on such systems, but again, little has been attempted experimentally. More complex coupling schemes would allow one to look for spatio-temporal effects such as waves, spatio-temporal chaos and other complex phenomena currently being investigated [Kaneko, 1989] in the non-linear dynamics field. Of course, the practical difficulties associated with controlling the coupling strength are formidable. For nearest neighbor interactions, for example, the number of interactions scales with N (2N for a 2-D square array). Even if it is assumed that all coupling strengths are equal, one still needs order N separate coupling elements (with equal strengths): a single resistor, for example, cannot be used. For the most general possible coupling scheme, N^2 individually controllable coupling elements are required. In addition, one would like to accommodate the possibility of both positive and negative coupling strengths (an option which was not available even in our experiment).

Finally, it is worth considering modifications to the oscillators themselves. Recall that each oscillator has associated with it two capacitors: one internal, which sets the natural frequency of oscillation, and one external which couples each oscillator to the others. The internal capacitor is in fact redundant in the limit of weak coupling. When the coupling resistance is zero the two capacitors may simply be added together in parallel. We believe the elimination of the internal capacitor would simplify the equations governing the circuit, without materially affecting its behavior.

A more interesting variation on the oscillator circuit, in which we retain the internal capacitor, is as follows: recall that currently the oscillators are single-terminal devices. That is, each oscillator has a single 'input' terminal which is connected through some arbitrary coupling network to all the other input terminals. Alternatively, we could treat each

oscillator as a two-terminal device: one input terminal and one output terminal. In the most general possible coupling scheme, each output terminal would be coupled by arbitrary resistive weights to each of the input terminals. This system is closely akin to the usual model of a neural network, except for the capacitor. Its advantages are that it eliminates entirely the need for any sort of capacitive coupling. The coupling can be purely resistive. In addition it is elegant, since the internal resistor used to charge the internal capacitor can be viewed as a self-coupling: it is a diagonal element in the matrix of weights which connect the outputs with the inputs.

REFERENCES

Bélair, J. [1986] "Periodic pulsatile stimulation of a nonlinear oscillator", *J. Math. Biol.* **24**, 217-232.

Brailove, A. A. [1992] "The Dynamics of Two Pulse-Coupled Relaxation Oscillators", *Int. J. Bifurcation and Chaos* **2**, 341-352.

Brown, B. N., *et. al.* [1975] "A Linked Oscillator Model of Electrical Activity in the Human Small Intestine", *Am. J. Physiol.* **229**, 384-388.

Buck, J. & Buck, E. [1976] "Synchronous Fireflies", *Scientific American* **234**, 74-85

Buck, J. [1988] "Synchronous Rhythmic Flashing of Fireflies. II", *Quart. Rev. Biol.* **63**, 265-289.

Cohen, A. H., Holmes, P. J. & Rand, R. H. [1982] "The Nature of the Coupling Between Segmental Oscillators of the Lamprey Spinal Generator for Locomotion: A Mathematical Model", *J. Math. Biology* **13**, 345-369

Cumming, A. & Linsay, P. S. [1988] "Quasiperiodicity and Chaos in a System with Three Competing Frequencies", *Phys. Rev. Lett.* **60**, 2719-2722.

Daido, H. [1987] "Discrete-Time Population Dynamics of Interacting Self-Oscillators", *Prog. Theor. Phys.* **75**, 1460-1463.

Daido, H. [1992] "Quasientrainment and Slow Relaxation in a Population of Oscillators with Random and Frustrated Interactions", *Phys. Rev. Lett.* **68**, 1073-1076.

Elliot, R. A., *et. al.* [1985] "Dynamic Characteristics of Phase-Locked Multiple Quantum Well Injection Lasers", *IEEE J. Quantum Elec.* **QE-21**, 598-602.

Floyd, S. & Jacobson, V. [1993] "The Synchronization of Periodic Routing Messages", Preprint.

Grebogi, C. & Ott, E. [1983] "Crises, Sudden Changes in Chaotic Attractors, and Transient Chaos", *Physica 7D* , 181-200.

Grebogi, C., Ott, E. & Yorke, J. A. [1985] "Super Persistent Chaotic Transients", *Ergod. Th. & Dynam. Sys.* **5**, 181-200.

Grebogi, C., Ott, E. & Yorke, J. A. [1988] "Unstable Periodic Orbits and the Dimension of Multifractal Chaotic Attractors", *Phys. Rev. A* **37**, 1711-1724.

Hadley, P., Beasly, M. R. & Wiesenfeld, K. [1988a] "Phase locking of Josephson junction arrays", *Appl. Phys. Lett.* **52**, 1619-1621.

Hadley, P., Beasly, M. R. & Wiesenfeld, K. [1988b] "Phase locking of Josephson-junction series arrays", *Phys. Rev. B.* **38**, 8712-8719.

Honerkamp, J. [1983] "The Heart as a System of Coupled Nonlinear Oscillators", *J. Math. Biology* **18**, 69-88.

Horowitz, P. & Hill, W. [1989] *The Art of Electronics, 2nd ed.* (Cambridge University Press, Cambridge) Chap. 5, p. 285.

Huygens, C. [1673] *The Pendulum Clock or Geometrical Demonstrations Concerning the Motion of Pendula as Applied to Clocks* (Iowa State University Press), Richard Blackwell, Translator, 1986. p.30.

Jain, A. K., Likharev, K. K., Lukens, J. E. & Sauvageau, J. E. [1984] "Mutual Phase-Locking in Josephson Junction Arrays", *Physics Reports* **109**, 309-426.

Kaneko, K. [1989] "Spatiotemporal Chaos in One- and Two-Dimensional Coupled Map Lattices", *Physica D* **37**, 60-82.

Kaneko, K. [1991] "Globally Coupled Circle Maps", *Physica D* **54**, 5-19.

Kaneko, K. [1992] "Mean Field Fluctuation of a Network of Chaotic Elements", *Physica D* **55**, 368-384.

Keener, J. P., Hoppensteadt, F. C. & Rinzel, J. [1981] "Integrate-and-fire models of nerve membrane response to oscillatory input", *SIAM J. Appl. Math.* **41**, 503-517.

Kopell, N. & Washburn, R. B. [1982] *IEEE Transactions on Circuits and Systems* **CAS-29**, 738.

Kuramoto, Y. & Nishikawa, I. [1987] "Statistical Macrodynamics of Large Dynamical Systems. Case of a Phase Transition in Oscillator Communities", *J. Stat. Phys.* **49**, 569-605.

Kuramoto, Y. [1984] *Chemical Oscillations, Waves, and Turbulence* (Springer-Verlag, Berlin) pp. 1-54.

Linsay, P. S. & Cumming, A. W. [1989] "Three-Frequency Quasiperiodicity, Phase-Locking and the Onset of Chaos", *Physica D* **40**, 196-217.

Lorenz, E. N., [1963] "Deterministic nonperiodic flow", *J. Atmos. Sci.* **20**, 130.

McClintock, M. K. [1971] "Menstrual Synchrony and Suppression", *Nature* **229**, 244-245.

Mirollo, R. E. & Strogatz, S. H. [1990] "Synchronization of pulse-coupled biological oscillators", *SIAM J. Appl. Math.* **50**, 1645-1662.

Müller, B. & Reinhardt, J. [1990] *Neural Networks* (Springer-Verlag, Berlin) Chap. 3, Chap. 15.

Newhouse, S., Ruelle, D. & Takens, F., [1978] "Occurrence of Strange Axiom A Attractors Near Quasi Periodic Flows on T^m, $m \geq 3$", *Commun. Math Phys.* **64**, 35.

Niebur, E., Schuster, H. & Kammen, D. [1991], "Collective Frequencies and Metastability in Networks of Limit-Cycle Oscillators with Time Delay", *Phys. Rev. Lett.* **67**, 2753-2756.

Omata, S., Yamaguchi, Y. & Shimizu, H. [1988] "Entrainment Among Coupled Limit Cycle Oscillators with Frustration", *Physica D* **31**, 397-408.

Peskin, C. S. [1975] *Mathematical Aspects of Heart Physiology* (Courant Institute of Mathematical Sciences, New York University, New York) pp. 268-278.

Poincaré, H., [1881] "Sur les courbes définies par une équation différentialle", *J. Math.* **3-7**, 375.

Ruelle, D. & Takens, F., [1971] "On the Nature of Turbulence", *Commun. Math Phys.* **20**, 167.

Smale, S., [1967] "Differentiable dynamical systems", *Bull. Amer. Math. Soc.* **73**, 747.

Smith, H. M. [1935] "Synchronous Flashing of Fireflies", *Science* **82**, 151.

Strogatz, S. H. & Mirollo, R. E. [1988] "Phase-Locking and Critical Phenomena in Lattices of Coupled Nonlinear Oscillators with Random Intrinsic Frequencies", *Physica D* **31**, 143-168.

Torre, V. [1976] "A Theory of Synchronization of Heart Pacemaker Cells", *J. Theor. Biol.* **61**, 55-71.

Treese, W. [1992] "Self-Synchronization Phenomena in Computer Networks", personal communication.

Tsodyks, M., Mitkov, I. & Sompolinsky, H. [1993] "Pattern of Synchrony in Inhomogeneous Networks of Oscillators with Pulse Interactions", *Phys. Rev. Lett.* **71**, 1280-1284.

Wang, S. S. & Winful, H. G. [1988] "Dynamics of phase-locked semiconductor laser arrays", *Appl. Phys. Lett.* **52**, 1774-1776.

Winfree, A. T. [1967] "Biological Rhythms and the Behavior of Populations of Coupled Oscillators", *J. Theoret. Biol.* **16**, 15-42.

Winful, H. G. & Wang, S. S. [1988] "Stability of phase locking in coupled semiconductor laser arrays", *Appl. Phys. Lett.* **53**, 1894-1896.

APPENDIX

This appendix contains the computer code used to acquire and analyze experimental data. The files are, in order:

AcquireDMA.c

FixedPtCluster.cp

```
//--------------------------------------
//
//      File:  AcquireDMA.c
//      By:        Adam Brailove
//
//--------------------------------------

#include <CursorCtl.h>
#include <Memory.h>
#include <StdLib.h>
#include <StdDef.h>
#include <StdIO.h>
#include <String.h>
#include <Types.h>
#include <Events.h>
#include <OSUtils.h>

#ifndef __MATH__
#include <Math.h>
#endif

#ifndef __SANE__
#include <SANE.h>
#endif

#include "Inner90:MPW:AAB:MyCHeaders:NIBoards.h"
#include "Inner90:MPW:AAB:MyCHeaders:NB-DIO-32F.h"
#include "Inner90:MPW:AAB:MyCHeaders:NB-DMA-8-G.h"

// --- Modes ---
#define    NORMAL 0
#define    CALIB  1

void Phi(int Nref, int *tref, int N, int *t, int *Nphi, float *phi);
int FindLocking(float *phi, float *phi_ref, int iphi_end, float epsilon);
float Phi_FixedPoint(float *phi_ref, float *phi, int iphi_lock, int iphi_end);
extended posmod(extended x, extended y);

/* ------------ Main -------------- */

void
main(char /* argc */, char *argv[])
{
    int                iOsc, nOsc;       // Population of the board.
    unsigned short     MasterfreqDiv = 2;    // Divide master clock to 5 Mhz (divider
must be >= 2).
    unsigned short     freqDivide;
    extended       sampleFreq;

    int                iRun, nRuns, nSamples;
    int                j;
    int                nSwitches[16], nSwitchesMin;
    int                iLockPhase[16], iStartPhase; // allLockedPhase;
    extended       period[16], phaseShift[16];
    long           *tau[16];
    unsigned short     *theData;
    long           *DataCopy;     //  an integer array for use with the NI-DSP.
    unsigned char  initRate[16], initState[16];
    int                mode;

    int                Nphi[16], iphi, iphi_end, iphi_all_locked;
    float          *phi[16];

    char           *initFile;
```

```
    FILE            *initFilePtr;
    char            *phasefile;
    FILE            *phasefileptr;

    void            DoAcquire(int nSamples, unsigned short* theData,  unsigned short
MasterfreqDiv,
                                        unsigned short freqDivide,  unsigned char*
initRate,
                                        unsigned char* initState, int nOsc, Boolean
doInit);
    void            DoInit(FILE *initFilePtr, char *initState, char *initRate, int
nOsc);
    long            SwitchTime(long* data, long n, long bitmask, long* SwitchTimeArray,
                                                    long nSTArray, long*
nSwitches);
    long            SwitchingTime(long* data, long n, long bitmask, long*
SwitchTimeArray,
                                                    long nSTArray, long*
nSwitches);
    extended        FindPhaseShift(timeShift, period);
    int                ArrayMin(int *intArray, int n);
    int                ArrayMax(int *intArray, int n);
    int                Min (int a, int b);
    int                Max (int a, int b);

    void            DSPChkErr(char*, short);
    short           OpenDSPBoard(void);
    const int       MAXPHIARRAY = 5000;// Maximum size of phi array. MOD: could be done
dynamically...

    // ------ Get command line input
    nSamples = atoi(argv[1]);        // Enter number of samples.
    nRuns = atoi(argv[2]);           // Enter number of master loops to perform.
    freqDivide = atoi(argv[3]);      // Enter sampling frequency divider: fSample =
5Mhz/(2*freqDivide)
    nOsc = atoi(argv[4]);            // Enter number of oscillators on board (In order,
starting from #0)
    initFile  = argv[5];          // Enter init filename string.
    phasefile = argv[6];          // Enter file for tau differences

    if (strcmp(initFile,"calib")) {  // If NOT calib...
       mode = NORMAL;
       initFilePtr = fopen(initFile, "r");     // Open file, get file pointer.  Mod:
Need to handle errors...
    } else {                      // if IS calib...
       mode = CALIB;
    }
    // ------ Allocate memory for the data
    theData = malloc (nSamples*2);
    if (theData == NULL) {exit(1);}

    // ------ Allocate memory for the data
    DataCopy = (long *)NewPtr((Size)(nSamples*sizeof(long)));
    if (DataCopy == NULL) {exit(1);}

    // ------ Allocate memory for the switching time arrays.
    for (iOsc=0;iOsc<nOsc;iOsc++){
       tau[iOsc] = (long *)NewPtr((Size)(nSamples*sizeof(long)/2));
       if (tau[iOsc] == NULL) {exit(1);}
    }

    // ------ Allocate memory for phi.-- MOD: could be done dynamically...
    for (iOsc=0;iOsc<nOsc;iOsc++){
       phi[iOsc] = (float *)NewPtr((Size)(MAXPHIARRAY*sizeof(float)));
```

```
        if (phi[iOsc] == NULL) {exit(1);}
    }

    // ------ Calculate sampling frequency in Hz., Max sampling frequency = approx 350
KHz
    sampleFreq = 10000000/(MasterfreqDiv*freqDivide*2);
    if (freqDivide < 2) {
        printf ("ERROR: freqDivide must be larger\n");
        exit(1);
    }

    // ---- Output Header Info.
    printf("Sampling Frequency = %f Hz\n",sampleFreq);
    printf("Sampling Period = %f sec\n",1/sampleFreq);
    printf("Number of Samples = %d\n",nSamples);
    printf("Number of Runs = %d\n",nRuns);
    printf("Number of Oscillators = %d\n",nOsc);
    printf("InitFile = %s\n",initFile);
    printf("\n\n");

    InitCursorCtl(NULL);

    //DSPChkErr("OpenDSPBoard", OpenDSPBoard());   //  open the DSP board and report
any errors.

    // ------ Master Loop
    for(iRun = 0;iRun<nRuns;iRun++) {
        if (iRun % 10 == 0) fprintf(stderr,"*Run %d\n",iRun);
        RotateCursor(iRun);

        // ---- Set the Initialization arrays
        if (mode != CALIB) DoInit (initFilePtr, initState, initRate, nOsc);

        // ---- Acquire the data.
        DoAcquire (nSamples, theData, 2, freqDivide, initRate, initState, nOsc, (mode
!= CALIB));

        //  copy data to an array of longs
        for(j = 0; j < nSamples; j++) DataCopy[j] = theData[j];

        // ---- do switching time (tau) calculation
        for (iOsc=0;iOsc<nOsc;iOsc++) {
            SwitchTime(DataCopy, nSamples, 0x00000001<<iOsc, tau[iOsc], nSamples/2,
&nSwitches[iOsc]);
            //DSPChkErr("SwitchTime",
                //SwitchingTime(DataCopy, nSamples, 0x00000001<<iOsc, tau[iOsc],
nSamples/2, &nSwitches[iOsc]));
//printf("%d\t",nSwitches[iOsc]);
        }
//printf("\n");

        nSwitchesMin =  ArrayMin(nSwitches, nOsc);

        // ---- Calculate phases
        for(iOsc=0;iOsc<nOsc;iOsc++) {
            Nphi[iOsc] = nSwitchesMin;
            Phi(nSwitches[0], tau[0], nSwitches[iOsc], tau[iOsc], &Nphi[iOsc],
phi[iOsc]);
//printf("%d\t",Nphi[iOsc]);
        }
//printf("phi[0][250] = %f\n",phi[0][250]);
        iphi_end = ArrayMin(Nphi, nOsc);
//printf("\n");
//printf("nSwitchesMin = %d\n",nSwitchesMin);
```

```
//printf("iphi_end = %d\n",iphi_end);

       // ---- Find phase at which each oscillator locks to osc#0.
       for(iOsc=0;iOsc<nOsc;iOsc++) {
          iLockPhase[iOsc] = 1 + FindLocking (phi[iOsc], phi[0], iphi_end, 0.2);
//printf("%d\t",iLockPhase[iOsc]);
//printf("\n");
       }
       iphi_all_locked = ArrayMax(iLockPhase, nOsc);
//printf("iAll Locked = %d\n",iphi_all_locked);
//printf("\n");

       // ---- Find oscillator periods and phase shifts
       if (mode == CALIB)
          iStartPhase = 0;      // use the whole data stream
       else
          iStartPhase = iphi_all_locked;       // use only the locked data

//printf("from: i,phi,t:%d, %f, %d\n",iStartPhase, phi[0][iStartPhase],
tau[0][iStartPhase]);
//printf("to: i,phi,t:%d, %f, %d\n\n",iphi_end-1, phi[0][iphi_end-1], tau[0][iphi_end-
1]);

       for(iOsc=0;iOsc<nOsc;iOsc++) {
          period[iOsc] = (extended) (tau[0][iphi_end-1]-tau[0][iStartPhase]) /
                     (extended) (phi[iOsc][iphi_end-1]-phi[iOsc][iStartPhase]);
                     // MUST use tau's of reference oscillator!! = tau[0]
          //phaseShift[iOsc] = FindPhaseShift (deltaTau[iOsc], period[iOsc]); What
the hell was this?!
          phaseShift[iOsc] = Phi_FixedPoint(phi[0], phi[iOsc], iStartPhase,
iphi_end);
       }

       // ---- Output Data.

       if (mode != CALIB)  {
          for(iOsc=1;iOsc<nOsc;iOsc++)     printf("%5.3f\t",posmod(phaseShift[iOsc],
1.0));
          for(iOsc=1;iOsc<nOsc;iOsc++)     printf("%d\t",tau[0][iLockPhase[iOsc]]);
       }
       for(iOsc=0;iOsc<nOsc;iOsc++)     printf("%7.3f\t",period[iOsc]);

       printf("\n");

       // ---- Print phase differences
       //phasefileptr = fopen(phasefile, "w");     //  open the file

       //if(phasefileptr != NULL) {
       //  for(iphi=0;iphi<iphi_end;iphi++) {
       //     fprintf(phasefileptr, "%d\t%d\t%10.3f\t", iphi, tau[0][iphi],
phi[0][iphi]);

       //     for(iOsc=0;iOsc<nOsc;iOsc++) {
       //        fprintf(phasefileptr, "%10.3f\t", phi[iOsc][iphi]-phi[0][iphi]);
       //     }
       //     fprintf(phasefileptr, "\n");
       //  }
       //  fclose(phasefileptr);
       //}

    } // End of master loop.

    // ---- print phase history of last run
    if(!strcmp(phasefile,"phases")) {
```

```
        for(iphi=0;iphi<iphi_end;iphi++) {
            printf("%d\t%d\t%10.3f\t", iphi, tau[0][iphi], phi[0][iphi]);

            for(iOsc=0;iOsc<nOsc;iOsc++) {
                printf("%10.3f\t", phi[iOsc][iphi]-phi[0][iphi]);
            }
            printf("\n");
        }
    }

    fflush(stdout);

    exit(0);

} // === End of main  ================================================================

void DoInit(FILE *initFilePtr, char *initState, char *initRate, int nOsc)
{
    int               iState, iRate, iOsc;

    for(iOsc=0;iOsc<nOsc;iOsc++) {
        if (fscanf (initFilePtr, "%d,%d", &iState, &iRate) != 2) {
            rewind(initFilePtr);      // Start at top of file again
            fscanf (initFilePtr, "%d,%d", &iState, &iRate);
        }
        initState[iOsc]  = iState;   initRate[iOsc] = iRate;
    }
    while (getc(initFilePtr) != '\n') ;     // Skip to next line. Works properly for
nOsc < file width.
}

void DoAcquire (int nSamples, unsigned short* theData,  unsigned short MasterfreqDiv,
unsigned short freqDivide,  unsigned char* initRate,  unsigned char* initState, int
nOsc, Boolean doInit)
{
    unsigned short* dataSource = 0xFBF40000; // WHY WHY WHY ??? Why
not:(DIOSLOT+PORTA);  This duplicates stuff in InitPorts()...
    int        j;

    InitPorts();              // Initialize the port addresses

    MasterClock(MasterfreqDiv);          // Produce a 5 Mhz master clock
    AMDClock (3, freqDivide, 1);         // Set Clock #3 at 5 Mhz/(2*5) = 500 Khz and
go.

     /* --- Initialize the oscillators --- */
     if (doInit) {
        DACMode();                       /* Set mode first! */
        StopOscillators();               /* Must be stopped before init! */
        for (j=0;j<100;j++)  {
            Init1Board (0, initRate, nOsc);     /* Init the rate */
        }
        for (j=0;j<100;j++)  {
            Init1Board (0, initState, nOsc);        /* Init the state.*/
        }
        IdleDAC();                       /* Idle the DAC at 0 volts */
    }
    DMASetup();                  // Setup the general characteristics of the DMA board.
    ProgramChannel0 (theData, dataSource, 2*nSamples);     // Program the DMA channel.

     /* --- Aquire data --- */
    AcquireDMAMode();         /* Set mode first! */

    AddressBoard(0);          /* Address board zero */
```

```
    AssertData();             /* Assert the data always, because only one board */
    StartOscillators();          /* Let the oscillators run !!  */

    ClockChannel0 ();         // Start the DMA transfer !!

    WaitForChannel0();           // Poll the DMA board for a completion signal.
}

long SwitchTime (long* data, long n, long bitmask, long* SwitchTimeArray, long, long*
nSwitches)
{
    long   i, switches;

    switches = 0;

    for (i=0;i<n-1;i++) {
        if ( (data[i+1] & bitmask) > (data[i] & bitmask) ) {
            SwitchTimeArray[switches] = i; // Record switch time of sample just BEFORE
transition
            switches++;    // increment switch count
        }
    }

//fprintf(stderr,"*%d\t",switches);
    *nSwitches = switches;    // Return number of transitions found
    return switches;      // Return number of transitions found
}

int FindLockingPhase (int *tauTgt, int *tauRef, int n, extended *tauShift)
    //  Returns the last phase at which the two oscillators were locked.
{
    int        i, deltaPhi, deltaPhiTot;

    deltaPhiTot = *tauTgt - *tauRef;

    for (i=1;i<n;i++) {
        tauTgt++;
        tauRef++;
        deltaPhi = *tauTgt - *tauRef;
        if (abs(deltaPhi*i - deltaPhiTot) > 2*i) {
            *tauShift = (extended) deltaPhiTot/i;
            return(i-1);
        }
        deltaPhiTot += deltaPhi;
    }
    *tauShift = (extended) deltaPhiTot/ i;
    return(i-1);
}

float Phi_FixedPoint(float *phi_ref, float *phi, int iphi_lock, int iphi_end)
{
    int        i;
    float  avg=0;

    for(i=iphi_lock;i<iphi_end;i++) {
       avg += phi[i]-phi_ref[i];
    }
    avg = avg/(float) (iphi_end-iphi_lock);
    return avg;
}

extended FindPhaseShift (extended timeShift, extended period)
{
    extended       phaseShift;
```

```
    phaseShift = timeShift/period;
    if (phaseShift < 0.0) phaseShift += 1.0; // put in range 0.0 to 1.0
    return phaseShift;
}

int ArrayMin(int *intArray, int n)
    // General purpose routine finds the minimum of an array of n integers
{
    int         *end = intArray + n;
    int         min = *intArray;

    while (intArray<end) {
        if (*intArray < min) min = *intArray;
        intArray++;
    }
    return min;
}

int ArrayMax(int *intArray, int n)
    // General purpose routine finds the maximum of an array of n integers
{
    int         *end = intArray + n;
    int         max = *intArray;

    while (intArray<end) {
        if (*intArray > max) max = *intArray;
        intArray++;
    }
    return max;
}

int Min (int a, int b)
{
    return (a < b ? a : b);
}

int Max (int a, int b)
{
    return (a > b ? a : b);
}

extended posmod(extended x, extended y)
{
    return x>=0 ? fmod(x, y) : y + fmod(x, y);
}

void Phi(int Nref, int *tref, int N, int *t, int *Nphi, float *phi)
{
    int         i, k=0, t1;

    for (i=0;i<Nref;i++) {    // loop through reference transition times
        t1 = tref[i];         // the time at which phi is to be calculated

        if (t1 < t[0]) {
            phi[i] = 0;
        } else if (t1 >= t[N-1]) {
            *Nphi = i;
            return;
        } else if (i == *Nphi) {
            return;
        } else {
            while (t1 >= t[k+1]) k++;
            phi[i] = (float) k + ((float) (t1-t[k]))/((float) (t[k+1]-t[k]));
```

```
        }

    }
}

int FindLocking(float *phi, float *phi_ref, int iphi_end, float epsilon)
{
    int        iphi;
    float   Dphi, Dphi_end, delta;

    Dphi_end = phi[iphi_end-1]-phi_ref[iphi_end-1];

    for (iphi=iphi_end-1;iphi>=0;iphi--) {
//fprintf(stderr, "%d\t",iphi);
        Dphi = phi[iphi]-phi_ref[iphi];
        delta = fabs(Dphi_end-Dphi);
//fprintf(stderr, "%f\t",delta);
        if(delta > epsilon) return iphi;
//fprintf(stderr, "\n");
    }
}
```

```
//-------------------------------------
//
//      File:  FixedPtCluster.cp
//      By:        Adam Brailove
//
//-------------------------------------

#include <StdLib.h>
#include <StdDef.h>
#include <StdIO.h>
#ifndef __MATH__
#include <Math.h>
#endif

#ifndef __SANE__
#include <SANE.h>
#endif

#ifndef __MathLib__
#include "HardDrive:MPW:CWork:CPlusLib:mathlib.h"
#endif

const int MAXOSC=16;

typedef struct {
    int        index;
    float  phase;
} IndexPhase;

typedef struct {
    int            irun;
    IndexPhase     iphase[MAXOSC];
    float      lockphase;
    float      period;
    int            nosc;
} RunRec;

int getline(char *s, int lim);
int ArrayMax(int *intArray, int n);
void PrintRunRec(RunRec *r);

typedef int (*COMPFUNTYPE) (const void *, const void *);
int Compar(IndexPhase *e1, IndexPhase *e2);
int ComparRunRec(RunRec *e1, RunRec *e2);

void main()
{
    const int  MAXLINE = 100, MAXRUNS = 11000;
    const char     full_output = 0;
    float      sampleFreq, samplePer;
    int            nSamples, nRuns, nOsc;
    char       initFile[MAXLINE], date[MAXLINE], topology[MAXLINE],
resistance[MAXLINE], capacitance[MAXLINE];

    int            iOsc, iRun;
    int            phi[MAXOSC];
    float      phaseShift[MAXOSC], period[MAXOSC];
    RunRec     *runrec;

    getline(date, MAXLINE);
    getline(topology, MAXLINE);
    getline(resistance, MAXLINE);
    getline(capacitance, MAXLINE);
```

```
    scanf("Sampling Frequency = %f Hz\n",&sampleFreq);
    scanf("Sampling Period = %f sec\n",&samplePer);
    scanf("Number of Samples = %d\n",&nSamples);
    scanf("Number of Runs = %d\n",&nRuns);
    scanf("Number of Oscillators = %d\n",&nOsc);
    scanf("InitFile = %s\n",initFile);
    scanf("\n\n");

    fprintf(stderr, "Data acquired %s",date);
    fprintf(stderr, "%s",topology);
    fprintf(stderr, "%s",resistance);
    fprintf(stderr, "%s",capacitance);
    fprintf(stderr, "Sampling Frequency = %f Hz\n",sampleFreq);
    fprintf(stderr, "Sampling Period = %f sec\n",1/sampleFreq);
    fprintf(stderr, "Number of Samples = %d\n",nSamples);
    fprintf(stderr, "Number of Runs = %d\n",nRuns);
    fprintf(stderr, "Number of Oscillators = %d\n",nOsc);
    fprintf(stderr, "InitFile = %s\n",initFile);
    fprintf(stderr, "\n\n");

    // --- Allocate array
    runrec = new RunRec[MAXRUNS];

    //nRuns = 100; // Temporary debugging

    int    iLockedRun = 0;
    for(iRun=0;iRun<nRuns;iRun++) {
        // --- Read in row of data
        for(iOsc=1;iOsc<nOsc;iOsc++) scanf("%f",&phaseShift[iOsc]);
        for(iOsc=1;iOsc<nOsc;iOsc++) scanf("%d",&phi[iOsc]);
        for(iOsc=0;iOsc<nOsc;iOsc++) scanf("%f",&period[iOsc]);
        scanf("\n");


        // --- Did it lock?
        int lockedPhase =  ArrayMax(&phi[1], nOsc-1);
        if (lockedPhase < 0.92*((float) nSamples)) {   // It locked
            //for(iOsc=1;iOsc<nOsc;iOsc++)   fprintf(stderr,
"%5.3f\t",phaseShift[iOsc]);
            //for(iOsc=1;iOsc<nOsc;iOsc++)   fprintf(stderr, "%d\t",phi[iOsc]);
            //for(iOsc=0;iOsc<nOsc;iOsc++)   fprintf(stderr, "%7.3f\t",period[iOsc]);
            //fprintf(stderr, "\n");

            // --- Init runrec
            runrec[iLockedRun].irun = iRun;
            for(iOsc=1;iOsc<nOsc;iOsc++) {
                runrec[iLockedRun].iphase[iOsc].index = iOsc;
                runrec[iLockedRun].iphase[iOsc].phase = phaseShift[iOsc];
            }
            runrec[iLockedRun].lockphase = lockedPhase;
            runrec[iLockedRun].period = period[0];  // Could avg all Nosc
            runrec[iLockedRun].nosc = nOsc;

            //fprintf(stderr, "\nN:");
            //PrintRunRec(&runrec[iLockedRun], nOsc);
            //fprintf(stderr, "\n");
            // --- sort phases of each run
            //qsort(&(runrec[iLockedRun].iphase[1]), nOsc-1, sizeof(IndexPhase),
(COMPFUNTYPE) Compar);
            //PrintRunRec(&runrec[iLockedRun]);
            //fprintf(stderr, "\n");

            // --- next run
            iLockedRun++;
```

```
        }

    }
    int nLockedRuns = iLockedRun;

    // --- sort runrecs by firing order
    qsort(runrec, nLockedRuns, sizeof(RunRec), (COMPFUNTYPE) ComparRunRec);

    // --- print sorted
    fprintf(stderr, "\n-- Sorted Fixed Points --\n");
    int FPcount=1;     // Fixed point counter
    int    FPmultiplicity = 1;   // Counts number of initial states ending at this FP
    PrintRunRec(&runrec[0]);
    for(iRun=1;iRun<nLockedRuns;iRun++) {
        if(ComparRunRec(&runrec[iRun-1], &runrec[iRun])) {
            fprintf(stderr, "%d\n", FPmultiplicity);
            FPmultiplicity = 0;
            PrintRunRec(&runrec[iRun]);
            FPcount++;
        }
        FPmultiplicity++;
    }

    fprintf(stderr, "%d\n", FPmultiplicity);
    fprintf(stderr, "Runs Locked = %d\nFixed Points Found = %d\n\n",nLockedRuns,
FPcount);

    // --- print full sorted list
    if (full_output) {
        PrintRunRec(&runrec[0]);
        fprintf(stderr, "\n");
        for(iRun=1;iRun<nLockedRuns;iRun++) {
            if(ComparRunRec(&runrec[iRun-1], &runrec[iRun]))
                fprintf(stderr, "--------------------------\n");
            PrintRunRec(&runrec[iRun]);
            fprintf(stderr, "\n");
        }
    }

    exit(0);
}

int Compar(IndexPhase *e1, IndexPhase *e2)
{
    float d = e1->phase - e2->phase;

    if (fabs(d) < 0.004) {    // within Ambiguity radius
        if (e1->index > e2->index) return 1;
        else return -1;
    } else {
        if (d > 0.0) return 1;
        else return -1;
    }
}

int ComparRunRec(RunRec *e1, RunRec *e2)
{
    int        i;
    const float    box_radius = 0.01;

    for (i=1;i<e1->nosc;i++) {
        float d = e1->iphase[i].phase - e2->iphase[i].phase;
        if (fabs(d) >= box_radius) { // if they are not near...
            if (d>0) return 1;
```

```
            if (d<0) return -1;
        }
    }

    return 0;
}

void PrintRunRec(RunRec *r)
{
    int     iOsc, nOsc = r->nosc;

    fprintf(stderr, "%4d) \t",r->irun);
    for(iOsc=1;iOsc<nOsc;iOsc++)
        fprintf(stderr, "%2d,",(r->iphase[iOsc]).index);
    fprintf(stderr, "\t");
    for(iOsc=1;iOsc<nOsc;iOsc++)
        fprintf(stderr, "%5.3f\t",(r->iphase[iOsc]).phase,);
    fprintf(stderr, "%7.3f\t",r->period);
    fprintf(stderr, "%11.3f\t",r->lockphase);
}

int getline(char *s, int lim)
{
    int c, i;

    i=0;
    while (--lim>0 && (c=getchar())!= EOF && c!='\n')
        s[i++] = c;
    if (c=='\n')
        s[i++] = c;
    s[i] = '\0';
    return i;
}

int ArrayMax(int *intArray, int n)
    // General purpose routine finds the maximum of an array of n integers
{
    int         *end = intArray + n;
    int         max = *intArray;

    while (intArray<end) {
        if (*intArray > max) max = *intArray;
        intArray++;
    }
    return max;
}
```